Universidade do Estado do Rio de Janeiro

Centro de Tecnologia e Ciências

Instituto de Química

Universidad de Cantabria

Programa de Doctorado en Ingeniería Química, de la Energía y de Procesos

Escuela de Doctorado

Antoniel Carlos Carolino Campos

Membranas compósitas de poli(uretano-ureia) com sistemas de Ag NP/ativador e $AgBF_4$/$BMImBF_4$ para separação de olefinas/parafinas leves

Rio de Janeiro

2018

Antoniel Carlos Carolino Campos

Membranas compósitas de poli(uretano-ureia) com sistemas de Ag NP/ativador e $AgBF_4$/BMImBF_4 para separação de olefinas/parafinas leves

Tese apresentada, como requisito parcial para obtenção do título de Doutor, ao Programa de Pós-graduação em Engenharia Química, da Universidade do Estado do Rio de Janeiro e ao *Programa de Doctorado en Ingeniería Química, de la Energía y de Procesos*, da *Universidad de Cantabria* em regime de cotutela internacional entre as duas universidades.

Orientador: Prof. Dr. Rodrigo Azevedo dos Reis (Universidade do Estado do Rio de Janeiro)

Orientador: Prof. Dr. Alfredo Ortiz Sainz de Aja (*Universidad de Cantabria*)

Rio de Janeiro

2018

CATALOGAÇÃO NA FONTE
UERJ/REDE SIRIUS/CTC/Q

C198m Campos, Antoniel Carlos Carolino

Membranas compósitas de poli(uretano-ureia) com sistemas de Ag NP/ativador e $AgBF_4$/$BMImBF_4$ para separação de olefinas/parafinas leves. / Antoniel Carlos Carolino Campos. – 2018.
119 f.

Orientador: Rodrigo Azevedo dos Reis
Alfredo Ortiz Sainz de Aja

Tese (Doutorado) – Universidade do Estado do Rio de Janeiro, Instituto de Química.

1. Nanopartículas - Teses. 2. Prata – Teses. 3. Indústria petroquímica – Teses I. Reis, Rodrigo Azevedo dos II. Aja, Alfredo Ortiz Sainz de III. Universidade do Estado do Rio de Janeiro. Instituto de Química. IV. Título.

CDU 541.68

Antoniel Carlos Carolino Campos

Membranas compósitas de poli(uretano-ureia) com sistemas de Ag NP/ativador e $AgBF_4$/$BMImBF_4$ para separação de olefinas/parafinas leves

Data da aprovação: 20 de junho de 2018

Banca Examinadora:

_____
Prof. Dr. Rodrigo Azevedo dos Reis (Orientador)
Instituto de Química - Universidade do Estado do Rio de Janeiro

_____
Prof. Dr. Alfredo Ortiz Sainz de Aja (Orientador)
Departamento de Ingenierías Química y Biomolecular - Universidad de Cantabria

_____
Prof. Dr. Márcio Luis Lyra Paredes
Instituto de Química - Universidade do Estado do Rio de Janeiro

_____
Prof. Dr. Eugenio Daniel Gorri Cirella
Departamento de Ingenierías Química y Biomolecular - Universidad de Cantabria

_____
Prof. Dr. Alberto Claudio Habert
Programa de Engenharia Química /COPPE - Universidade Federal do Rio de Janeiro

_____
Profa. Dra. Helen Conceição Ferraz
Programa de Engenharia Química /COPPE - Universidade Federal do Rio de Janeiro

_____
Prof. Dr. Karim Dahmouche
Polo de Xerém da Universidade Federal do Rio de Janeiro

Rio de Janeiro

2018

RESUMO

CAMPOS, A. C. C. Membranas compósitas de poli(uretano-ureia) com sistemas de Ag NP/ativador e $AgBF_4$/$BMImBF_4$ para separação de olefinas/parafinas leves. 2018. 119 f. Tese (Doutorado em Engenharia Química) - Instituto de Química, Universidade do Estado do Rio de Janeiro, Rio de Janeiro, 2018.

Olefinas leves são principalmente produzidas pelo craqueamento a vapor da nafta, que está entre os processos mais intensos em energia da indústria petroquímica. Na busca por processos energicamente mais eficientes, algumas alternativas têm sido propostas para substituir parcialmente ou se combinar com a destilação criogênica, que é a tecnologia convencional para separação de parafinas e olefinas. Com esse objetivo, membranas de transporte facilitado, principalmente com o cátion Ag^+ como carreador seletivo, têm recebido grande atenção devido a sua alta seletividade e permeança fornecida. Entretanto, para ser usada industrialmente, a indesejada instabilidade associada ao cátion Ag^+ deve ser considerada. Agentes contaminantes e materiais de membranas poliméricas são fonte de desativação do Ag^+. Nos anos recentes, muitos avanços no desempenho da separação têm sido reportados, mas o desafio atual ainda é manter a seletividade em longos períodos de processo de separação. Nesse sentido, este trabalho traz uma revisão das perspectivas de soluções para a instabilidade das membranas para essa separação. Entre as alternativas que têm sido propostas para solucionar a potencial causa de desativação do Ag^+, este trabalho foca no uso de Ag NP como carreador e IL para a estabilização de Ag^+. A matriz polimérica investigada como material foram os poli(uretanos ureia)s (WPUU) sintetizados a partir de dispersão aquosa. O objetivo geral da Tese é o preparo de membranas compósitas com sistemas de Ag NP/ativador e $AgBF_4$/$BMImBF_4$ para a separação de olefinas e parafinas leves. Foi possível preparar com sucesso membranas de WPUU/Ag NP com até 50% (m/m) de prata. O transporte facilitado de olefinas não foi alcançado, mesmo com o uso de ativadores, $BMImBF_4$ e p-Bq. Membranas de WPUU/$AgBF_4$ com mais de 50% (m/m) de $AgBF_4$ apresentaram o transporte facilitado de olefinas. Entretanto, o fluxo de olefina diminuiu devido à perda de umidade durante os experimentos com gases secos e a intensa interação Ag^+/grupo éter presente na matriz de WPUU. IL ($BMImBF_4$) foi introduzido nas membranas eletrólitas preparadas. O IL foi capaz de suavizar a interação Ag^+/grupo éter proporcionando um aumento da seletividade final quando comparado com membranas sem o IL. Antes da queda do fluxo de olefina, a máxima permeança (13,94 GPU) e seletividade (97,5) foram alcançadas na membrana com razão mássica de 1 WPUU: 2 $AgBF_4$: 0.5 IL. Esse resultado conseguiu superar o desempenho mínimo para a substituição de colunas convencionais de separação para C3. Foi possível recuperar (84%) do fluxo de olefina quando o nível de umidade da membrana foi recuperado. Esse resultado sugere que a fonte inicial de queda no fluxo de olefina não é o problema de redução do Ag^+, mas a perda de umidade, que possivelemente acarretou na indisponibilidade do Ag^+ para interação com a olefina.

Palavras-chave: Separação olefina/parafina. Membrana de transporte facilitado. Sais de prata. Nanopartículas de prata. Desativação de carreador. Poli(uretano-ureia).

ABSTRACT

CAMPOS, A. C. C. *Poly(urethane urea) composite membranes with AgNP/Activator and $AgBF_4$/$BMImBF_4$ systems for olefins/paraffins separations.* 2018. 119 f. Tese (Doutorado em Engenharia Química) - Instituto de Química, Universidade do Estado do Rio de Janeiro, Rio de Janeiro, 2018.

Light olefins are mainly produced by the naphtha steam cracking, which is among the more energy intensive processes in the petrochemical industry. To save energy, some alternatives have been proposed to partially replace or combine with cryogenic distillation, the conventional technology to separate olefins and paraffins. Within this aim, facilitated transport membranes, mainly with Ag^+ cations as selective carriers, have received great attention owing to the high selectivity and permeance provided. However, the undesirable instability associated to the Ag^+ cation should be considered. Poisonous agents and polymer membrane materials are sources of Ag^+ deactivation. In recent years, great achievements on the separation performance have been reported, but the current challenge is to maintain the selectivity in long-term separation processes. Among alternatives that have been proposed to overcome the potential causes of Ag^+ deactivation, this Thesis focuses on the use of Ag NP as carrier and IL for Ag^+ stabilization. The polymer matrix investigated as membrane material are waterborne poly(urethane urea)s (WPUU). The general goal of the work is to prepare membranes with Ag NP/activator and $AgBF_4$/$BMImBF_4$ systems for light olefins/paraffins separation. It was possible to prepare successfully WPUU/Ag NP membranes up to 50 wt% of silver content. The facilitated transport of olefin was not reached, even with the use of activators, $BMImBF_4$ and p-Bq. WPUU/$AgBF_4$ membranes with more than 50 wt% of $AgBF_4$ provided facilitated transport of olefin. However, the olefin flux decreased due to the moisture loss during the experiments with dried gases and the intensive Ag^+/ether interaction in WPUU matrix. IL ($BMImBF_4$) was introduced to the electrolyte membranes prepared. IL was able to smooth Ag^+/ether interaction leading to an increase of the final selectivity when compared with membrane without IL. Before the olefin flux drop, the maximum olefin permeance (13.94 GPU) and selectivity (97.5) was achieved in 1 WPUU: 2 $AgBF_4$: 0.5 IL (weight ratio) membrane. This result reached the minimum performance required to replace C3 splitters. It was possible to recovery (84%) the olefin flux when the moisture level of the membrane was recovered. This result suggests that the initial source of olefin flux decline was not the Ag^+ reduction problem, but the moisture loss, which led to Ag^+ cations unfeasibility for olefin interaction.

Keywords: Olefin/paraffin separations. Facilitated transport membranes. Silver salts. Silver nanoparticles. Carrier poisoning. Poly(urethane urea).

RESUMEN

CAMPOS, A. C. C. *Membranas compuestas de poli(uretano-urea) con Ag NP/activador y $AgBF_4$/$BMImBF_4$ para la separación de olefinas/parafinas ligeras.* 2018. 119 f. Tese (Doutorado em Engenharia Química) - Instituto de Química, Universidade do Estado do Rio de Janeiro, Rio de Janeiro, 2018.

Las olefinas ligeras son producidas principalmente mediante el craqueo a vapor de las naftas, siendo este uno de los procesos más intensivos en energía de la industria petroquímica. Con el objetivo de disminuir el consumo energético, en los últimos años se han propuesto diferentes alternativas para sustituir parcialmente o combinar con la destilación criogénica, tecnología convencional para la separación de mezclas olefina/parafina. En este sentido, se destacan las membranas de transporte facilitado, que contienen el catión Ag^+ como cargador selectivo, proporcionando a estos materiales una alta selectividad y permeabilidad. Sin embargo, para ser empleada industrialmente, se debe considerar la inestabilidad asociada al catión Ag^+. Diferentes agentes contaminantes, así como algunos elementos en la composición de las membranas poliméricas son fuente de desactivación de la Ag^+. En los últimos años, se han reportado muchos avances en el desempeño de esta separación, pero el desafío actual sigue siendo mantener la selectividad en largos períodos de tiempo. Entre las alternativas que han sido propuestas para solucionar la potencial causa de desactivación del catión Ag^+, esta Tesis se centra en el uso de Ag NP como transportador y el uso de IL para la estabilización de Ag^+. La matriz polimérica investigada como material fue los poli(uretanos urea)s (WPUU) sintetizados a partir de dispersiones acuosas. Fue posible preparar con éxito membranas de WPUU/Ag NP hasta 50% (m/m) de plata. El transporte facilitado de olefinas no fue alcanzado, mismo con el uso de activadores, $BMImBF_4$ y p-Bq. Por otro lado, el transporte facilitado de olefinas se alcanzó en las membranas de $AgBF_4$/$BMImBF_4$/WPUU. Sin embargo, la membrana evidenció una dependencia con su humidificación para ser estable en experimentos de permeación de larga duración.

Palabras clave. Separación olefina/parafina. Membrana de transporte facilitado. Sales de plata. Nanopartículas de plata. Desactivación de cargador. Poli (uretano-urea).

LIST OF FIGURES

Figura 1 – Production of propylene by process..... 16
Figura 2 – Representation of solution-diffusion mechanism..... 21
Figura 3 – Representation of the facilitated transport mechanism in membranes..... 25
Figura 4 – π complexation between olefin and Ag^+..... 27
Figura 5 – Supported liquid membrane..... 28
Figura 6 – Ion-exchange membranes..... 29
Figura 7 – Interaction between the functional groups of POZ with the Ag^+..... 32
Figura 8 – Schematic representation of the possible polarization mechanism of the Ag NP surface by 7,7,8,8-tetracyanoquinodimethane (TCNQ)..... 37
Figura 9 – Chemical structure of PVDF-HFP and $BMImBF_4$..... 41
Figura 10 – Chemical structure of Pebax®..... 43
Figura 11 – Schematic illustration of a usual thin film composite membrane used for industrial gas separations..... 45
Figura 12 – Representation of rigid and flexible domains structure in a segmented PU..... 50
Figura 13 – Scheme of prepolymer formation and chain extension during the synthesis of WPU and WPUU..... 52
Figura 14 – Structure of WPU and WPUU particles in water medium. The scheme shows an anionic ionomer..... 53
Figura 15 – Steric stabilization scheme (in the enlarged part, a small polar portion of the stabilizing macromolecule anchors the surface of the NP)..... 56
Figura 16 – Illustration of overall free energy change ΔG as function of the growth particle size r..... 57
Figura 17 – Experimental apparatus for the synthesis of Ag NP in WPUU aqueous dispersion..... 60
Figura 18 – TEM images of WPUU/Ag NP membranes..... 63
Figura 19 – SAXS data of WPUU/Ag NP membranes..... 63
Figura 20 – Fits of SAXS data..... 64
Figura 21– XRD patterns of Ag NP and WPUU/Ag NP membranes..... 66
Figura 22 – Comparison between FTIR spectra of the WPUU and Ag NP 10%..... 68
Figura 23 – Comparison between FTIR spectra of the WPUU and 50% Ag NP*..... 69
Figura 24 – FTIR spectra of $AgBF_4$ and H_2O..... 79
Figura 25 – FTIR spectra of WPUU/$AgBF_4$ films..... 80

Figura 26 – FTIR spectra of WPUU/IL and WPUU/$AgBF_4$/IL films..... 80
Figura 27 – Flux of propylene, propane, and selectivity vs. permeation time for WPUU/$AgBF_4$ membranes..... 82
Figura 28 – Flux of propylene and propane vs. permeation time for WPUU/$AgBF_4$ membranes in the initial time of the experiments..... 84
Figura 29 – Flux of propylene, propane, and selectivity vs. permeation time for the membrane with high $AgBF_4$ content..... 85
Figura 30 – Flux of propylene, propane, and selectivity vs. permeation time for membrane with high $AgBF_4$ content in the initial time of the experiments... 86
Figura 31 – Flux of propylene and propane vs. permeation for 1 WPUU: 1 $AgBF_4$: 0.25 IL membrane. In this experiment, the permeation cell was opened and closed to restart the run..... 90
Figura 32 – Slopes of power-law region from log I(q) vs. log q and respective nanofiller morphology..... 116

LIST OF TABLES

Table 1 – Data used to calculate the feedstock share for the steam cracker in 2016..... 16

Table 2 – Steam cracker yields for ethane and naphtha..... 16

Table 3 – Sections of SC process and the energy involved..... 17

Table 4 – Data used to calculate the total energy consumption of the steam cracker and the SC separation section in 2016..... 18

Table 5 – Results of long-term permeation tests of various electrolyte membranes..... 33

Table 6 – Deactivation reaction of silver cation (Ag^+)..... 33

Table 7 – Main results of metallic nanoparticles as carriers for membrane facilitated transport of olefins..... 39

Table 8 – Chemical structures of activator agents for Ag NP..... 40

Table 9 – Results of membrane performance with ionic liquids for protection against the reduction of Ag^+..... 40

Table 10 – Results of the deactivation and regeneration processes of Pebax® 2533 + 80 wt% $AgBF_4$ membrane with original selectivity of 40 and olefin permeance of 87 GPU..... 43

Table 11 – Results of facilitated transport membranes based on highly fluorinated polymers..... 46

Table 12 – SAXS results for the WPUU/Ag NP membranes..... 65

Table 13 – Area ratios of the FTIR bands in N–H region of WPUU and 50% Ag NP*membranes..... 69

Table 14 – Thermal degradation data of the WPUU/Ag NP membranes from batch A of WPUU..... 70

Table 15 – Thermal degradation data of the WPUU/Ag NP membranes from batch B of WPUU..... 70

Table 16 – WPUU/Ag NP membranes prepared for gas permeation experiments..... 74

Table 17 – $AgBF_4$/WPUU membranes prepared for gas permeation experiments..... 75

Table 18 – Permeability of CO_2, C_2H_6 and C_2H_4 in WPUU/Ag NP membranes..... 78

Table 19 – Permeability of C_3H_8 and C_3H_6 in WPUU/Ag NP membranes..... 78

Table 20 – Results for the WPUU/$AgBF_4$ membranes..... 84

Table 21 – Results for the WPUU/$AgBF_4$ membranes at the end of gas permeation experiments..... 88

TABLE OF CONTENTS

	INTRODUCTION……..	11
1	**BACKGROUND AND THEORY**……..…	15
1.1	**Production of light olefins**……...	15
1.2	**Energy consumption of steam creaking process**……	16
1.3	**Applicability of membrane technology for olefin/paraffin separations**…..	19
1.4	**Solution-diffusion mechanism**……	20
1.5	**Facilitated transport membranes for olefin/paraffin separation**…….	24
1.5.1	Chemical interaction for olefin separation: Olefin π complexation……..….	25
1.5.2	Supported liquid membrane……...	27
1.5.3	Ion exchange membranes……..	28
1.5.4	Electrolyte membranes……..	30
1.6	**Challenges to avoid carrier instability**……...	35
1.7	**Some alternatives to overcome the Ag^+ deactivation**……	36
1.7.1	Silver nanoparticles as carrier……	36
1.7.2	Ionic liquids for the stabilization of Ag^+……	40
1.7.3	In situ regeneration using oxidizing agents……	42
1.7.4	Use of highly fluorinated polymers/ Current technological options……..……	44
1.8	**Summary and conclusions**……..…	47
2	**POLY(URETHANE UREA)/Ag NP COMPOSITES MEMBRANES**…...	50
2.1	**Waterborne poly(urethane urea)s**……..……	50
2.2	**Ag NP synthesis**……	55
2.3	**Experimental**…….....	59
2.3.1	Materials……	59
2.3.2	Preparation of WPUU/Ag NP composites…….	59
2.3.3	Characterizations……...	61
2.4	**Results**……..	62
2.4.1	Transmission electron microscopy (TEM) and Small Angle X-ray Scattering (SAXS)……..	62
2.4.2	X-ray diffraction (XRD)……...…….	66
2.4.3	Infrared Spectroscopy (FTIR)……...	67

2.4.4 Thermal Stability…….……. 69
2.5 **Conclusions**…….. 71
3 **OLEFIN/PARAFFIN GAS PERMEATION**……. 72
3.1 **Introduction**……. 72
3.2 **Experimental**……... 73
3.2.1 Materials…… 73
3.2.2 Membranes preparation……. 73
3.2.2.1 Membranes based on WPUU/Ag NP……. 73
3.2.2.2 Membranes based on WPUU/$AgBF_4$…… 74
3.2.3 Gas permeation tests…….. 75
3.2.3.1 Simple gas experiments……. 75
3.2.3.2 Mixture gas experiments……... 76
3.3 **Results**…….. 76
3.3.1 Membranes based on WPUU/Ag NP……..... 76
3.3.2 Membranes based on WPUU/$AgBF_4$…… 78
3.3.2.1 Infrared Spectroscopy (FTIR)……... 78
3.3.2.2 Gas permeation…….. 81
3.4 **Conclusions**…….. 89
GENERAL CONCLUSIONS……. 90
CHALLENGES FOR FUTURE RESEARCHES……. 91
REFERENCES…… 93
APPENDIX — Brief description of the main analytical techniques used to characterize the composites materials studied in this Thesis…….. 113

INTRODUCTION

Light olefins are the principal raw material to the petrochemical industry.[1] In 2016, the global ethylene and propylene production was 146 and 99 million tons, and the expected of demand growth rate, until 2025, is 3.6%/year and 4.0%/year, respectively.[2] Steam cracking (SC) is the main industrial process to manufacture light olefins from naphtha or light alkanes.[2–5] In the petrochemical industry, SC is among the more energy intensive processes, and in 2016, the worldwide consumption has been estimated to be about 3.0×10^{15} BTU.[6,7] After pyrolysis, the separation section is the second largest energy consumption step in SC (about 7.5×10^{14} BTU).[2,5–7] The justification for this consumption is based on the cryogenic distillation of the cracked gases.[6,8,9]

Membrane processes have been proposed to save energy in the separation section by replacing or integrating with the current cryogenic distillation technology.[10–17] Membrane technology has achieved very promising results, specifically regarding the olefin/paraffin separations.[18–24] In a recent study, Lee et al.[25] identified the optimum membrane performance required to replace one typical C3 splitter. They found that a set of membrane modules with propylene permeance of 11.3 GPU (1 GPU = 1×10^{-6} cm^3 (STP)/cm^2 s cmHg) and selectivity of 68 could substitute for a typical distillation process. Since the replacement of the distillation column by membrane units with optimum performance is technically viable, the great challenge for membrane technology is to reach the suitable selectivity and permeability for the process and keep them over long-term operation. The operational conditions in which the membrane should be used are severe and can lead to performance loss along the operation.[23,24,26–28]

Among membrane technologies, the alternatives based only on the solution-diffusion mechanism are not effective enough to discriminate olefin/paraffin pairs. The similarity between the physicochemical properties of alkenes and alkanes is the main drawback that all dense-type membranes assigned to separation face.[29] The carbon molecular sieve membranes suffer the same problem since there is a tiny difference between the molecular diameter of the molecules to be separated.[15] Nevertheless, many efforts have been focused on improving separation using mixed matrix membranes by introduction of zeolites,[30,31] organic and metal−organic frameworks,[32–36] in the polymer matrix. Other works focused on carbon molecular sieve membranes[10,37,38] that are brittle, and it is difficult to scale up production.[25] To overcome these discriminative issues between the molecules, the facilitated transport of olefins has been explored, increasing simultaneously the permeance and the selectivity of the separation. The facilitated transport can be defined as a process in which chemically distinct

carrier species form complexes with a specific component in the feed stream, thereby increasing the flux of this component relative to other components.[39] The facilitated transport membranes have surpassed the upper bound of the Robeson diagram for the olefin/paraffin separation in the past few years,[22,40] demonstrating the greater potential of this technological option.

The majority of studies investigates the facilitated transport membranes using carrier agents, which bind with olefins by the π-complexion reaction.[19,41] Generally, transport membranes using silver (Ag) salts as carrier agents have been demonstrating better selectivity and permeability, when compared to passive transport membranes.[40] Despite the superior separation properties of those systems, in general, some Ag salts carrier agents do not have enough stability to keep a long-term performance separation.[28] As an attempt to solve this problem, many authors have been pointing out to carrier agents based on Ag nanoparticles (NP), as promising chemical stable carriers for facilitated transport membranes.[19,42–46]

Metal nanoparticles (NP) have been extensively exploited in the formation of polymeric nanocomposites with many functional properties. The main features added to the polymers by the addition of NP are conductivity,[47] antibacterial,[48,49] magnetic[50], and catalytic characteristics.[51] The difficulties in dealing with metal NP are their instability (due to the tendency of agglomeration caused by high free surface energy), oxidation by air, humidity, etc. By introducing NP into dielectric polymer matrices, many problems of stabilization and manipulation of metal NP are solved.[52]

Metal NP prepared by chemical processes, generally, are structures with better particle size, shape, and lower polydispersity;[53] however, it brings up additional challenges to NP synthesis. In the specific case of Ag NP synthesis, the chemical reduction in water medium is the most widely used method.[54,55] To synthesize Ag NP via chemical reduction, there are basically three elements: precursor salt, stabilizing and reducing agent. There are a variety of possible combinations involving several types of these three elements. Nevertheless, the most used and cheapest syntheses involves the use of $AgNO_3$ as precursor salt[56] and $NaBH_4$ as reducing agent.[57] Since chemical reduction is an easy method to reproduce, it is relevant when the goals is to scale-up the production of Ag NP. Stabilizers may also vary widely, depending on the system, but generally they have surfactant properties, which protect the surface of NP against agglomeration.

Membranes of waterborne poly(urethane urea)s (WPUU) have been researched as a material for gas permeation.[58–64] WPUU have internal emulsifiers in their structure, which are responsible for their dispersion stability in water, since it is prepared in aqueous medium. In water, internal emulsifier, urethane, and urea groups face the aqueous medium, while the

flexible segments, composed by more hydrophobic domains turn inwardly. In principle, the WPUU conformation in aqueous dispersion can provide the basic characteristics of a stabilizing agent for Ag NP synthesis via chemical reduction in water. Polar segments placed at the external surface of WPUU colloid particles can anchor the freshly synthesized NP, ensuring a nanoscale approximation without collision and agglomeration throughout their synthesis.[55,64] Preliminary, the possibility of using WPUU dispersion eliminates the need of an additional stabilizing agent, affording an advantage to the synthesis of Ag NP in WPUU dispersion.

Another factor to be considered is that in all works dealing with membranes for olefins facilitated transport, only commercial polymers are used as matrix for membranes.[22,26,72,73,43,65–71] The use of a versatile polymer as WPUU may be useful to achieve properties in which is necessary to make a certain modification in the formulation and consequently in the polymer structure/properties. Moreover, the material preparation in aqueous medium is eco-friendly, avoiding the use of undesirable volatile organic compounds. Therefore, the strategy of using WPUU as matrix for WPUU/Ag NP membranes applied to olefin/paraffin separation is reasonable to be proposed.

To act as carrier, Ag NP require a suitable activator agent[42–44,71,72,74,75] to polarize their surface to form a partial charge, which is responsible by the interaction with olefins.[43,76] For the experiments in this Thesis, it was chosen p-benzoquinone (p-BQ) and 1-butil-3-methilimidazolium tetrafluoroborate ($BMImBF_4$) due to the lower price of these activator agents comparing with other compounds. The concentration of Ag NP inside the polymer matrix should be higher than 30 wt% and NP should have diameters smaller than 30 nm to achieve the facilitated transport.[46]

Other alternative that literature has shown as promising is the introduction of ionic liquids (IL) to stabilize Ag^+ salts in facilitated transport membranes. Relate to this option, Ortiz et al.[22,77] developed a material with promising characteristics for the separation of light olefins/paraffins. Composite films of poly (vinylidene fluoride-co-hexafluoropropylene) (PVDF-HFP)/$BMImBF_4$–$AgBF_4$ reached C_3H_6/C_3H_8 mixture selectivity of 700 and propylene permeability of 6630 Barrer (*ca.* 55 GPU) in long-term permeation tests for 10 days. This remarkable performance motivated the use of this system ($AgBF_4$/$BMImBF_4$) in membrane of WPUU as attempt to overcome Ag^+ cation deactivation.

Therefore, the general objective of this Thesis is to investigate the gas transport behavior in WPUU membranes with Ag NP/activator and $AgBF_4$/$BMImBF_4$ systems. The specific goals of the Thesis are:

(i) to prepare WPUU/Ag NP membranes, analyze them using transmission electron microscopy (TEM), small angle scattering X-ray (SAXS), X-ray diffraction (XRD), Fourier transform infrared spectroscopy (FTIR), thermogravimetric analysis (TGA), and perform permeation tests with pure CO_2, C_2H_6, C_2H_4, and equimolar C_3H_6/C_3H_8 binary mixtures;

(ii) to prepare WPUU/$AgBF_4$ membranes, analyze them using FTIR, and test them in gas permeation experiments with equimolar C_3H_6/ C_3H_8 binary mixtures.

This manuscript is organized as follows:

Considering the potential applicability of the membrane technology for light olefins/paraffins separation, the goal of Chapter 1 is to critically review the development of facilitated transport membrane for this separation, highlighting the challenges and main drawbacks surpassed during the last decades. A comprehensive analysis of the instability/deactivation problems confronted by distinct kinds of membranes is carried out. The alkene/alkane membrane separation technology is presented describing the source of poisonous agents for the principal carrier used, i.e., the Ag^+ cation. Finally, some recent strategies are pointed out as options that try to overcome the Ag^+ deactivation by smart solutions.

Chapter 2 describes the WPUU material and the approach for Ag NP synthesis. The aim is to prepare and characterize WPUU/Ag NP membranes by TEM, SAXS, XRD, FTIR, and TGA to check the morphology of Ag NP and their influence on chemical and thermal features of WPUU.

Chapter 3 collects all gas permeation tests of the Thesis. The objective is to prepare Ag NP/activator/WPUU and $AgBF_4$/$BMImBF_4$/WPUU membranes and after investigating the gas transport behavior through these membranes. The activators used were p-Bq and $BMImBF_4$. For $AgBF_4$/$BMImBF_4$/WPUU membranes, FTIR was applied to investigate the influence of Ag^+ cation on WPUU matrix. Moreover, the FTIR results were used to correlate the polymer structure modification with gas transport behavior.

Finally, it is found the general conclusions of this Thesis and an overview of the challenges and prospects for future researches.

1 BACKGROUND AND THEORY

1.1 Production of light olefins

Light olefins are the principal raw material to the petrochemical industry. They are used as the precursor for a variety of thermoplastic polymers, synthetic rubber, and solvents. The applicability of this input ranges from the electronic devices to food and pharmaceutical products. There is no doubt that these building block molecules are needful for the majority of goods used by modern society.[1] Regarding the present scenario, the global demand for ethylene and propylene, which are the most important light olefins, has been increasing over the last decades.[78,79] In 2016, the global ethylene and propylene production were 146 and 99 million tons and expected of demand growth rate, until 2025, is 3.6%/year and 4.0%/year, respectively.[2] These numbers show the expansion trend in consumption of light olefins that is closely related to the consumption pattern of the global population over the last years.

The steam creaking (SC) is the principal process to obtain light olefins, and in the near future, probably it should be the leading technology, mainly to the production of ethylene. Nevertheless, there are other potential mature alternatives to the SC, such as the catalytic dehydrogenation of light alkanes,[80] the oxidative coupling of methane[81] and syngas-based routes (Fischer-Tropsch synthesis and methanol synthesis followed by methanol to olefins).[82] At present, all cited technologies are not economically competitive compared to the SC.[3] The main feedstock to the SC is the naphtha (*ca.* 61 %), but light alkanes, such as ethane, have been increasing their share (*ca.* 33 %) (Table 1).[2,5] Since 2008, the light alkanes market share has been growing due to the exploitation of shale gas[4] in the United State of America, as a result, the ethane price has become competitive.[3]

Table 2[5,6] shows the SC yield by feedstock, and it can be seen that propylene is a by-product of SC and should be produced from additional processes to reach the current demand. Generally, propylene also is manufactured as a by-product from fluid catalytic crackers (FCC) and produced in smaller scale from propane dehydrogenation process, and metathesis (Figure 1).[2,3,83]In the case of FCC, since the propylene demand is rising, most refineries tries to maximize the propylene production modifying the FCC process to reach the gap in the market.[83]

Table 1 – Data used to calculate the feedstock share for the steam cracker in 2016

Feedstock	Global ethylene production by feedstock (Mt)[2]	Yield by weight of feedstock (wt%)[5]	Feedstock(Mt)	FeedstockShare (%)
Naphtha	63	30	210	61
Ethane	52	80	65	19
Propane	13	45	29	8
Butane	7	37	19	6
Gas oil	5	25	20	6
Coal	3	–	–	–
Other	2	–	–	–

Note: We considered all ethylene was produced by the steam cracker.
Source: The author, 2018.

Table 2 – Steam cracker yields for ethane and naphtha

	Yield by weight of feedstock (wt%)		
Feedstock	**Ethylene**	**Propylene**	**Butadiene**
Ethane	80-84	1.0 -1.6	1.0-1.4
Naphtha	29-34	13-16	4-5

Source: The author, 2018.

Figure 1 – Production of propylene by process

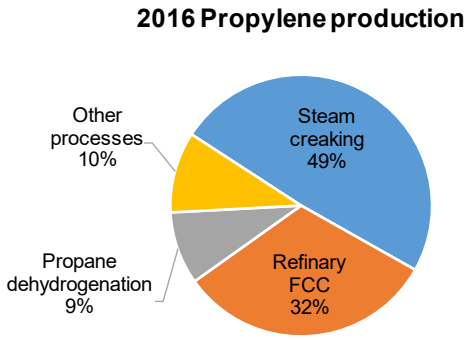

Source: The author, 2018.

1.2 Energy consumption of steam creaking process

Regarding the petrochemical industry, SC is the most energy-intensive process, and, in 2016, it consumed *ca.* 3.0×10^{15} BTU.[6,7] In the petrochemical facilities, the SC unit is divided into 3 sections (Table 3). Most of the energy is applied in the pyrolysis section where the cracking of the feedstock takes place. Further, there is a compression section followed by a cleanup to remove acid gases (carbon dioxide and hydrogen sulfide) and water. Finally, the cracked gases enter in the separation section to fractionation/purification of the output products. After the pyrolysis, the separation section is the second large energy consumption step in SC.

The justification for this consumption is based on the cryogenic distillation of the cracked gases. Roughly, the cryogenic distillation consists on decreasing the gas stream temperature by a complex web of heat exchangers and compressors. Next, the cryogenic stream is fractioned by different distillation/separation columns in the desired final products of the SC.[6,8,9]

Table 3 – Sections of SC process and the energy involved.

Feedstock	Typical energy consumption (GJ/t of ethylene produced)[5,7]	The share (%) of energy consumption by SC sections		
		Pyrolysis	Compression	Separation
Ethane	17-19	47	22	31
Naphtha	23-27	65	15	20

Source: The author, 2018.

Many efforts have been undertaken to save energy in the different section of the SC. In the past years, the typical efficiency improvement rate in the SC units was *ca.* 1.7% per year.[84] In the pyrolysis and the compression section, the attention is devoted to increase the efficiency of the furnace, compressors and other related equipment. The operational condition of the cracking process also has been studied according to the different raw material looking for better energy yield of the pyrolysis.[8] In the separation section, alternative technologies, such as membrane processes and reactive absorption, have been proposed to replace or integrate with the current cryogenic distillation technology.[10–12] The reactive absorption takes places in large absorption/stripping columns containing silver or cooper salts.[13,85,86] In addition, other adsorbent materials such as zeolites,[87–89] porous organic frameworks,[90–92] and metal−organic frameworks (MOFs)[93–95] could also be applied. The membrane separation, which is well known for its energetic efficiency in gas separation,[14,15] uses polymer membranes,[29,96] mixed matrix membrane,[25,97,98] facilitated transport membranes[18–21] and carbon molecular sieves[37,38] for the separation. The membrane technology has been achieving the most promising results related to cracked gases separation, specifically regarding the olefin/paraffin separation.[22–24] The reactive absorption is also under development however in an earlier stage compared to the membranes.[13,99]

According to our estimate (Table 4), in 2016, the energy consumption in the separation processes, inside the SC unit, was *ca.* 7.5×10^{14} BTU.[2,5–7] Most of this energy is destined to the refrigeration system of the SC separation section that is used to achieve the cryogenic temperatures in the cracked gases stream.[6,8] These temperatures are reached by using a chilling

system integrated with compressors operating under high pressure (15-30 bar).[6] The refrigerant fluids should cover a broad range of temperature, -150 ºC to +10 ºC, to be applied in distinct parts of the chilling train and in the fractionation towers.[8] The fractionation processes take place in towers generically called demethanizer, deethanizer, depropanizer, debutanizer, C2 splitter, and C3 splitter.[8,25] These fractionation equipment types operate using distinct temperature and pressure conditions to separate the desired compounds. Related to the C2 and C3 splitters, which are distillation columns, the challenging task is separate compounds with similar boiling points. In C2 splitter, the ethylene and ethane ($\Delta T_{ethylene/ethane}$ = 15,2 ºC at 1atm)[100] are separated using a reflux rate of *ca.* 4, a column with 90-125 trays, and pressure operating of 17-28 bar. In C3 splitter, the propylene and propane ($\Delta T_{propylene/propane}$ = 5,7 ºC at 1atm)[100] are separated using a reflux rate of *ca.* 20, a column with 150-230 trays, and pressure operating of 18 bar.[8] In the case of C3 splitter, the high number of separation stages normally requires two connected distillation columns that raises up the capital cost investment related to this equipment type. These features make the C2 and C3 separations one of the most energy intense processes inside the SC separation section.[25]

Table 4 – Data used to calculate the total energy consumption of the steam cracker and the SC separation section in 2016

Feedstock	**Global ethylene production by feedstock (Mt)**	**Typical energy consumption (GJ/t of ethylene produced)**[6,7]	**Total energy consumption (10^{15} BTU)**	**Total energy consumption in separation section of steam cracker (10^{14} BTU)**
Light[a]	72	17-19	1.2-1.3	3.6-4.0
Heavy[b]	68	23-27	1.5-1.7	3.0-3.5
Total	140	–	2.6-3.0	6.6-7.5

Note: a – ethane, propane and butane; b – naphtha and gas oil. We assumed the propane, butane SC energy consumption equal to the ethane and the gas oil equal to the naphtha. We considered the energy consumption of SC separation process *ca*. 31% of the total energy consumption for ethane, propane and butane, and ca. 20% for naphtha and gas oil.
Source: The author, 2018.

As one of the advanced SC separation technologies, the membrane technology is thought to replace or integrate the C2 and C3 splitters. The estimate is that *ca.* 8% of all energy used in SC could be saved if membranes are applied just for olefin/paraffin separations.[6] The use of membranes in this separation is considered one of the most important applicability of this technology in the world since it could save a large amount of energy. Consequently, membrane technology could contribute with the lowering of gas emissions and pollution levels.[101] In a recent study, Lee et al.[25] identified the minimum required membrane performance

to replace one typical C3 splitter. They found that a membrane module with propylene permeance of 11.3 GPU (1GPU=1 × 10^{-6} cm^3 (STP)/cm^2 s cmHg) and selectivity of 68 could substitute a typical distillation process. Since it is viable the replacement of the distillation by membranes with this minimum performance, the great challenge to the membrane technology is reach the suitable selectivity and permeability for the process and keep them over long-term operation. The operational conditions in which the membrane should be used is severe and can lead to the performance loss along the operation. Regular substitutions due to the incapability to withstand the real operation condition is a drawback to a feasible application of the membrane separation. Therefore, many works try to figure out how to make the membranes more permeable and selective to the olefins, besides finding a way to keep the performance in long-term operation.[23,24,26–28]

Among membranes technologies, the alternatives based only on a solution-diffusion transport have had some difficulties to discriminate the olefin/paraffin pairs. The similarity between the physical and chemical properties of alkenes and alkanes is the main drawback to all dense-type membranes assigned to the separation.[29] The carbon molecular sieve membranes suffer of the same problem, since the difference between the molecular diameter of the molecules to be separated is tiny.[15] Nevertheless, many efforts have been developed trying to improve the separation using mixed matrix membrane by the introduction of zeolites,[30,31] organic and metal−organic frameworks[32–36] in the polymer matrix. Other works try to develop carbon molecular sieve membranes[10,37,38] that are brittle and difficult to scale-up the production.[25] To overcome these discriminative problems between the molecules, the facilitated transport of olefins has been explored, increasing simultaneously the permeance and the selectivity of the separation. The facilitated transport membranes have surpassed the upper bound of Robeson diagram for the olefin/paraffin separation in the last years,[22,40] demonstrating the greater potential of this technology option.

1.3 Applicability of membrane technology for olefin/paraffin separations

The gas separation technology using membranes is already industrially applied in cases such as the separation of nitrogen from air, CO_2 removal from natural gas, and the hydrogen recovery from steam refinery.[14,102] It should not sound strange the use of this technology in the light olefin/paraffin separations in which could save considerable energy compared to the current cryogenic distillation process. However, the best available polymer materials, which are used in the saturated/unsaturated hydrocarbon separation, under industrial conditions, only

present a real selectivity of 3-4. To be used in steam creaking plants in the replacement or integration with the cryogenic distillation, a higher selectivity should be achieved.[28,103] Besides the steam creaking plants, which is the main target application, there are other two potential areas where membrane technology could be applied for olefin/paraffin separations. As shown in the Figure 1, roughly, 1/3 of the propylene production is from FCC processes. In this case, the olefin/paraffin separation membranes should be used in the recovery of propylene from FCC off-gas streams.[83,84,103,104]

The membrane technology could also be applied in alkene/alkane separation from vent streams of some kinds of petrochemical reactors. For instance, in the production of polypropylene, the propylene monomer has a small amount of propane (for propylene polymer grade, *ca.* 0.5%[105]) that gradually builds up in the reactional system. The unreacted propane reaches concentrations of 20-30 vol.% inside the system. To control the accumulation of propane, there is a continuous purged flux from the process that usually is flared. For each mole of purged propane, 2-3 mol of propylene is lost together resulting in a 1-2% of the total plant propylene feed. The membrane separation is desired technology to be installed before the flare line avoiding the waste of propylene. This application is very attractive because selectivities of 3-5 could be suitable to the propylene recycling process. In addition, the purged stream usually has low level of sulfur and acetylene compounds resulting in a milder condition operation and lower performance need (selectivity and permeance) than in steam creaking process.[106] Even individually, the small-scale separations of olefins from reactor vent streams when taken together, could represent a huge opportunity of saving money and a way to introduce commercial olefin/paraffin membrane units. Maybe, this market niche can represent a previous favorable step before the attempt to replace the distillation in the steam cracking process or in the FCC off-gas streams that involves huge challenges to be overcome.[103,106,107]

1.4 Solution-diffusion mechanism

The driving force that motivates gas molecules to cross a dense membrane can be expressed by the difference in partial pressure between the feed and the permeate side (Figure 2).[108] Under the process conditions, this partial pressure difference (concentration difference) represents the chemical potential gradient that is responsible for the gas flow. Initially, the gases are solubilized (sorption) in the membrane, afterward the diffusion of the molecules through the membrane takes place; and on the lower partial pressure side, desorption occurs. These steps are known as solution-diffusion mechanism.[108]

Figure 2 – Representation of solution-diffusion mechanism

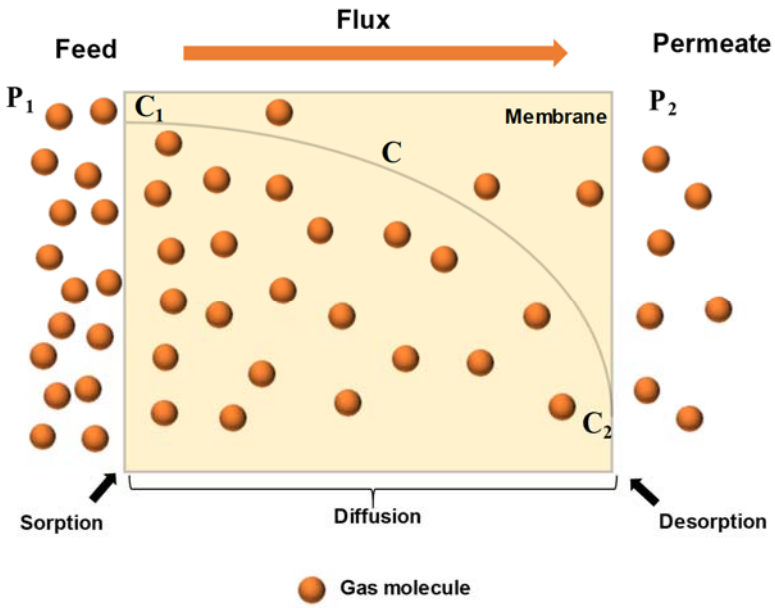

Source: The author, 2018.

Sorption is the thermodynamic step of permeation.[108] The gas molecules concentration C_i in the membrane is in thermodynamic equilibrium with the molecules of that gas in the gas phase under partial pressure p_i. In the mathematical modeling of this equilibrium, an approach is adopted that involves the fugacity coefficient for the gas phase (ideal gas as a reference state) and activity coefficient for the polymer phase (ideal solution as a reference state). By manipulating mathematical relationships, it is possible to obtain the definition of the coefficient of sorption or solubility S_i, which is approximately independent of the concentration. In the mathematical approach of this equilibrium, on both sides of the membrane (feed and permeate), the coefficient S_i is considered equal in both interfaces of gas with the polymer. Thus, a linear relationship can be obtained between S_i and p_i, as expressed in Equation (1). The sorption parameter is influenced mainly by the balance of three effects: (i) condensability of the gas molecules, (ii) gas / polymer interactions; and (iii) segmental mobility of the polymer.[109]

$$C_i = S_i \, p_i \tag{1}$$

Taken as example the light olefins/paraffins, the light paraffins are more condensable than olefins, so they have a higher coefficient of solubility compared to olefins.[109,110] The selectivity provided by the sorption coefficient is not enough for a desired separation. To be more selective towards the olefins, the polymer necessarily needs to make preferential

interaction with those molecules. Therefore, polymers that present groups capable (polar groups as polyether)[110,111] of performing this interaction may be considered as potential material for the separation of light olefins/paraffins.

Diffusion is the kinetic step of permeation that is related to the movement of gas molecules across the membrane.[108] The total flux through the dense film thickness is represented only by the diffusive flux J_i , given by *Fick's law*, in which D_i is the gas diffusion coefficient in the polymer. By integrating the *Fick's law* expression along the membrane thickness δ , the following Equation (2) is obtained:

$$J_i = \frac{D_i\,(C_i^f - C_i^p)}{\delta} \tag{2}$$

In Equation (2), the superscripts f and p refer to the feed side and the permeate side, respectively. The diffusion coefficient D is determined mainly by the following effects: (i) size and shape of the permeant molecule, (ii) gas interaction inside the polymer matrix; and (iii) plasticizing effects of the permeant on the polymer caused by the high volumetric fraction of the gas in the membrane.[112] The differentiation between light olefins and paraffins in the diffusional step is very inexpressive, since these molecules have very similar sizes. Replacing Equation (1) in (2), it is possible to express J_i as Equation (3), in which P_i is the gas permeability in the membrane. P_i can be defined as the product between D_i and S_i, $\mathrm{P}_i = \mathrm{D}_i\mathrm{S}_i$. The ratio P_i/δ is also known as gas permeance and it shows the gas flux by the partial pressure difference ($\mathrm{J}_i/\Delta\, p_i$), i.e., reflects the productivity of the membrane in the separation process.

$$J_i = \frac{\mathrm{P}_i}{\delta}\left(p_i^f - p_i^p\right) \tag{3}$$

Dense membranes for gas separation are generally synthesized from polymeric material. Preliminary information regarding the affinity of a such polymeric membrane for a specific gas is provided by the ideal selectivity $\alpha_{i/j}^{id}$ that is calculated according to Equation (4), with P_i and P_j as permeability values of i and j gases, respectively. The $\alpha_{i/j}^{id}$ is different from the real selectivity $\alpha_{i/j}$ (Equation (5)) that represents the separation factor of the membrane when the operation involves a gas mixture. This factor is calculated by the quotient of molar fractions (y) ratios of two key components of the mixture in the permeate and feed stream.

$$\alpha_{i/j}^{id} = \frac{\mathrm{P}_i}{\mathrm{P}_j} \tag{4}$$

$$\alpha_{i/j} = \frac{(y_i^p / y_j^p)}{(y_i^f / y_j^f)} \tag{5}$$

The practical differences between ideal and real selectivities are the effects caused by permeation of a gas mixture. As the gas permeates through the polymer, the volumetric fraction thereof increases inside polymer matrix.[109] Thereafter, the higher concentration of gas molecules in the membrane leads to an segmental mobility increase of the polymer chains. This phenomenon significantly alters the diffusion coefficient and is best known as plasticization.[112]

The polymeric materials used for gas permeation can exhibit vitreous or elastomeric characteristics. Vitreous and elastomeric polymers have different behaviors related to the permeability of different gas molecules. Vitreous polymers discriminate molecules mostly in the diffusion step. Larger molecules have more difficulty to move through the pre-existing vacancies inside the vitreous polymer matrixes, which have lower segmental mobility. Therefore, in general, the larger the molecule, the lower the permeability in this type of polymer.[109]

In elastomeric polymers, the dominant step is sorption. The more condensable the gas molecules, the easier the solubilization in the polymer matrixes. This usually means that the larger molecules, which are more condensable, have greater permeability in this type of polymer. Elastomers have higher segmental mobility and consequently, higher probability of local segmental density fluctuation. For this reason, the activation energy for a diffusional jump in elastomeric polymers is considered lower and not much influenced by the size of the penetrating molecule, making the diffusional step less selective.[109]

The use of block copolymers that can share vitreous and elastomeric features in their polymer backbone may be one of the alternatives to reach the best performance regarding trade-off between selectivity and permeability. Tailormade block copolymers can also provide "virtual" crosslinking that may improve the plasticization resistance of membrane during the gas separation processes.[41,70,113,114] For instance, polyurethanes[58,62,115,116] and poly(ether-block-amide) (Pebax®)[117–120] have this quality, since they present regions with elastomeric and vitreous characteristics. Depending on the formulation, suitable features can be achieved for specific uses.

1.5 Facilitated transport membranes for olefin/paraffin separation

The development of new membranes based on polymeric materials or the modification of polymer structures that provide suitable selectivities for the olefin/paraffin separation has been largely investigated.[121–123] As the polymer films have become more selective to the olefins, they lose productivity due to the trade-off between selectivity and permeation flux, therefore, leading to the technical unfeasibility of the separation process.[15,124] Films where mass transport is based only on the solution-diffusion mechanism have shown, as best results, ideal selectivity of 27 (C_3H_6/C_3H_8) and 0.8 Barrer of propylene permeability.[123,124] These values are significantly lower than the performance reported for facilitated transport films that have shown mixture selectivities (C_2H_4/C_2H_6) higher than 100.[40]

The facilitated transport mechanism, when it takes place, plays in a complementary mechanism to the solution-diffusion transport. In the facilitated transport, a carrier agent interacts reversibly and selectively with the target molecule, that results in the increase in the driving force for the permeation flux of target molecule, and therefore, the permeate is enriched. This kind of transport is not accessible to the inert molecules that are not able to interact with the carrier agent, so that their concentration decreases in the permeate side (Figure 3). Thus, the facilitated transport membrane has a superior selectivity compared to the passive (solution-diffusion) membrane.[27,40,125,126] The carriers need to be effectively dispersed over the natural diffusional path of the gases (in the direction of the concentration gradient) and be present at a concentration high enough for transport activation. Furthermore, the carriers also need to be ready to the interaction with the target molecules inside the membrane, i.e., the carriers should be not poisoned.[42,43] In addition, the facilitated transport has the potential to save energy in separation processes since it improves simultaneously selectivity and permeability values of the membranes, differently of the passive transport.[40]

A useful way to describe or classify the facilitated transport membranes is to evaluate them regarding carrier mobility. In general, there are three possible classifications:[19] (i) mobile carrier membranes, in which the carriers move freely through diffusional path; (ii) semi-mobile carrier membranes, in which the carriers also move freely, however it is restrict to the local segmental density fluctuation that represents a much higher activation cost energy for diffusion than that required in mobile carrier membranes; and (iii) fixed-site carrier membranes, in which carriers are chemically bonded to the polymer segments and can only vibrate within a limited nanospace.

Figure 3 – Representation of the facilitated transport mechanism in membranes

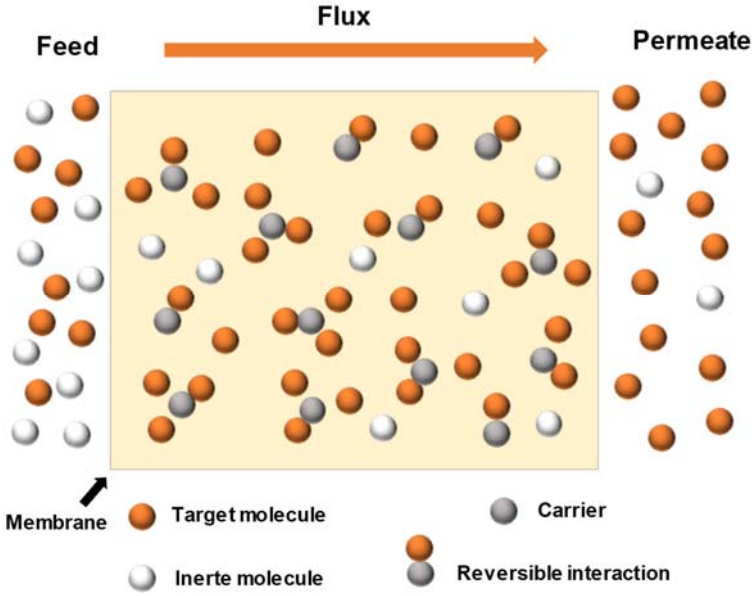

Source: The author, 2018.

In mobile carrier membranes, the carriers move like a boat navigating between both sides of the membrane. A low viscosity of the medium is required to the transport in this kind of membrane. Generally, the main component of the medium whereby the carriers move are aqueous solutions or compounds with low viscosity as ionic liquids. Therefore, mobile carrier membranes are usually liquid membranes and they need a support to be used in most membrane separations.[19]

Regarding semi-mobile and fixed carrier membranes, polymeric materials are used as host matrix. Cussler *et al.*[127] proposed the jump mechanism for transport within the fixed-site carrier membranes, in which the target molecules cross the membrane by jumps from carrier to carrier. The idea of the solute acting as *Tarzan* came from the early XX century and was the inspiration for the jumping mechanism elaborated in 1989. The thinking of Cussler et al.[127] was that the carriers placed in chain, from a determined concentration inside the polymer matrix could achieve facilitated diffusion. Since carriers are covalently bounded to the matrix or fixed in a nanospace, the solution-diffusion mechanism is limited compared to the mobile carrier membranes. The distinct features between mobile carrier and fixed-site carrier membranes can be combined to generate an intermediate behavior in semi-mobile carrier membranes, in which the vehicular and the jumping mechanism can take place simultaneously to some extent.[19,127]

1.5.1 Chemical interaction for olefin separation: Olefin π complexation

The formation of complexes between some metals and the double bond of olefins has been well known for a long time. Nevertheless, only in 1827, the first metal−olefin complex was identified. The referred compound was platinum(II)-ethene, which was known as the Zeise complex. In the beginning of the 20th century, the first ideas of using silver(I) (Ag^+) salts in olefin absorption systems arose. However, only in 1951, Dewar[128] gave a satisfactory explanation to the interaction mechanism between the ethene and Ag+. Shortly after, Chatt and Duncanson[129] advanced the Dewar`s explanation presenting the interaction mechanism called π-bond complexation.[13] This complexation takes places when the bonding orbital of the olefin donate electronic density to the empty outermost orbital of the Ag^+ (5s) making a σ bond. The strength of this bond depends on the magnitude of the metal (*e.g.* silver, cooper, and gold) positive charge. The second bond formed is a π bond, resulting from the backdonation of the electronic density from the outermost atomic orbital 4d, which is electronic completed, to the π*- antibonding molecular orbital of the olefin (Figure 4).[130,131]

In 1960, Scholander[132] published a pioneer work that explored the facilitated transport in liquid membranes containing hemoglobin as a carrier agent for oxygen transport. Thereafter, works that described membranes of facilitated transport have grown for several applications.[109] Over the following decades to the present day, the facilitated transport mechanism has attracted great attention of many researchers due to the separation potential compared to the simple mechanism of passive transport.

Practically, the development of facilitated transport membranes for light olefin/paraffin separations have been based on the feature of the reversible interaction among olefins and some transition metals, especially silver, copper, and gold. Additionally, the π complexation should be strong enough to favor the interaction between the metal and at the same time allow the complexation reversibility under the appropriate operational conditions. Among transition metals, silver has one singularity related to π complexation. The silver electro- negativity is 2.2, in the range of 1.6−2.3, in which the reversible complexation can take place.[133] In addition, the silver salts that have been applied in facilitated transport of olefins have the lowest lattice energies compared to other metallic salts that can be also used for this goal. A salt with low lattice energy favors the solubility of the metal cation, and hence, it also favors its availability for the interaction with the olefin.[27,134] Owing to these features, silver is the metal most widely used in the preparation of facilitated transport membranes for olefin/ paraffin separation. Nevertheless, the use of copper is the second option due to the lower price of this metal.[25] The price is a critical issue when the final goal is to scale up the production of this kind of membrane, and therefore, it should be considered. However, up to now, the use of the Cu^+ cation has not

proved to be a feasible option for the facilitated transport of olefins due to the stability issues of this cation against oxidizing agents,[135] although some promising studies have recently been published about the use of ionic liquids as solvents that stabilize cuprous ions.[136]

Figure 4 – π complexation between olefin and Ag^+

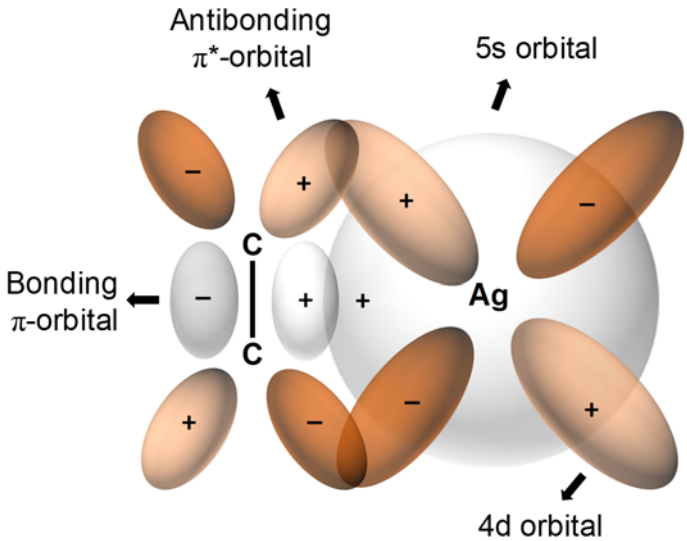

Source: The author, 2018.

On the basis of mainly the use of silver salts, the principal carrier, facilitated transport membranes for olefin/paraffin separations started to be developed initially as supported liquid membranes. After, in the search for superior mechanical stability, ion exchange and electrolyte membranes were applied to the olefin/paraffin separations.

1.5.2 Supported liquid membrane

In 1973, Steigelmann and Hughes[137], working in the Standard Oil Company, started to develop films of cellulose acetate with silver nitrate solution in the pores of the membrane (support) (Figure 5). The solution is held in the pores of the support by capillary forces. The best initial result achieved for mixture selectivity (C_2H_4/C_2H_6) was *ca* 1280 and a mixture permeance of 30 GPU. Motivated by the preliminary results, they have developed these films for more than 10 years.[138] However, spite of all efforts, they have not had success in the commercialization of this technology. The main problem found by them was the poor stability of the Ag^+ solution in the membrane pores. During the separation process, the solution was gradually swept out from the pores due to the dragging effect of the gas stream, dropping the selectivity of the process. To solve this problem, some subsequent works[27,139–142] have focused

on improving the stability of the solutions inside the pores of the membranes. However, the inherent instability of the supported liquid membranes continues to be a limiting feature in the commercial application of this membrane configuration.

Common performances of supported liquid membranes show selectivity values (α) ranging from 100 (α of C_3H_6/C_3H_8 using triethylene glycol/$AgBF_4$ 43 wt.% with humidified feed stream)[139] to 1000 (α of C_2H_4/C_2H_6 using $AgNO_3$ 4 M with humidified feed stream)[143] and permeances from 4 to 27 GPU of olefin, respectively. High permeances are achieved due to low mass transport resistance through liquid medium. The use of humidified feed stream is required to avoid the drying of solution held in support pores. The support can be prepared of microporous membranes made of cellulose, polyvinilydene diflouride (PVDF), and polytetrafluoroethylene (PTFE).[139,143–145] Indeed, the disadvantage for this membrane configuration are the real risks of dragging out the carrier solution from support pores.

Figure 5 – Supported liquid membrane

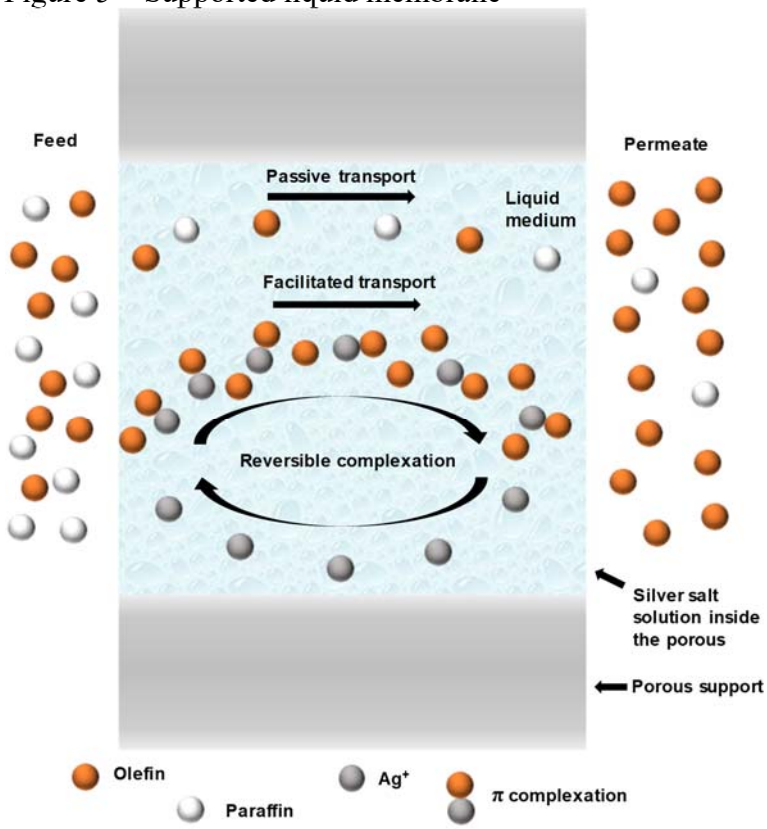

Source: The author, 2018.

1.5.3 Ion exchange membranes

In the 1980s, to solve the problems with the supported liquid membranes resulting from the Ag^+ solution sweeping out by the passage of the gas stream, LeBlanc and coworkes[146]

proposed the use of ion-exchange membranes. From this work, several other groups started to research this kind of strategy.[18,147–153] The ion-exchange membranes are generally prepared by the addition of the silver salt to the membrane, which is formed by a polymer functionalized with an acid group, (*e.g.* sulfonic acid group) able to exchange H^+ for the Ag^+. To achieve the ion-exchange, the polymer should be immersed in the Ag^+ solution or other metallic salt solution. Next, the membrane should be humidified. Without water, the Ag^+ ions are so strongly attached to the anionic sites in the membrane that makes very difficult the interaction with the olefin (Figure 6). Working with humidified feed streams, several interesting works have been reported in literature. For instance, Eriksen et al.[147] applied Nafion (N-117), which was pre swollen in glycerine and soaked in aqueous $AgBF_4$ 6 M, for separation of C_2H_4/C_2H_6 (1:1 molar ratio) humidified stream. The membrane provided a selectivity of 1930 and C_2H_4 permeability of 26,800 Barrer or *ca.* 83 GPU.

Figure 6 – Ion-exchange membranes

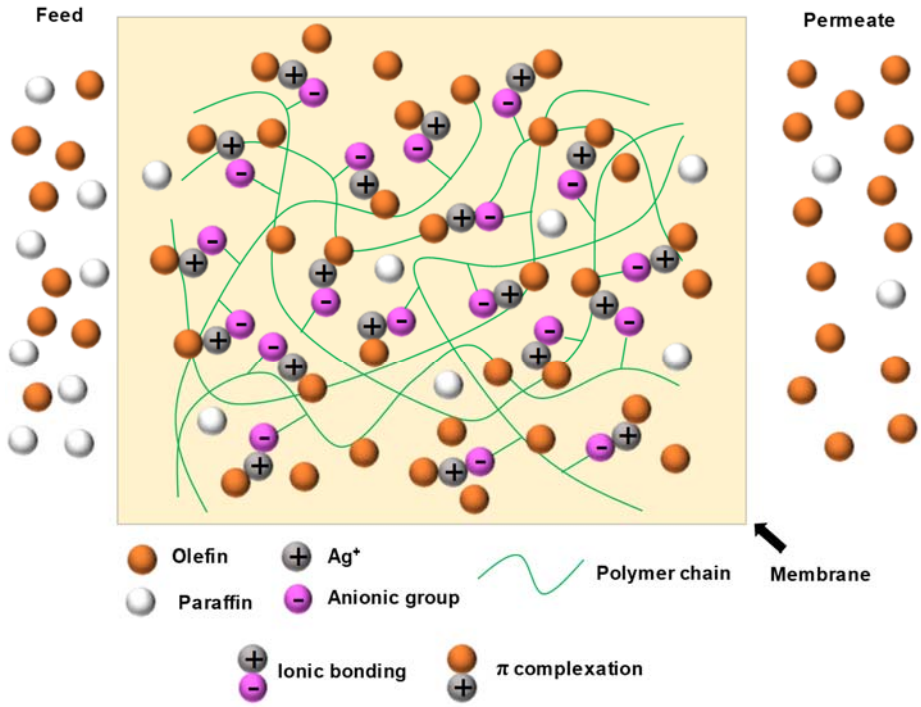

Source: The author, 2018.

As the carrier agent cannot be easily swept out from the membrane by the gas streams, the ion-exchange membranes have a vast advantage compared to supported liquid membranes. Despite their advantages, ion-exchange membranes formed by an ion-exchange polymer are usually more expensive and the required humidification is not desirable because it requires an additional operation step aimed at drying the outlet gas streams from the membrane unit.[27,28]

For this kind of membrane configuration, olefin/paraffin selectivity values between 290 and 1900, and olefin permeances ranging from 5 GPU to 83 GPU have been reported (always with humidified feed streams). The main polymeric materials used as matrix for ion-exchange membranes are Nafion and sulfonated polyphenyleneoxide.[146,147]

1.5.4 Electrolyte membranes

During the 1990s and 2000s, to overcome the problems originated from the humidification dependence of the ion-exchange membranes, the development of dense materials denominated as polymer electrolyte membranes took place.[20,154–156] Among others, the research groups of Ingo Pinnau[155,157–159] and Yong Soo Kang[69,156,160–162] stood out during the past few years. Pinnau and Toy[155] reported that it was possible to dissolve silver salts in a hydrophilic polymer with polar functional groups able to coordinate with Ag^+ ion, *e.g.* polyether. In this kind of membrane, the facilitated transport was developed without humidification of the flowing gas, which represented a great achievement compared to the ion-exchange membranes. Kang et al.[40,126,134,156,163,164] followed this method and dissolved silver salts in others polar polymer matrices as poly(2-ethyl-2-oxazoline) (POZ), polyvinylpyrrolidone (PVP) and poly(styrene-b-butadiene-b-styrene) (SBS). The results obtained with polymer electrolyte materials have by far exceeded the previous results of supported liquid and ion-exchange membranes. In 2006, the Kang`s group,[40] using the polymer electrolyte membranes with different silver salts and polymers, was able to surpass the upper bound of Robeson diagram with selectivities and permeabilities never achieved before. For instance, the ideal separation factor (pure gas permeation) of propylene/propane was above 10,000 with 45 GPU of propylene permeance.[134] In the permeation of gas mixtures, the selectivity dropped to 40–60 due to the plasticization effect that occurred in the membranes.[126]

Inside the polymer matrix, the Ag^+ cations can be arranged as free ions, ion pairs or higher order aggregates.[165] In this context, the term "free ions" should be understood as the Ag^+ cations dissolved in the polymer matrix. The best way for the salt to be in the membrane is in the form of free ion, because the silver is more available to the interaction with the olefin.[69,165–167] To reach the desired amount of free ions in the electrolyte membrane, normally, the polymer should have suitable functional groups (*e.g.* ether, amide, lactam, ester, alcohol and aromatic or aliphatic double bond) to interact with the Ag^+ cations (Figure 7a). Polymers like poly(2-ethyl-2-oxazoline) (POZ), poly(ethylene oxide) (PEO), polyvinylpyrrolidone (PVP), polymethacrylates (PMA), poly(vinyl alcohol) (PVA), poly(styrene-b-butadiene-b-styrene)

(SBS), poly(ethylene phthalate) (PEP),[40,126,134,156,163,164] polyurethanes (PU) based on polyether or polyester[21,70,168,169] and poly(ether-block-amide) (best known under the trademark Pebax®)[28,117,119] are used as suitable polymer matrix to maintain the dissolution of the silver salts in solid electrolyte membranes. The lower lattice energy of the salt is also crucial in this point to provide an easier way to dissolve the compound. Regarding this aspect, $AgBF_4$ is the most widely used salt due to its lowest lattice energy among ordinary silver salts for this purpose.[27,134] At this point, in an attempt to increase the degree of salt dissociation inside the polymer electrolytes, a couple of investigations have proposed the addition of asparagine[170] in the POZ/$AgBF_4$ membranes and the use of a mixture of silver salts[171,172] to improve the salt dissociation inside the polymer matrix.

Nevertheless, the interaction among the polymer functional group and the Ag^+ salt may cause the reduction of Ag^+ cation to Ag^0 metallic. Over the time, the Ag^0 growth and agglomeration cause the formation of some defects or holes at the interface between the metal particle and the polymer chains. Without discrimination, the gases can easily pass through this path with lower mass transport resistance that leads to selectivity loss in long-term permeation experiments.[26] Trying to solve this problem, several works have investigated solutions to overcome this drawback. In 2001, Jose et al.[173] retarded the formation of Ag^0 by incorporating phthalates to the membranes of PVP/$AgBF_4$ (Table 5). The stabilization of Ag^+ cation is due to the strong interaction between the carbonyl groups of phthalates and the Ag^+ that plays a key factor in slowing down the reduction induced by the lactam group of PVP. This was the pioneer work that started to report long-term experiments regarding the stability of polymer membranes containing silver salts. In attempt to avoid the Ag^0 growth and agglomeration, Park et al.[65] added a non-ionic surfactant (*n*-octyl β-D-glucopyranoside (8G1)) to the same kind of membrane to provide a steric hindrance effect hampering the metal particles coalescence. The protective layer onto the surface of formed silver particles was responsible to maintain the stability of membrane performance for 30 days (Table 5). However, the reduction problems were not solved by this strategy.

The reduction of Ag^+ by polymers like POZ normally results in an increase of H^+ ion concentration in the medium.[174] This is possible because the membrane contained a small amount of water favored by the hygroscopicity of salts like $AgBF_4$.[175] To suppress the Ag^+ reduction process, Kim et al.[161] proposed the introduction of HBF_4 in POZ/$AgBF_4$ membranes. The goal was to shift the equilibrium of the reduction reaction toward the regeneration of Ag^+, preventing the formation of metallic silver. To investigate this proposal, they performed permeation tests under UV irradiation. As a result, it was found that tiny amounts of HBF_4

could indeed suppress the reduction of Ag^+. A POZ/$AgBF_4$ membrane with the molar ratio of 1[carbonyl oxygen]:1[Ag^+] exhibited a selectivity of *ca.* 100 (50:50 vol.% of C_2H_4/C_2H_6) but, after 4 h under UV irradiation, the selectivity dropped to 1. When HBF_4 was introduced in the membrane with the molar ration of 1[carbonyl oxygen]:1[Ag^+]:0.2[HBF_4], the selectivity was maintained in the same initial value after 4 h under UV irradiation, thus having suppressed the Ag^+ reduction process inside the material. Although this procedure has been effective in laboratory studies, it seems an alternative difficult to implement on a large scale.

Figure 7 – Interaction between the functional groups of POZ with the Ag^+

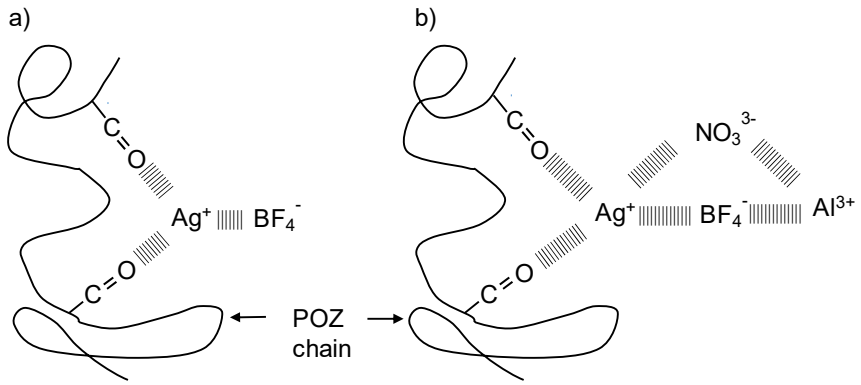

Legend: a) Interaction between the functional groups of POZ (amide C=O) with the Ag^+ from $AgBF_4$ and b) the mutual interaction between the Ag^+/NO_3^- and Al^{3+}/BF_4^- that weakens the former interaction between the C=O group of polymer.
Source: The author, 2018.

On the other hand, Kang et al.[67] interestingly suggested the introduction of $Al(NO_3)_3$ in POZ/$AgBF_4$ membranes (Table 5) to suppress Ag^+ ion reduction. The function of $Al(NO_3)_3$ is to weaken the interaction between the functional group of the polymer and the Ag^+ due to the favorable electrostatic interaction between Ag^+ and NO_3^-.[176,177] The mutual interaction between the ions, i.e. Ag^+/NO_3^- and Al^{3+}/BF_4^-, is responsible for changing the chemical environment of the Ag^+. Compared to the neat POZ/$AgBF_4$, the presence of $Al(NO_3)_3$ decreases the binding energy of the valence electron in the silver atom, which is verified by X-ray photoelectron spectroscopy (XPS) analysis. By modifying the electronic density of the silver atom, it is possible to adjust the intensity of the interaction between the Ag^+ and polymer functional group, reducing the oxidative power of the Ag^+ (Figure 7b). Using this strategy, it was possible to maintain the selectivity of the membrane for 14 days in long-term permeation tests.[67]

Table 5 – Results of long-term permeation tests of various electrolyte membranes

Polymer	Carrier/ stabilizer Fraction (%)	Separation performance (days)	Selectivity[c]	Mixed gas permeance (GPU)	Olefin purity (mol%)	Reference
Electrolyte membranes of polar matrix						
PVP	$AgBF_4$/DOP 50.0[a*]/2.0[b*]	4.2	160	7.5	99.4	In 2001, Jose et al.[173]
PVP	$AgBF_4$/DPP 50.0[a*]/2.0[b*]	4.2	135	10	99.3	In 2001, Jose et al.[173]
PVP	$AgBF_4$/DBP 50.0[a*]/2.0[b*]	4.2	85	9	98.8	In 2001, Jose et al.[173]
PVP	$AgBF_4$/8G1 49.8/0.5[a]	30	50	34	98.0	In 2003, Park *et al.*[65]
PVP	$AgBF_4$/8G1 49.9/0.2[a]	30	60	34	98.4	In 2003, Park *et al.*[65]
PEP	$AgNO_3$ 50.0[a]	7	16.2	5.4	94.2	In 2006, Kang et al.[66]
POZ	$AgBF_4$/ $Al(NO_3)_3$* 47.6/4.8[a]	14	21	4.8	95.5	In 2013, Kang et al.[67]
PEO	$AgBF_4$/ $Al(NO_3)_3$* 49.9/0.2[a]	10	10	20	90.9	In 2015, Song et al.[68]
PVP	$AgCF_3SO_3$/ $Al(NO_3)_3$* 49.9/0.2[a]	4	5	0.5	83.3	In 2015, Sung et al.[176]
PVP	$AgCF_3SO_3$/ $Al(NO_3)_3$*/ $BMImBF_4$ 43.6/4.1/8.7[a]	4	9	0.5	90.0	In 2016, Park and Kang[178]
PVA	$AgBF_4$/ $Al(NO_3)_3$* 49.3/1.5[a]	6	17	11	94.0	In 2017, Park et al.[26]
Electrolyte membranes of inert matrix						
PDMS	$AgBF_4$ 73[b]	7	200	15	99.5	In 2004, Kim et al.[69]

Note: a - molar fraction; b - weight fraction; a* - molar fraction relates only to the polymer; b* - weight fraction relates only to the polymer; c - mixed gas (50:50 vol % of propylene/propane mixture); *Al(NO3)3·9H2O; PVP – polyvinylpyrrolidone; PEP – poly(ethylene phthalate); POZ – poly(2-ethyl-2-oxazoline); PEO – poly(ethylene oxide); PVA – poly(vinyl alcohol); PDMS – polydimethylsiloxane DOP – dioctyl phthalate; DPP – diphenyl phthalate; DPB – dibutyl phthalate; 8G1 – n-octyl β-D-glucopyranoside.

Source: The author, 2018.

Also in an attempt to solve the problems related to the essential instability of Ag^+ inside polar polymer matrices, Kang et al.[69] showed a way to disperse silver salts in polydimethylsiloxane (PDMS), which is an inert polymer matrix, and yet reach the facilitated transport (Table 5). The Ag^+ does not share the same interaction observed in polar matrixes, leading to the formation of silver salt aggregates trapped in the polymer domains. At first glance, it seemed that it would not work, since the preferable interaction with the olefin takes place with silver free ions. However, in permeation tests, when the olefinic gases began to pass through the membrane, the olefin complexation gradually dissolved the silver salt aggregates into free ions, promoting the facilitated transport. The time to reach the dissolution is *ca.* 100

h, after that, steady-state transport is achieved. Following this approach, it was possible to reach mixed gas selectivity of *ca*. 200, propylene permeance of *ca.* 15 GPU and keep the values constant for one week. This remarkable result brought the knowledge that introduction of silver salt in inert polymers, i.e. polymers that do not have functional groups to dissolve the silver salt, is feasible; and yet, they can promote the facilitated transport of olefins.

In the set of electrolyte membranes, the longest-term permeation test was performed in a PVP/$AgBF_4$/n-octyl β-D-glucopyranoside (8G1) membrane. Along 30 days, the presence of non-ionic surfactant (8G1) provided a stable membrane performance (mixture selectivity C_3H_6/C_3H_8 = 60 and mixed gas permeance of 34 GPU) with the highest permeance reported for electrolyte membranes.[65] The introduction of 8G1 only avoided the Ag^0 growth and agglomeration, however the reduction problems remained unsolved. Among attempts that indeed try to protect Ag^+ cation against reduction, POZ/$AgBF_4$/$Al(NO_3)_3$ membrane showed a stable performance (mixture selectivity C_3H_6/C_3H_8 = 21 and mixed gas permeance of 4.8 GPU) for 14 days.[67] The highest selectivity value was found in PDMS/$AgBF_4$ membrane with a stable performance (mixture selectivity C_3H_6/C_3H_8 = 200 and mixed gas permeance of 15 GPU) for 7 days.[69] In general, the selectivity values can vary from 5 to 200 and the mixed gas permeance from 0.5 to 34 GPU.[65,69,176] The time reported in long-term permeation tests ranges from 4 to 30 days.[69,176,178]

PVP is the most used polymer for electrolyte membranes of polar matrix; however, membranes made of PDMS, which is an inert matrix, have shown the highest selectivity values. Despite all efforts, the selectivity loss caused by Ag^+ cation reduction remains unsolved for permeation tests longer than 2 weeks. Considering simultaneously selectivity, permeance, and separation stability, the best result is performed by PDMS/$AgBF_4$ membrane, indicating that the use of inert matrixes is a promising strategy to develop new electrolyte membranes for olefin/paraffin separation. To avoid the reduction of Ag^+ inside the polymer matrix, besides the silicone-based polymers, other polymer class, which is well known by its intrinsic inertness, is thought to be used as membrane material. Fluoropolymers have been used in the latest works trying to solve the problem of Ag^+ instability.[22,179] In general, since Ag^+ is a stronger oxidant, the aim is that the polymer to be used as membrane does not have any group that could be oxidized by the Ag^+ cation.

1.6 Challenges to avoid carrier instability

Taking into account the results reached at laboratory scale by using polymer membranes with silver salts[40], the search for higher selectivities and permeabilities in the separation process is no more a big challenge. However, the maintenance of the membrane performance in long-term operation conditions has become a new target to be surpassed. Ag^+ cations incorporated in the electrolyte membranes report instability problems related to the tendency of them to react with other species, deactivating or poisoning the agent carrier in long-term operation.[28,103] The photoreduction or the exposition to reductant gases, *e.g.* hydrogen, inactivates the Ag^+ cation due to its reduction to metallic silver (Ag^0). The decontrolled formation of Ag^0 in the membrane can damage it with negative influence on the separation performance. The Ag^+ cation also can react with hydrogen sulfide (H_2S) and acetylene (C_2H_2) forming undesired compounds, principally silver acetylide that is extremely explosive and can pose a significant risk to the process. The deactivation reaction of Ag^+ are summarized in Table 6. It is worth emphasizing that small amounts (*ca.* 10 ppm) of these contaminants in the gas stream is enough to drastically decrease the process selectivity, in less than one week, impairing the membrane use.[28]

Table 6 – Deactivation reaction of silver cation (Ag^+)

Reaction	Description
$Ag^+ + e^- \xrightarrow{uv} Ag^0$	Photoredution
$2Ag^+ + H_2 \rightarrow 2Ag^0 + 2H^+$	Reduction by H_2
$C_2H_2 + 2AgX \rightarrow Ag_2C_2 + 2HX$	Formation of silver acetylide
$H_2S + 2AgX \rightarrow Ag_2S + 2HX$	Formation of silver sulfide

Note: X is an anionic component of silver salt
Source: The author, 2018.

Normally, the olefin/paraffin stream from naphtha steam cracking, which aims to be separated by membrane technology, contains some silver poisonous agents in low concentration, in ppm range. In the naphtha cracking furnace, it is necessary to operate with *ca.* 20 ppm of sulfur compounds in the feedstock to prevent the formation of undesired carbon monoxide. The function of sulfur is to passivate the nickel and iron catalysts sites in the cracking coil material of the furnace. The H_2S formed in the cracked gases is removed together with the CO_2 in the compression section using caustic solvents in absorption towers. Usually, CO_2 and H_2S concentration in the overhead stream of the absorption towers is below 0.2 ppm.[6,8]

Usually, hydrogen reduced compounds and acetylene (C2 and C3) are some byproducts of the SC. Hydrogen is removed at the lowest temperatures achieved in the chilling train,

together with methane; they are overhead products of the demethanizer.[25] The acetylene species, i.e. acetylene, methylacetylene (MA), and propadiene (PD), are removed by catalytic hydrogenation processes that transform them into more saturated hydrocarbons. The content of acetylenic compounds in the outlet of the hydrogenation process is <0.5 ppm.[8] Typically, the specification of polymer grade ethylene and propylene from the SC is <1 ppm of H_2 and <4 ppm of acetylene species.[105]

This severe scenario corresponds to a typical petrochemical plant where membranes are intended to be implemented. In addition, there are other challenges not related to silver poisoning. To replace or integrate C2 and C3 splitters, the membrane should treat a feed stream under a pressure of 5-20 bar and produce a permeate stream at 1−3 bar. Governed by these conditions, plasticization effects may occur even in the most rigid polymer membranes.[11,180] Thus, withstanding the negative influence of contaminants and avoid plasticization issues are essential challenges to be overcome by the next generation membranes.

1.7 Some alternatives to overcome the Ag^+ deactivation

In this context, some research groups have focused their efforts on proposing strategies to mitigate and/or overcome the problems imposed to the separation by the deactivation of the carrier. In the scientific literature, the most prominent efforts, proposing different solution lines to these problems, seem to not have a clear consensus on what would be the most promising strategy. The alternatives, which use dense polymeric films, are (i) the use of metallic nanoparticles as carrier, mainly silver nanoparticles, (ii) the use of ionic liquids for the stabilization of Ag^+, (iii) *in situ* regeneration of electrolyte polymeric membrane by using oxidizing agents, and (iv) the use of highly fluorinated polymers.

1.7.1 Silver nanoparticles as carrier

As already seen, the reduction of Ag^+ to Ag^0 throughout the separation process causes deactivation of the carrier and consequently the loss of membrane selectivity. In 2004, Kang et al.,[42] when performing permeation tests on a polymeric membrane with silver salts, noticed that the selectivity was reduced from 52 to 31 in 150 h of experiment. In parallel, it was observed the formation of metallic silver nanoparticles (Ag NP), whose size increased from 14.75 to 27.75 nm. It should be noted that, even at the beginning of the experiment, Ag NP were formed, pointing to the difficulty in avoiding Ag^+ reduction. What was remarkable in this experimental

observation was that, even with Ag NP of 27.75 nm in the membrane, the selectivity did not fall abruptly, only 40% reduction was observed. The hypothesis proposed for the maintenance of the Ag carrier properties was the formation of a partial charge polarization on the Ag NP surface. The phenomena observed by these authors has initiated a new study framework involving facilitated transport nanocomposite membranes of light olefins in place of Ag^+ salts. The great advantage of this replacement is that the problems of reduction deactivation involving the Ag^+ ion would be bypassed. This would allow the maintenance of the separation properties of the membranes in long-term operation.[76]

In 2007, Kang et al.[43] presented the first paper introducing the idea of Ag NP as carrier for the facilitated transport of olefins. To polarize the surface of Ag NP more efficiently, p-benzoquinone (p-BQ), an electron acceptor, was used to this goal, since the polymer matrix (EPR-poly(ethylene-co-propylene)) used was non-polar. The membrane selectivity achieved working with 50:50 v/v propylene/propane mixtures was 11 (Table 7). After this work, others studies have begun to explore new molecules to polarize the surface of the Ag NP,[24,44,71,75,181] always aiming to improve the selectivity of separation. Figure 8 shows a schematic representation of the possible polarization mechanism of the Ag NP surface by 7,7,8,8-tetracyanoquinodimethane (TCNQ).

Figure 8 – Schematic representation of the possible polarization mechanism of the Ag NP surface by 7,7,8,8-tetracyanoquinodimethane (TCNQ)

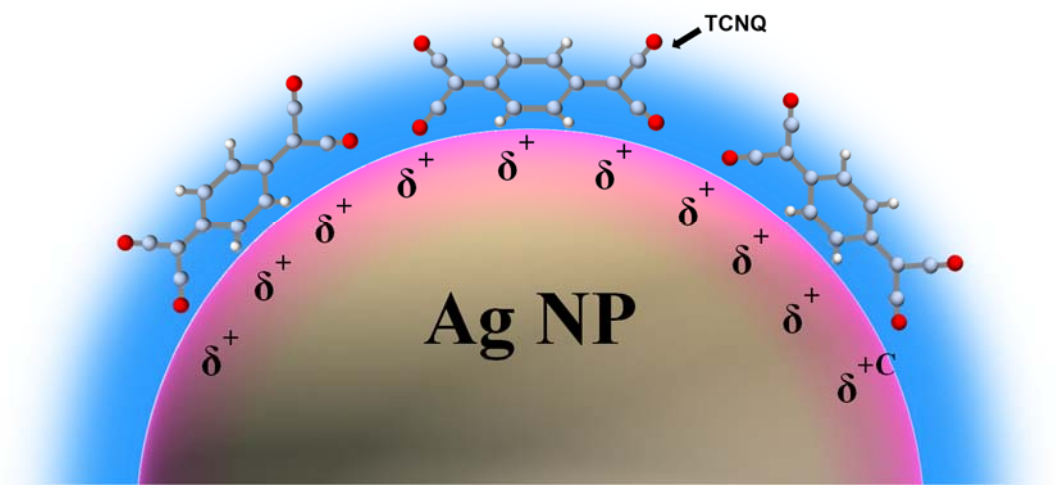

Source: The author, 2018.

Table 7 shows the most promising results observed for the separation of light olefin/paraffin mixtures by membranes using Ag NP and Table 8 presents the chemical structures of activator compounds for Ag NP. Analyzing Table 7, there is a clear evolution in the carrier properties of

the Ag NP due, mainly, to the suitable choice of the polarizing agent of the NP surface, but other factors are important such as the nanoparticle concentration, its size in the polymer matrix, and its adequate dispersion along the diffusional gas pathway. Although the concentration may vary from one work to another, it is noted that a concentration higher than 30 wt% of Ag NP, relative to the composite material, is required. In all works, where the facilitated transport of olefins by Ag NP with activator is verified, the NP have diameters smaller than 30 nm.[46] Therefore, Ag NP with sizes below this value can further improve the transport of the olefinic gases. Experimentally, the formation of the induced dipole on the interface between the Ag NP and the activator is checked by the X-ray photoelectron spectroscopy analysis (XPS). By changing the binding energy of the $d_{5/2}$ and $d_{3/2}$ silver orbitals to higher values, it is possible to verify the polarization of the NP surface.[43,71] Lee et al.[46] have reported an interesting study where the partial positive charge density of the surface of Ag NP was modulated by addition of TCNQ. These authors found that the amount of propylene adsorbed on the surface of the Ag NP could be correlated with the silver binding energy.

The membranes with Ag NP have reached higher selectivity values compared to membranes made of PVP[71] with the same weight ratio of Ag^+ and with the advantage of being resistant to light and hydrogen gas.[24] To further investigate the viability of Ag NP as promising carriers for the facilitated transport of olefins, Kang et al.[24] verified the deactivation resistance against C_2H_2. Surprisingly, the NP activated with TCNQ as a polarizing agent proved to be resistant to the formation of silver acetylide. Therefore, this is an additional evidence of the superior chemical stability that the Ag NP reports compared to Ag^+ salts. To become even more feasible, the chemical stability of Ag NP membranes against hydrogen sulfide and other sulfur compounds needs to be investigated. Other source of instability for the separation is the inherent instability of the polarizing agents, which is few mentioned in the literature. Compounds like p-BQ, TCNQ and tetrathiafulvalene (TTF) work as electron acceptor; thus, they have a tendency of withdrawing electrons from other molecules. This feature makes polarizing agents susceptible to chemical attack similarly as it is found in Ag^+ cation. For instance, depending on the condition, p-BQ can easily withdraw electrons from other chemical species and consequently being transformed in hydroquinone,[182,183] which is unable to polarize the surface of Ag NP. Therefore, p-BQ could be deactivated as polarizing agent by suffering a reduction process.

Table 7 – Main results of metallic nanoparticles as carriers for membrane facilitated transport of olefins

Polymer	Carrier/ activator Fraction (%)	Separation performance (days)	Selectivity[c]	Total permeance (GPU)	Olefin purity (mol%)	Reference
EPR	Ag NP/p-BQ 35.1/29.8[b]	3.5	11	0.45	91.7	In 2007, Kang et al.[43]
PVP	Au NP 81.1[b]	—	22	1.2	95.7	In 2008, Kang et al.[125]
SLM*	Ag NP/ $BMImBF_4$ 41.2/58.8[b]	5	17	2.7	94.4	In 2008, Kang et al.[44]
POZ	Ag NP/PVP 29.8/35.1[b]	15	21	1.3	95.5	In 2008, Kang and Kang[42,74]
PVP	Ag NP/ TCNQ 33.1/0.7[b]	5.5	50	3.5	98.0	In 2011, Chae et al.[71]
PVP	Ag NP/TTF 33.3/33.3[a]	—	145	2.5	99.3	In 2014, Choi et al.[75]
PEO	Ag NP/p-BQ 27.8/2.8[a]	10	10	15	90.9	In 2014, Hong et al.[72]
PVP	Ag NP/ F4-TCNQ 48.8/2.4[b]	1.5	112	1.8	99.1	In 2014, Chae et al.[181]
PU	Ag NP/$(OTf)^-$ 21.0/29.1[b]	—	24.4[d]	—	—	In 2016, Rezende et al.[73]

Note: a - molar fraction; b - weight fraction; c - mixed gas (50:50 vol % of propylene/propane mixture); *Supported liquid membranes. Support of polyester microporous membrane; EPR – poly(ethylene-co-propylene); PVP – polyvinylpyrrolidone; POZ – poly(2-ethyl-2-oxazoline); PEO – poly(ethylene oxide); Ag NP – silver nanoparticle; Au NP – gold nanoparticle; p-BQ – p-benzoquinone; BMImBF4 – 1-butyl-3-methylimidazolium tetrafluoroborate; TCNQ – 7,7,8,8-tetracyanoquinodimethane; TTF – tetrathiafulvalene.
Source: The author, 2018.

Other aspect that should be addressed is related to the permeance of this kind of membranes. Generally, the flux of Ag NP membranes need to be improved. For industrial application, high fluxes are required because it is necessary to reach the target high production of industrial plants. Thus, Hong et al.[72] prepared a membrane of poly(ethylene oxide) with Ag NP activated by p-benzoquinone seeking out the permeance increase. The composite membrane showed a selectivity of 10 and a mixed-gas permeance of 15 GPU for 10 days, the highest permeance reported for Ag NP membranes.

The use of Ag NP was also tested in membranes of polyurethane (ether based) (PU). Rezende et al.[73] measured the sorption values of propylene and propane in Ag NP/PU membranes (Table 7), in which the Ag NP were synthesized *in situ* into PU matrix using UV light radiation and silver triflate ($AgCF_3SO_3$) as salt precursor. It was found an ideal solubility selectivity of 24.4 in the Ag NP/PU membranes that could indicate an essential contribution of the sorption selectivity in propylene/propane separation by this kind of membrane.

Table 8 – Chemical structures of activator agents for Ag NP

Activator	Chemical structure	Reference
p-BQ		In 2007, Kang et al.[43]and in 2014, Hong et al.[72]
$BMImBF_4$		In 2008, Kang et al.[44]
PVP*		In 2008, Kang and Kang[42,74]
TCNQ		In 2011, Chae et al.[71]
TTF		In 2014, Choi et al.[75]

Note: p-BQ: p-benzoquinone – BMImBF4 – 1-butil-3-methilimidazolium tetrafluoroborate; PVP* – polyvinilpirrolidone crosslinked (this activator was introduced as a stabilazer during the Ag NP synthesis); TCNQ – 7,7,8,8-tetracianequinodimethane; and TTF – tetrathiafulvalene.
Source: The author, 2018.

1.7.2 Ionic liquids for the stabilization of Ag^+

The introduction of ionic liquids (IL) to stabilize Ag^+ salts in facilitated transport membranes is another alternative that the literature has reported as promising. For instance, the use of POZ/$AgNO_3$ membranes could reach stable separation performance (mixed gas permeance of 5.6 and selectivity of 32) during 150 h by the addition of small amount of 1-butyl-3-methylimidazolium nitrate ($BMImNO_3$).[167] Another example is the use of PVP/$AgBF_4$ membrane with $BMImNO_3$ that was able to maintain a selectivity of 7.2 with 3.6 GPU nearly constant along 160 h of permeation (Table 9).[184]

In the search for higher stability, in the last few years, dense composite membranes incorporating ionic liquids have received much attention.[22,178,184–187] In this configuration, IL/Ag^+ system is embedded in the polymer so that Ag^+ cations are distributed between the polymer matrix and a liquid phase entrapped inside it. This Ag^+ distribution through the membrane promotes the fixed and mobile carrier facilitated transport mechanisms, leading to higher permeabilities and selectivities.[188] In this line, Ortiz et al.[22,189] developed a material with promising characteristics for the separation of light olefin/paraffin mixtures. Previous to the

material choice, a thorough investigation on the most suitable IL to form the IL/silver salt pair was carried out[77,190]. Among several pairs, 1-butyl-3-methylimidazolium tetrafluoroborate/silver tetrafluoroborate ($BMImBF_4/AgBF_4$) was selected. Additionally, the fluoropolymer poly (vinylidene fluoride-co-hexafluoropropylene) (PVDF-HFP) (Figure 9) was used as polymer matrix to avoid the potential reduction of Ag^+ by the polymer chain.

Table 9 – Results of membrane performance with ionic liquids for protection against the reduction of Ag^+.

Polymer	Carrier/ stabilizer Fraction (%)[a]	Separation performance (days)	Selectivity[b]	Mixed gas permeance (GPU)	Olefin purity (mol%)	Reference
POZ	$AgNO_3$/ $BMImNO_3$ 58.8/7.0	6	32	5.6	84.8	In 2006, Kang et al.[167]
PVP[f]	$AgBF_4$/ $BMImNO_3$ 8.9/86.6	6.5	7.2	3.6	87.8	In 2007, Kang et al.[184]
PVDF-HFP	$AgBF_4$/ $BMImBF_4$ 60.2/7.8	10	700	55[d] 6630[e]	99.9	In 2013, Fallanza et al.[22]
TPU	$AgBF_4$/ $BMImBF_4$ 10/20	—	18.3[c]	3000[e]	94.8	In 2017, Wang et al.[70]
TPU	$Ag(Tf_2N)$/ $BMImTf_2N$ 10/20	—	9[c]	8398[e]	90.0	In 2017, Wang et al.[70]
TPU	$Ag(Tf_2N)$ 30	—	38[c]	8512[e]	97.4	In 2017, Wang et al.[70]

Note: a - weight fraction; b - mixed gas (50:50 vol % of propylene/propane mixture); c – tests under 2 bar transmembrane pressure; d – olefin permeance; e – olefin permeability in Barrer; POZ – poly(2-ethyl-2-oxazoline); PVP – polyvinylpyrrolidone; PVDF-HFP – poly (vinylidene fluoride-*co*-hexafluoropropylene); TPU – thermoplastic polyurethane Elastollan®; $BMImNO_3$ – 1-butyl-3-methylimidazolium nitrate; $BMImBF_4$ – 1-butyl-3-methylimidazolium tetrafluoroborate; $BMImTf_2N$ – 1-butyl-3-methylimidazolium bis(tri fluoromethanesulfonyl)imide.

Source: The author, 2018.

Figure 9 – Chemical structure of PVDF-HFP and $BMImBF_4$

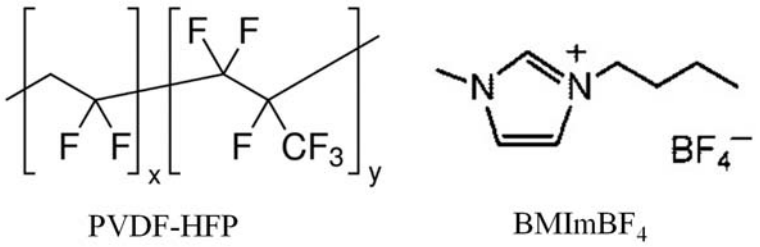

Source: The author, 2018.

The results obtained with the composite films of PVDF-HFP/BMImBF$_4$–AgBF$_4$ behave satisfactorily providing a mixture selectivity C_3H_6/C_3H_8 = 700, and propylene permeability of 6630 Barrer or *ca.* 55 GPU in the separation process (Table 9**)**. This remarkable performance was maintained for 10 days. The IL could stabilize the Ag^+ in a long-term experiment in this kind of membrane. To prove the potential of this type of material it is necessary to perform tests under the presence of the deactivating agents and verify the behavior of the composite membranes with ionic liquid against the simulated industrial operational conditions.[22]

On the other hand, different tests were made using thermoplastic polyurethanes (TPU)/IL membranes, but without taking into account the problems related to instability of the olefins transport. Wang et al.[70] synthesized several PU membranes with different silver salt/IL pairs. The IL used contained the 1-butyl-3-methylimidazolium cation ($BMIm^+$). Among all membranes prepared with IL, the highest selectivity (C_3H_6/C_3H_8 = 18.3) was found for the AgBF$_4$/BMImBF$_4$/TPU (weight fraction 10/20/70) membrane. The highest olefin permeability (8400 Barrer) was observed for the Ag(Tf$_2$N)/BMImTf$_2$N/TPU (weight fraction % 10/20/70) membrane. In general, the IL enhanced the selectivity of the TPU membranes by favoring the coordination of olefin with the Ag^+ ions inside the dense polymeric matrix. However, the best result (C_3H_6/C_3H_8 = 38 and 8512 Barrer) were reported for the Ag(Tf$_2$N)/TPU (weight fraction % 10/20/70) membrane without adding IL (Table 9).

1.7.3 In situ regeneration using oxidizing agents

Merkel et al.[28] have continued the research line focused on the development of polymer electrolyte membranes using polyethers which can provide a facilitated transport without the matrix humidification. This group further discussed the instability of the Ag^+ cation caused by deactivating agents listed in Table 10. The material used to produce the membranes was the Pebax® 2533 (Figure 10) with various levels of silver tetrafluorobate (AgBF$_4$). It is an elastomeric thermoplastic material composed of blocks of polyether (PE) and polyamide (PA). Specifically, the poly (ether-b-amide) used was prepared from nylon 12 and polytetramethylene oxide.

The Pebax® 2533/AgBF$_4$ membranes were tested against the deactivating agents in the separation of ethylene/ethane mixtures, and as expected, the selectivity in the separation process has collapsed. However, by exposing these membranes to hydrogen peroxide vapors combined with tetrafluoroboric acid (H_2O_2/HBF$_4$) or immersing directly in a bath of H_2O_2/HBF$_4$, the

membranes were able to return partially or completely to the original selectivity values (Table 10).

This *in situ* regeneration, by using these oxidative treatments, has reversed the deactivation caused by light, H_2 and C_2H_2; however, the membranes deactivated by H_2S have not shown any reversion. In the light and H_2 cases, the explanation for the regeneration is that the Ag^0 formed in the deactivation process is oxidized and returns to the Ag^+ form, becoming active again for the facilitated transport. However, the deactivation process caused by H_2 seems to be more aggressive than light deactivation, since the required time to restore the same level of selectivity was longer in the case of H_2 deactivation (60 h). According to Merkel et al.,[28] the understanding of the phenomenon involved in the regeneration of membranes inactivated by C_2H_2 still demands more detailed studies. Nevertheless, taking into account the chemical reaction of silver acetylide formation it can be thought that the regeneration is not caused by the oxidizing agent itself, but by the presence of HBF_4, which shifts the equilibrium of the reduction reaction toward the Ag^+ regeneration.[191]

Table 10 – Results of the deactivation and regeneration processes of Pebax® 2533 + 80 wt% $AgBF_4$ membrane with original selectivity of 40 and olefin permeance of 87 GPU

Deactivation process	**Selectivity[a] drop**	**Regeneration process**	**Selectivity[a] regeneration**
Membrane exposed to ambient light for 34 days	-95%	Immersion in a H_2O_2/HBF_4 bath[b] for 30 s	100%
Membrane exposed to ambient light for 34 days	-95%	Contact with the H_2O_2/HBF_4 vapors[c] for 16 h	50%
7 days of hydrogen permeation	-95%	Contact with the H_2O_2/HBF_4 vapors for 60 h	50%
Membrane exposed to 10 ppm of acetylene in the ethylene feed for 5 days	-85%	Immersion in a bath of H_2O_2/HBF_4 for 60 s	69%
Membrane exposed to 10 ppm of hydrogen sulfide in the ethylene feed for 7 days	-92%	Immersion in a bath of H_2O_2/HBF_4 or contact with the H_2O_2/HBF_4 vapors	0%

Note: a – mixed gas (65:35 vol % of ethylene/ethane); b - 1:1 mixture of 35 wt% H_2O_2 in water and 50 wt% HBF_4 in water; c - membrane in contact with the vapor of a 1:1 H_2O_2/HBF_4 aqueous solutions at room temperature.
Source: Adapted from Merkel et al. (2013)[28]

Figure 10 – Chemical structure of Pebax®

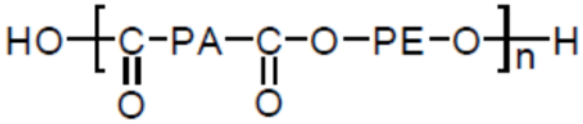

Source: The author, 2018.

From the possibility of *in situ* membrane regeneration, the research group believes that it will be possible to extend the service life of the membrane by applying cyclic regeneration steps, thus enabling the practical application of the membranes made of Pebax® 2533/$AgBF_4$. Analyzing this proposal, it is noted that the deactivation by H_2S was not solved and the cyclic regeneration steps should be evaluated against the commercial application feasibility of the technology.

1.7.4 Use of highly fluorinated polymers/ Current technological options

In 2016, the Compact Membrane Systems (CMS) Company has unveiled the separation system called Optiperm. By this olefin/paraffin separation system, the Company has claimed resistance against common poisonous agents in feed stream, including hydrogen and acetylene. The Company promises a high return with small financial investment. For instance, the Company describes a typical application of olefin/paraffin separation in a polypropylene reactor purge stream that costs <$1M to installation, <$500K per year of operating cost and an internal rate of return of >150%.[192,193]

The base for the stability of the Ag^+ inside the polymer matrix is the use of a highly fluorinated polymer that is extremely chemically and thermally resistant. Specifically, the fluorinate polymer with sulfonate functional group is used.[23] The Ag^+ is added to the polymer matrix by ion-exchange with the H^+ of the sulfonic groups. Unlike the previous works,[27,147,150,152] in which the membrane was immersed in the Ag^+ water solution to achieve the ion-exchange, now, the polymer and the Ag^+ salt are solubilized in the same solvent and after, the solution is cast to form the polymeric film. This material is called silver ionomer and it is responsible for the facilitated transport of olefins.[23]

As a typical structure of thin film composite membrane used for industrial gas separations, the CMS`s membrane has different layers joined together, each one with specific function, as shown in the Figure 11. The selective layer has the task of distinguishing the molecules to be separated and it should be thin (0.1-1μm) to provide high permeances. A thin layer does not have enough mechanical strength and it is necessary deposit it onto the surface of a porous support (150–200 μm) with negligible mass transport resistance. Normally, the support has small porous (< 100 nm) on the surface.[194,195]

When the thickness of the selective layer become closer to the porous diameter of the support, it takes place a geometric restriction in the diffusion of the gases, leading to a substantial decreasing of the gas flux.[196,197] To solve this problem, usually, it is added a third

layer between the support and the selective layer, called gutter layer. The gutter layer is a high diffusion layer composed by a very permeable polymer. Its purpose is to channel the outgoing gases from selective layer into the surface pores of the support. By this channel effect, the geometric restriction is reduced compared to the two-layer configuration. The optimum thin composite membrane performance is reached when the thickness of the gutter layer is in the range of 1–2 times the pore radius of the support.[194] In addition to the former three layers, another high diffusion layer can be added to protect the selective layer and plug any defects eventually present. This protective layer prevents damage during the manipulation of the membrane and protects the exposed surface of the selective layer from contaminants present in the stream to be separated.[194,195]

Figure 11 – Schematic illustration of a usual thin film composite membrane used for industrial gas separations

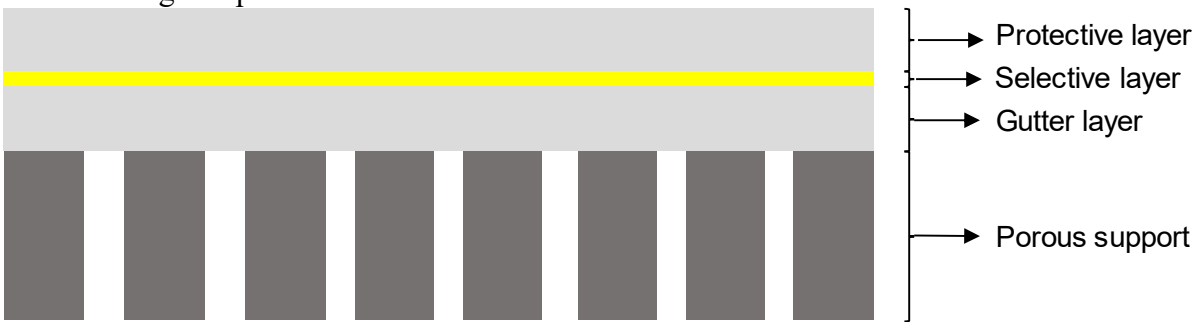

Source: The author, 2018.

In the CMS`s Optiperm system,[23] the high diffusion and the selective layers are composed of a custom fluoropolymer designing for a specific function according to the layer assignment. The high diffusion layers should be made preferably of a glassy polymer containing tough functional groups against the oxidation by the Ag^+. Perfluoroether and chlorotrifluoroethylene are useful polymers to be applied in the high diffusion layers, rather than primary and secondary alcohol, iodo, bromo, and aldehyde. For the selective layer, the polymer should be more inert than the high diffusion layer, preferably should be use an amorphous perfluoropolymer searching the maximus protection for the Ag^+. The fluoropolymer inertness and the protection offered by the protective layer are responsible for the stability and resistance against poisonous agents during the separation process. Another source of inherent reduction of the Ag^+ is the direct contact between the selective layer and the porous support. Usually, the polymer from which the support is made has small amount of incidental organic vapor or other chemicals. Besides, the oxidable organic groups in the own polymer chain of the support could reduce the Ag^+. Thus, another protection factor is also attributed to the gutter

layer, but in this case, the protection is associated to avoid the direct contact between the selective layer and the support.

In the patent assigned to CMS,[23] the claims are mainly related to the material used in the preparation of the membrane. The best results (Table 11) were achieved by using the following materials for the membrane layers. The high diffusion layers are composed by the Teflon® AF 2400, a copolymer with a high molar percentage (83%) of perfluoro(2,2-dimethyl-1,3-dioxole) (PDD) and 17% of tetrafluoroethylene. The porous support is made of PAN350, an ultrafilter made from polyacrylonitrile. Two selective layers with the same amount of silver salt ($AgNO_3$) are employed. One layer has higher permeance and lower selectivity (selective layer 1) and another has lower productivity and higher selectivity (selective layer 2). The selective layer 1 is composed by a silver ionomer of sulfonic acid based on the PDD/VF (vinyl fluoride)/PPSF (perfluoro sulfonylfluorideethylvinyl ether) terpolymer (T_g 58 °C). The selective layer 2 is made of the Aquivion®D79-25BS,[179] a perfluorosulfonic acid polymer made from perfluorosulfonylfluoridevinyl ether monomer. In the patent, there are no long-term stability and resistance against poisonous agents tests. The permeation tests were conducted using humidification (relative humidity greater than 90%) of the feed stream and N_2 as a sweep gas.

Table 11 – Results of facilitated transport membranes based on highly fluorinated polymers

Polymer	Carrier Fraction (%)[a]	Selectivity[b]	Total permeance (GPU)	Olefin purity (mol%)
(PDD/VF/PPSF)/	$AgNO_3$ 16.7[b]	95.5	278.9	96.0
Aquivion®D79-25BS	$AgNO_3$ 16.7[b]	52.1	317.37	92.9

Note: a - weight fraction; b - mixed gas (20:80 vol % of propylene/propane mixture); PDD – perfluoro(2,2-dimethyl-1,3-dioxole); VF – vinyl fluoride ; PPSF – perfluoro sulfonylfluorideethylvinyl ether.
Source: Adapted from Majumdar et al. *(*2016*)*.[23]

Regarding the humidification need issue related to the ion-exchange membrane,[198] Feiring et al.[199] tested different sweep gas configurations for checking the hole of the moisture and the sweep gas in highly fluorinated silver ionomer membranes. In the configuration 1, they humidified the sweep gas (N_2 under 2.8 kPa) and the feed mixture (10:90 vol % of propylene/propane under 414 kPa). In the configuration 2, the feed was not humidified, and the sweep gas was a vapor from above a sealed tank of water under vacuum of 6.7 kPa absolute pressure. Finally, the configuration 3 employed a dried feed and vacuum. As expected, it was founded the best results for configuration 1. Surprisingly, the configuration 2 and 3 presented equivalent high olefin/paraffin selectivity but 30% and 60% lesser olefin permeance

respectively. Comparing the configurations 1 and 2, it seems that only the humidification of the permeate stream can supply the facilitated transport activity during the permeation, resulting in still notable high olefin permeance. The presence of the inert sweep gas in the permeate implies a further separation step. Thus, the configuration 2, which does not use the N_2 as sweep gas, shows an advantage since the permeate stream only has the olefin and an eventual small amount of paraffin. Nevertheless, the presence of water in the permeate was not avoided. A subsequent drying stage may be considered in the separation train, but it seems an easier task than removing the inert gas from the output stream of the membrane unit. To replace the inert sweep gas, the use of a vacuum pump should be taken in account and a tradeoff between energy consumption and permeance may be considered.

1.8 Summary and conclusions

The global demand of light olefins has experienced a significant growth related to the increasing demand of different polymers over the last decades. The principal process to produce olefins is the naphtha steam cracking process, the most energy intensive process in the petrochemical industry. In an attempt to save energy in the process, some alternatives have been proposed to replace or integrate with the current cryogenic distillation separation of olefins and paraffins. Among several technologies, facilitated transport membranes have stood out owing to the combination of high selectivity and permeance. However, to be used in the industrial separation, some instability issues should be considered.

The Ag^+ cation, the main carrier for the facilitated transport membrane, suffers deactivation by poisonous agents present in the gaseous stream to be separated. Even without the presence of deactivating agents, the Ag^+ cation can be reduced by the chemical environmental of the polymer matrix from which the membrane is made. After achieving superior performance by using silver salts dissolved or dispersed in polymer matrix, the current arduous task is to maintain the selectivity in long-term separation process. To attain this goal, some clever alternatives have been proposed to overcome the hurdle.

By adding small amounts of HBF_4 or non-ionic surfactants, it is possible to confer certain stability to Ag^+ cation. In addition, the introduction of $Al(NO_3)_3$ in electrolyte membranes can weaken the interaction between the functional group of the polymer and the Ag^+ salt, providing a more stable chemical environment to the Ag^+. A remarkable result was reached with a POZ/$AgBF_4$/$Al(NO_3)_3$ membrane. The selectivity was maintained for 14 days. The use of another interesting carrier, Ag NP, overcome the problem related to the reduction of

Ag^+. To be useful, the Ag NP should be activated by a suitable polarizing agent. Experimental tests showed the resistance of Ag NP against acetylene, which is one of the poisonous agents. Therefore, Ag NP reveal higher resistance compared to Ag^+. The best results reached by Ag NP composite membranes achieved a selectivity of 10 and a mixed-gas permeance of 15 GPU for 10 days.

To avoid the Ag^+ cation reduction inside the polymer matrix, more inert polymers have begun to be applied as a host matrix to silver salts. Specially fluoropolymers, which are well known by their intrinsic inertness, have been used as material to the preparation of Ag^+ facilitated transport membranes. A PVDF-HFP matrix was used for hosting a system of $AgBF_4$/BMImBF_4. IL have been demonstrated as another type of agents able to stabilize Ag^+ against reduction. Joining together these features, a membrane of PVDF-HFP/BMImBF_4–$AgBF_4$ reported a mixture selectivity of 700 and propylene permeability of 6630 Barrer (*ca.* 55 GPU) in a 10 days separation test. Claiming resistance against common poisonous agents in the feed stream, a thin film composite membrane based on a highly fluorinated polymer was developed by Compact Membrane Systems Company. Beyond the intrinsic inertness of the membrane material, additional protection arises from the configuration of the composite membrane. A thin separation layer composed by fluorinated silver ionomer, which is responsible for the facilitated transport of olefins, is between two high diffusion protective layers. This configuration seems to avoid the poisoning of the Ag^+ cation that are ionic bonded in the ion-exchange polymer; however, the membrane humidification dependence was not solved. If the problems related to poisoning are still present in the membrane process, other alternative is to try an *in situ* regeneration using vapor of the oxidizing system (H_2O_2/HBF_4) to recover the separation performance and extend the service life of the membrane.

Most of the results reported in the literature didn't consider the presence of poisonous agents in the permeation experiments. The main concern is still the stability of Ag^+ inside the polymer matrix, but it seems that this challenge has started to be overcome using stabilizing agents and inert polymer matrix. Issues related to the plasticization effects are not yet a problem discussed intensively by the works concentrated in the facilitated transport membrane for the olefin/paraffin separation. Probably, the future efforts will be dedicated to understand deeply the problems regarding the poisonous agents, trying to figure out a more robust solution. Due to the lower performance required and milder condition operation, the initial commercial application of the membrane technology to olefin/paraffin separation could be in the vent streams of some kinds of petrochemical reactors. This application could make a step forward

in the use of commercial olefin/paraffin membrane units before the challenging task aimed to replace the distillation unit in the steam cracking process or in the FCC off-gas streams.

2 POLY(URETHANE UREA)/Ag NP COMPOSITES MEMBRANES

2.1 Waterborne poly(urethane urea)s

Polyurethane (PU) and poly(urethane urea) (PUU) belong to a versatile polymer class, which have been extensively employed as fibers, foams, coatings, adhesives, elastomers, membranes, and biomaterials.[200–202] This polymer family can provide desirable properties for a range of application by tailoring the features of rigid and flexible segments present in the material. By a suitable formulation choice, it is possible to obtain from vitreous to elastomeric characteristics. The PU and PUU are formed by flexible polyol segments, most commonly based on polyethers or polyesthers; and by rigid segments formed by diisocyanates and chain extenders.[114,203] Morphologically, PU and PUU present, to some extent, a degree of microphase separation between rigid and flexible domains due to thermodynamic incompatibility between them.[200] The Figure 12 shows a representation of these domains in the polymer matrix. By controlling the microphase separation using a wide range of precursor monomers, it is possible to explore unusual properties for different applications.[204]

Figure 12 – Representation of rigid and flexible domains structure in a segmented PU

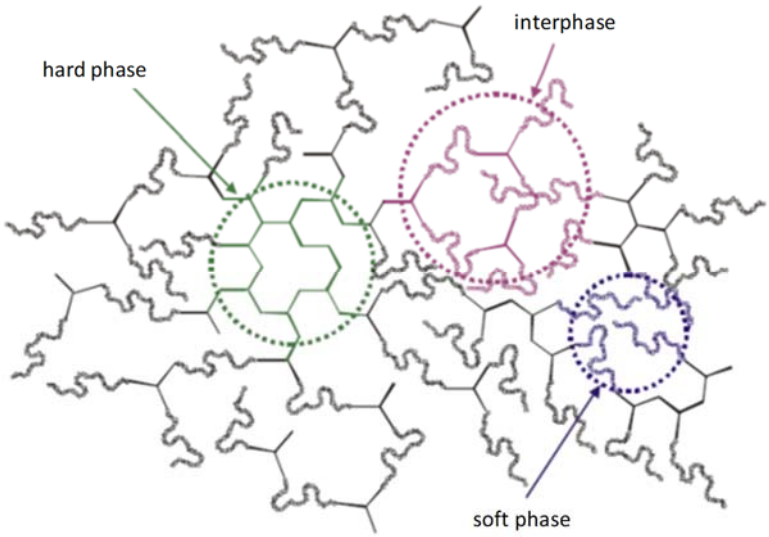

Source: This figure was reproduced from Król (2007).[204]

The final morphology and mechanical properties of material are governed primarily by multiples hydrogen bonds formed between proton donator (urethane and urea N-H) and proton acceptor (urethane and urea C=O, ester carbonyl and ether oxygen) groups.[113,205] PUU with bidentate hydrogen bonds generally exhibit a superior Young's modulus, tensile strength, and

extension properties compared to related PU.[206] In terms of thermal processability, in most cases, PU and PUU are processing from solution instead of thermal processes due to the thermal degradability of urea and urethane linkage.[207,208]

PU and PUU obtained from aqueous dispersion (WPU and WPUU) have been receiving great attention by replacing volatile organic compounds (VOC) in the preparation of coatings, membranes, adhesives, food packaging, and biomedical devices.[209] Thus, this replacement reduces safety risks and environment concerns compared to conventional PU and PUU formulations based on VOC.[210,211]

WPU and WPUU synthesis is usually initiated by the formation of a prepolymer using the reaction between a polyol and ionic segments (internal emulsifier) with an excess of diisocyanate, forming urethane bonds and terminal cyanate (NCO) groups.[210] Further, water is added to the prepolymer to formation of dispersion. The incorporation of ionic groups allows the stabilization of dispersion in aqueous medium. Afterwards, the terminal NCO groups can react with diols or diamines forming WPU or WPUU, respectively. This step is known as chain extension. The extension by using diamines results in polymer chains with urea groups. The extension by using diols results in urethane groups. Figure 13 schematizes the formation of prepolymer and chain extension step in the synthesis of the WPU and WPUU. In aqueous media, WPU and WPUU constitute particles in nanometric scale (<100nm) due to their ionic groups that act as internal emulsifier.[60,61] In these particles, internal emulsifier, urethane, and urea groups face the aqueous medium, while the flexible segments, composed by more hydrophobic domains turn inwardly (Figure 14).[210]

Membranes of waterborne poly(urethane urea) (WPUU) have been researched as a material for gas permeation. From 2002 to 2004, Coutinho et al.[58,59] studied the use of WPUU based on hydroxyl-terminated polybutadiene (HTPB) and poly (propylene glycol) (PPG) in CO_2 and N_2 permeations. In these works, the most expressive results were an ideal selectivity ($\alpha^{id}CO_2/N_2$) of 31.2 and 22.6 with CO_2 permeance of 0.025 and 1.57 GPU, respectively. Continuing the research line, in 2011, Barboza et al.[60,61] evaluated CO_2 permeability in WPUU/clay composites with different contents of poly (propylene glycol) (PPG) and block copolymer based on poly(ethylene glycol) and poly(propylene glycol) (EG-b-PG). By an increment in the copolymer content, it was observed an increase in CO_2 permeability related to the membranes with and without clay. In sequence, Pereira et al.[62,63] tested $\alpha^{id}CO_2/CH_4$ of WPUU membranes stimulated by the context of CO_2 removal from natural gas (CH_4). Using NCO/OH ratio of 1.5 in the prepolymer and varying the proportion of PPG and EG-b-PG in the precursor monomers, it was found a formulation with 25% PPG/75% EG-b-PG that presented

an $\alpha^{id}CO_2/CH_4$ of 54 and CO_2 permeability of 189 Barrer. This result was considered promising, since it was possible to cross the Robeson's 2008 upper bound for this separation.

Figure 13 – Scheme of prepolymer formation and chain extension during the synthesis of WPU and WPUU

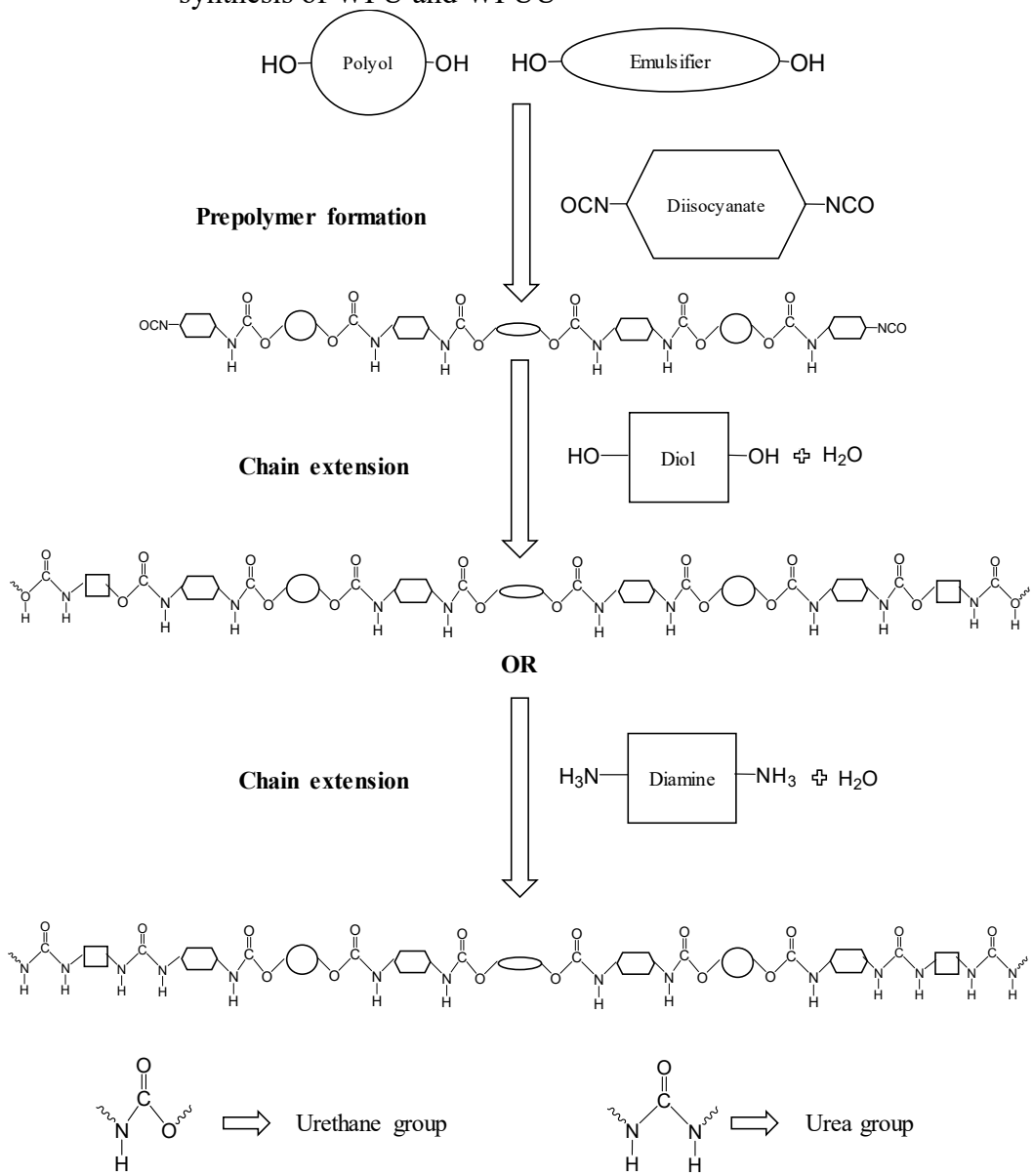

Source: The author, 2018.

Figure 14 – Structure of WPU and WPUU particles in water medium. The scheme shows an anionic ionomer

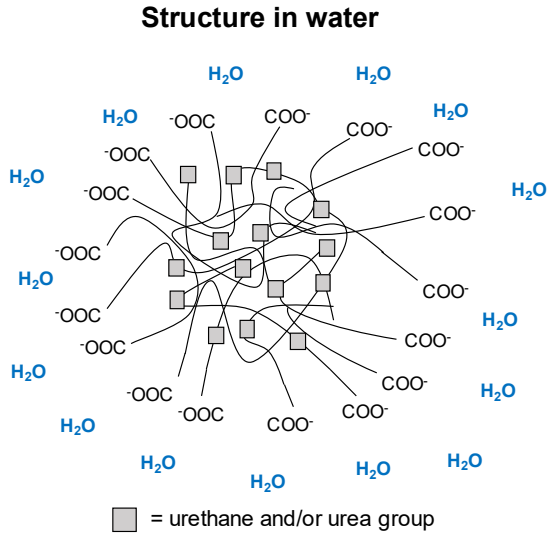

Source: The author, 2018.

From Pereira`s formulation[62,63] with noteworthy result for CO_2/CH_4 separation, in 2013, Campos[64] introduced powder Ag NP (coated with 4% of polyvinylpyrrolidone) in an WPUU dispersion by using a high intensity ultrasonic processor. After, α^{id} of olefin/paraffin was tested in the WPUU/Ag NP membranes with higher Ag NP content of 1wt%. It was not possible to achieve the facilitated transport of olefin through the membranes; however, it was the first work that investigated the permeability of petrochemical gases in the WPUU/Ag NP membranes. Also, CO_2 and N_2 permeabilities was evaluated as probe gases to investigate how Ag NP presence influenced the gas transport properties of the membranes. The results obtained by Fourier transform infrared spectroscopy (FTIR) and thermogravimetry (TGA) suggested an interaction between ether oxygen atoms of WPUU and Ag NP. The CO_2-philic feature of the material was impaired, since the polyol segments was obstructed by interactions with Ag NP, which were among ether linkages. CO_2 and C_2H_4 permeability values were reduced remarkably due to the ether groups obstruction. C_2H_6 and N_2 permeability values were decreased moderately because of the Ag NP aggregates formation, which intensified the tortuosity of the diffusion path in WPUU matrix.[64]

Respecting PUU, they have a suitable feature for gas separation membranes. PUU hard segments work as a strong “virtual” crosslinking that may improve the plasticization resistance of membrane during the gas separation processes.[70,113,114] Additionally, WPU and WPUU based materials obtained from water dispersion do not need thermal processes to be used, protecting

the products from thermal degradation and impeding polyols crystallization.[207] A desired requirement for a polymer to be use as Ag NP nanocomposite membrane for the olefin facilitated transport is to allow the gas access to the Ag NP surface. Polymers with high diffusional resistance do not favor the facilitated transport because they decrease the target molecule concentration around the carrier, hampering the jump mechanism.[27,41,212] Normally, elastomeric polymers should favor the permeation of more condensable gases. This is appropriate, since the larger molecules from the steam cracking products are light olefins and paraffins. As CO_2, olefins are apolar gases, however they can interact with the polar polymer domains through quadrupole moment. Many papers explore the ether oxygen of poly(ethylene glycol) (PEG) segments to improve the CO_2 solubility in membranes.[63,213,214] For WPUU with flexible polyether segments, it is possible to enhance the solubility of olefins compared to paraffins. The presence of PEG in the flexible segments ensures a greater interaction with olefinic gases, since the gas transport through membrane take places in these domains.[213] Probably, elastomeric polymers with higher CO_2-philic feature, in theory, also should show a higher olefin solubility, which may contribute in some way to the separation. However, very permeable polymers can impair the selectivity of the membrane, even if the facilitated transport is present. Due to high permeability to olefins and paraffins, a membrane could not be suitable to the separation, since the high flux of paraffin can decrease any selectivity to olefins. Thus, a tradeoff between elastomeric behavior of material and separation selectivity should be considered.

The polymer WPUU formulation used in Campos' s work[64] is elastomeric (T_g=-35ºC) and it has a higher CO_2-philic feature due to the presence of ether groups from PEG, hence the olefins permeability is greater than the paraffins (α^{id} ethene/ethane is 1.4). Although, paraffins should be more permeable, the opposite behavior takes place. Olefins, which are lesser condensable, are more permeable than paraffins due to the interaction between ether groups and alkenes.

Another factor to be considered is that in all works dealing with membranes for olefins facilitated transport, only commercial polymers are used as matrix for membranes.[22,26,72,73,43,65–71] The use of a versatile polymer as WPUU may be useful to achieve properties in which is necessary to make a certain modification in the formulation and consequently in the polymer structure/properties. Moreover, the material preparation in aqueous medium, avoiding the use of undesirable volatile organic compounds, is eco-friendly. Therefore, the strategy of using WPUU as matrix for WPUU/Ag NP membranes applied to olefin/paraffin separation is reasonable to be proposed.

2.2 Ag NP synthesis

In the preparation of nanocomposites materials there are two types of approach: bottom-up and top-down. Top-down strategy starts from bulk-scale materials and by using physical, chemical or mechanical processes the method can reduce the bulk material into nanoparticles. Bottom-up strategy starts with atoms or molecules to obtain nanoparticles.[53,54]

In top-down approach, usually, higher energy mechanical methods are used, such as mills that fragment the microparticles into smaller particles in nanometer scale. High energy laser, ultrasonic, thermal and lithographic methods can also be used.[215] Generally, the final material in this approach consists of nanoparticles with higher polydispersity, without a suitable size and shape control of the produced nanoparticles. Top-down strategy variations are related to the quality of dispersion provided by macroscopic processing factors such as design of the processing structure, mixing speed and residence time. There is a considerable limitation to the optimization of the process from these factors.[53,54]

In bottom-up approach, nanoparticle structures are generally constructed by chemical processes. This strategy produces structures with more complex shapes prepared from atoms or molecules. Better particle size, shape, and lower polydispersity control can be achieved. The methods involved in bottom-up strategy comprise precipitation, aerosol, and sol-gel processes.[53]

Metal nanoparticles (NP) have been extensively exploited in the formation of polymeric nanocomposites with many functional properties. The difficulties in dealing with metal NP are their instability (due to the tendency of agglomeration caused by high free surface energy), oxidation by air, humidity, etc. By introducing NP into dielectric polymer matrices, many problems of stabilization and manipulation of metal NP are solved.[52] The principal metals used in polymer nanocomposites are silver, gold, platinum, and copper. The main features added to the polymers by the addition of NP are conductivity,[47] antibacterial,[48,49] magnetic[50], and catalytic characteristics.[51] These special NP aspects arise from the increase of surface atoms as the size of NP decreases. In macroscopic materials, most atoms are internal, and a few are found in the basal planes of the surface. In NP, almost all atoms are in the surface (in corners or edges) providing to the material the characteristics of superficial atoms. This fact is the reason for special and unique features of NP.[53]

The bottom-up strategy is more efficient regarding the control of particle size; however, it brings up additional challenges to NP synthesis. In the specific case of Ag NP, focus of the Thesis, the Ag NP synthesis via chemical reduction in water medium is the most widely used

method.[54,55] To synthesize Ag NP via chemical reduction, there are basically three elements: (i) precursor salt, (ii) stabilizing, and (iii) reducing agent. There are a variety of possible combinations involving several types of these three elements. Nevertheless, the most used and cheapest syntheses involves the use of $AgNO_3$ as precursor salt[56] and $NaBH_4$ as reducing agent.[57] Since chemical reduction is an easy method to reproduce, it takes into account when goes is to scale-up the production of Ag NP. Stabilizers may also vary widely, depending on the system, but generally they have surfactant properties, which protect the surface of NP against agglomeration. Recently prepared NP anchor in the polar regions of the polymer, preventing the approximation of others NP and avoiding agglomeration (Figure 15).[55] Typically, polymers such as polyvinilpirrolidone (PVP), polyvinyl alcohol (PVA), and poly(N-isopropilacrilamide) are among the most used stabilizers.[55]

Figure 15 – Steric stabilization scheme (in the enlarged part, a small polar portion of the stabilizing macromolecule anchors the surface of the NP)

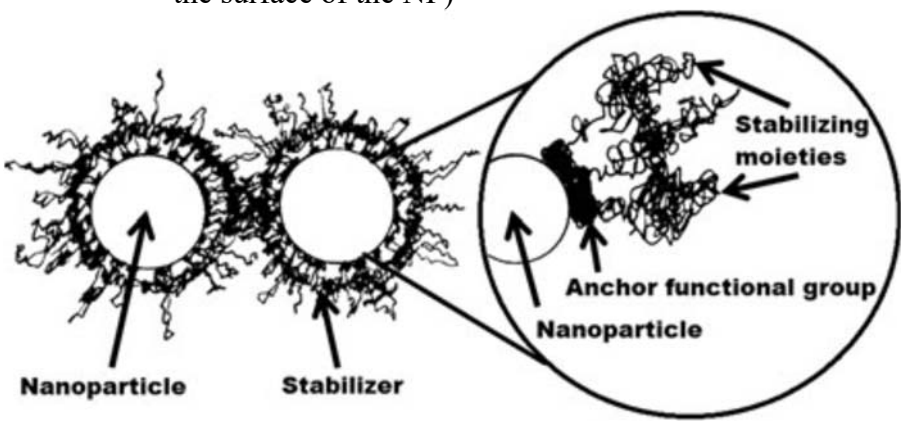

Source: This figure was reproduced from Tan and Cheong; Zhang (2011).[55]

As seen in the previous section, WPUU have internal emulsifiers in their structure, which are responsible for the dispersion stability in aqueous medium. In these particles, internal emulsifier, urethane, and urea groups face the aqueous medium, while the flexible segments, composed by more hydrophobic domains turn inwardly. As shown in Figure 14, WPUU particles are typical micellar structure in which the internal emulsifier, urethane, and urea groups, which are hydrophilic, are oriented towards the aqueous medium. On the other hand, flexible polyether segments, which are hydrophobic, are turned inwardly towards the polymer nanoparticle core.[210] In principle, the WPUU conformation in aqueous dispersion can provide the basic characteristics of a stabilizing agent for Ag NP synthesis. Polar segments placed at the external surface of WPUU colloid particles can anchor the freshly synthesized NP, ensuring

a nanoscale approximation without collision and agglomeration throughout their synthesis.[55,64] Preliminarily, the possibility of using WPUU dispersion eliminates the need of an additional stabilizing agent, affording an advantage to the synthesis of Ag NP in WPUU dispersion.

During the synthesis, the metallic NP formation has two steps: nucleation and growth. In the nucleation stage, the metal cation undergoes reduction and the recently formed metal atom moves randomly until collides with other atoms and cations forming a cluster. The nucleus will be formed as cations, atoms, and clusters collide. The nucleus that exceeds the activation energy (the maximum free energy ΔG*) should have a critical radius size r* (Figure 16).[216] Nuclei larger than critical size decrease their free energy and the process of NP growth becomes spontaneous. Nuclei smaller than the critical size are dissolved. After the nuclei formation, they can grow into NP via molecular addition or Ostwald ripening. Molecular addition consists in addition of metal atoms on the surface of the nucleus. The addition is extremely dependent on the nucleation rate. High nucleation rates result in many nuclei that tend to grow independently, providing small NP with better size distribution and more uniform shape. On the other hand, Ostwald ripening take places by collision and agglomeration between NP with the following dynamic: larger NP become larger and smaller NP become smaller until their dissolution.[55]

Figure 16 – Illustration of overall free energy change *ΔG* as function of the growth particle size r

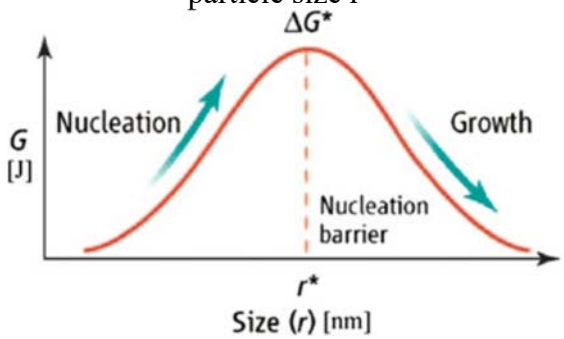

Source: This figure was reproduced from Zhang (2010).[217]

Comparatively, Ostwald ripening velocity is greater than molecular addition velocity; thus, it is much easier to synthesize large NP than smaller ones. Apparently, a high nucleation rate is essential to achieve smaller NP and it depends on the power of reducing agent, but this cannot be generalized because each reaction has its own growth dynamics. The influence of temperature on the growth process of NP depends on the reaction system employed, and it is not possible to obtain a clear trend of its influence.[55]

The Ag NP synthesis using WPUU dispersion as a stabilizing agent leads to performer the reaction in aqueous medium. This kind of synthesis is also known as *in situ* synthesis. Many applications require that NP should be dispersed in aqueous media and remain suspended with same chemical or physical properties over an extended period. The NP synthesis in aqueous medium has some difficulties that arise from the intense ionic interactions aggravated by increasing the ionic strength in the medium. These challenges are solved by using low reagent concentrations during the preparation of NP (*ca.* $5 \cdot 10^{-4}$M). To increase the concentration, stabilizing agents are sometimes used, but with further difficult to remove them at the end of the preparation when it is required.[218]

In contrast to the synthesis in aqueous medium, NP synthesized in organic media can be prepared at higher concentrations (above 1 mol/L of reagents) with higher monodispersity, predefined shapes and sizes when compared to the preparation in aqueous medium. NP prepared in organic medium are insoluble in water; thus, many works have been tried to create NP transfer methods from organic medium to aqueous medium because of the synthesis difficulties in water.[218] Although there is the possibility of synthesis in aqueous medium, it consists a challenge to be overcome due to problems that may occur during the process of Ag NP synthesis in WPUU dispersion.

The properties of Ag NP for light olefins/paraffins separation by facilitated transport membrane are directly related to the control of the surface area that is a consequence of size control during the synthesis. In addition, NP must be properly dispersed in the polymer matrix with suitable concentration to allow the olefin molecule migration from one carrier to another, characterizing the facilitated transport. The challenges for the preparation of WPUU/Ag NP membranes start in the reactional system by the control of Ag NP dispersion and concentration in WPUU dispersion. Ensuring the stability of Ag NP in aqueous medium, avoiding aggregation and precipitation, is the initial problem.[219–221]

From the previous paragraphs is possible to conclude:

(i) The $AgNO_3/NaBH_4$ reaction system is the simplest and most common; therefore, it is a reasonable option for Ag NP synthesis;

(ii) Due to the surfactant characteristics, WPUU aqueous dispersion can be used as a stabilizing agent for Ag NP synthesis;

(iii) $NaBH_4$ is a strong reducing agent[55] able to provide the necessary conditions for a higher nucleation rate (delaying Ostwald ripening), which favors the formation of small Ag NP with uniform size distribution;

(iv) With a high nucleation rate, it is not necessary to raise the reaction temperature. The temperature and stirring of the reaction system should be lowest as possible to minimize Ostwald ripening. Stirring should be sufficient to homogenize the reaction medium and must be stopped when the last amount of $AgNO_3$ is added in the reactional system.

These points are important to avoid the agglomeration of Ag NP.

2.3 Experimental

2.3.1 Materials

Powder sodium borohydride and silver nitrate (≥99.0%) were provide by Sigma-Aldrich. Block copolymer based on poly(ethylene glycol) and poly(propylene glycol) (EG-b-PG), number average molecular mass ($\bar{M}n$) = 1850 g·mol^{-1} and EG content of 7% in terms of molar mass, and poly (propylene glycol) (PPG), ($\bar{M}n$ = 1000 g·mol^{-1}) were kindly donated by Dow Brazil and data were reported by the manufacturer. Dimethylolpropionic acid (DMPA) purchased from Sigma-Aldrich; ethylenediamine (EDA, 99%) was provided by Acros Organics; isophorone diisocyanate (IPDI) was gently donated by Centro Técnico Aeroespacial (CTA); and triethylamine (TEA) purchased from Vetec.

2.3.2 Preparation of WPUU/Ag NP composites

The Ag NP synthesis proposed in this work follows the reaction[55]:

$$AgNO_{3(aq)} + NaBH_{4(aq)} + 3H_2O \rightarrow Ag^0 + 3{,}5\ H_{2(g)} + B(OH)_{3(aq)} + NaNO_{3(aq)}$$

In the reaction, the molar ratio of Ag:BH_4^- is 1:1. Usually, excess of reducing agent is used to ensure that all Ag^+ is reduced to Ag^0, in addition, the BH_4^- excess is responsible for stabilizing Ag NP in aqueous medium[222]. In the Ag NP synthesis of this thesis, it was not used a BH_4^- excess, since there was an expectation for the stabilization of Ag NP by the WPUU aqueous dispersion.

All WPUU aqueous dispersion used in this Thesis were prepared previously in the Laboratory of Sustainable Polymeric Materials from Rio de Janeiro State University under supervision of Professor Marcia Cerqueira Delpech. The PUU NCO-terminated (terminated

with isocyanate group) prepolymer was synthesized by reacting EG-b-PG, PPG, DMPA, and IPDI (NCO/OH equivalents-gram proportion of 1.5) at 95 °C during 30 min. The equivalents-gram proportion between the polyols (EG-b-PG, PPG, and DMPA) in the synthesis was 3:1:4. The carboxylic groups of DMPA were neutralized using TEA. The NCO-terminated prepolymer was dispersed in deionized water and then submitted to the chain extension reaction with EDA at 30°C, as reported in previous works.[60,62,210,223] WPUU dispersion with a solid content around 30% was prepared. Two different WPUU batches were produced, batch A and B. The batch will be indicated when final results of the analyses performed are influenced by batch type. Other formulation was synthesized by using the same methodology and reagents except by a different NCO/OH ratio of 2. The code for this formulation is WPUU(2). WPUU(2) was not characterized like WPUU, however this material will be used for some permeation tests in the next chapter.

Ag NP were prepared by the reduction *in situ* of Ag^+ using $NaBH_4$. The molar ratio of $Ag:BH_4^-$ was 1:1. Fifteen milliliters of WPUU (approximately 15 g) were added to 15 mL of deionized water, and then $NaBH_{4(s)}$ was added under mechanical stirring at 500 rpm. After the solubilization of the reducing agent, 20 mL of $AgNO_3$ solution were added with a flow rate of *ca.* 0.01 $mL \cdot s^{-1}$, under stirring at 500 rpm - 2000 rpm. Reactional system was at 10 °C during all procedures.[48,222,224–226] Figure 17 shows the experimental apparatus used for synthesizing the WPUU/Ag NP dispersions.

Figure 17 – Experimental apparatus for the synthesis of Ag NP in WPUU aqueous dispersion

Legend: 1 – mechanical stirrer (anchor blade); 2 – thermostatic bath; 3 – peristaltic pump; 4 – glass jacketed reaction; and 5 – $AgNO_3$ solution.
Source: The author, 2018.

At the end of the reaction, WPUU/Ag NP dispersions were cast onto Teflon plates and dried in a vacuum oven at 40 °C for one week. After drying process, the membranes were

removed from the plates for characterization. By using this methodology, the following membranes were prepared: 1 wt% (1% Ag NP), 2.5 wt% (2.5% Ag NP), 5 wt% (5% Ag NP), and 10 wt% (10% Ag NP). The percentages are relative to the amount of silver in the final dried composite material.

To the preparation of material with higher Ag NP content, a modification of the procedure described above was adopted. At the synthesis end, a precipitate was formed, and it was separated from the dispersion by filtration. The precipitate was introduced into a test tube containing water. After manual stirring, the tube was centrifuged (3000 rpm for 10 min). The precipitate at the tube bottom was separated from the supernatant. This procedure was performed 3 times. After the washing steps, the precipitate was solubilized in ethanol at 75° C for 15 min. After solubilization, the alcoholic solutions of WPUU/Ag NP were cast onto Teflon plates and dried in a vacuum oven at 35 °C for 24 h. Membranes with 30 wt% (30% Ag NP*) and 50 wt% (50% Ag NP*) were prepared by this methodology. For evaluation, the precipitate formed during the synthesis of 30% Ag NP* membrane was also investigated. The code for this material is 30% Ag NP_{ppt}.

2.3.3 Characterizations

The FTIR analysis were performed on a Perkin Elmer (Spectrum One) FT-IR spectrometer equipped with an attenuated total reflection (ATR) accessory, with a flat ZnSe plate, and dried films were collected at an angle of 42º. The measurements were obtained at 4 cm^{-1} of spectral resolution, 50 scans per spectrum and performed in triplicates for each film. The spectrum of the crystal was used as background.

WPUU/Ag NP composites were characterized using transmission electron microscopy (TEM) (JEM 2100, JEOL), operating at 80 kV. The SAXS data were collected at the wavelength λ = 1.49 Å using a MAR CCD 165 detector on the SAXS-2 beamline of the Brazilian National Synchrotron Light Laboratory (LNLS/Brazil) over a range of $0.007 < q < 0.2$ $Å^{-1}$ ($q = 4\pi \sin\theta/\lambda$, where 2θ is the scattering angle). The scattering patterns were measured at 25 °C for samples. The obtained scattering patterns were measured at 25 °C for samples and corrected for the instrument background, before being used for further analysis.

X-ray diffraction (XRD) measurements of the films were performed using a Rigaku Miniflex II diffractometer with Cu-Kα radiation (λ = 1.5405 Å). XRD data were collected in a conventional Bragg–Brentano θ/2θ geometry using a continuous scan ranging between $5º < 2\theta < 60º$ and step size of 0.05º.

Thermogravimetric analysis (TGA) measurements were carried out in N_2 flow (20 mL ·min^{-1}) for all the samples using a Dp Union SDT Q 600 TGA with a temperature scan rate of 20 °C·min^{-1}. WPUU/Ag NP films with mass ranging from 8 to 15 mg were placed in alumina crucibles and heated from 25 to 600 °C. During the heating period, the weight loss and temperature difference were recorded as a function of temperature. The films onset degradation temperature (T_{onset}) was defined by the intersection of a line tangent to the baseline with a line tangent to the inflection point of the differential weight loss (DTG) curves, as recommended by ASTM E2550-07 standard.[227] The thermal analyses were made in triplicates for each film.

2.4 Results

A brief description of the main analytical techniques used to characterize the composites materials studied in this Thesis is found in Appendix.

2.4.1 Transmission electron microscopy (TEM) and Small Angle X-ray Scattering (SAXS)

TEM images of the 1% Ag NP and 5% Ag NP membranes shows a suitable dispersion and diameters between 10 and 20 nm for the NP (Figure 18). SAXS data for WPUU, 1% Ag NP, 2.5% Ag NP, and 5% Ag NP membranes are shown in Figure 19. The fittings using the Beaucage unified model are in the Figure 20, it was considered NP with spherical shape and smooth surface. SAXS results are summarized in Table 12. It was found Ag NP diameters ranged from 3 to 7 nm with low polydispersity. In neat WPUU membrane, the mean distance between the rigid domains of the polymer was 6 nm. Probably, these rigid domains are clustered into domains with a fractal structure because the slope of the **log I(q) vs. log q** curve model is -3 in the second hierarchical level indicating a fractal surface.[228,229]

Analyzing the TEM and SAXS data, it can be concluded that the synthesized Ag NP are smaller than 10 nm. The black spots in TEM images possibly shows a nanoagglomerates of Ag NP that justifies larger diameters found by TEM compared to SAXS analysis. Additionally, the sample analyzed by TEM is from a region with high concentration of NP, since the SAXS results did not present a peak, which indicates a spatial correlation among NP.

It was achieved a suitable Ag NP dispersion in the WPUU matrix, since there was no formation of microclusters (larger than 100 nm). From the TEM images it is possible to observe a Ag NP homogeneous distribution in WPUU/Ag NP membranes. Additionally, a low polydispersity related to Ag NP diameters was found in the material showing that the synthesis

was able to provide Ag NP with uniform size. The adequate Ag NP dispersion in the membranes can be attributed to the stabilizer feature of WPUU aqueous dispersion that avoided the formation of large size agglomerates.

Figure 18 – TEM images of WPUU/Ag NP membranes

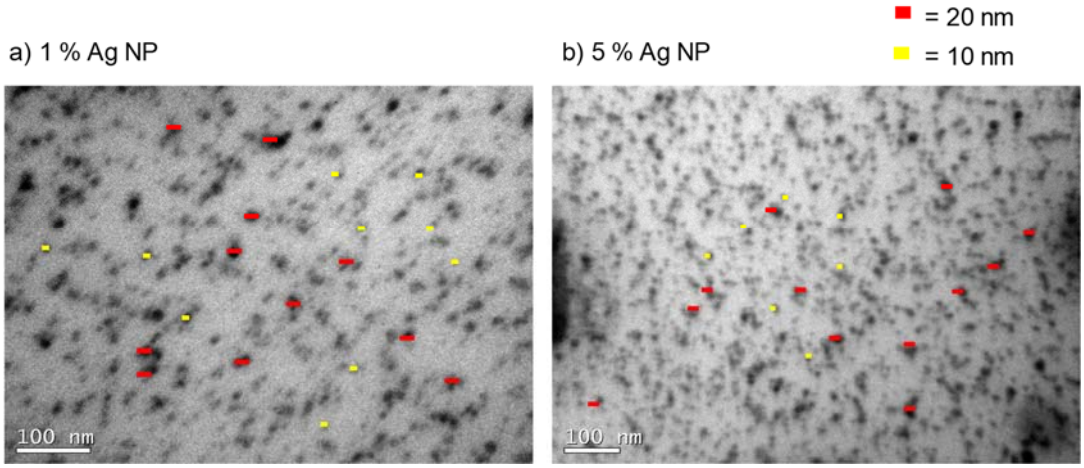

Legend: a)1% Ag NP; b)5% Ag NP.
Source: The author, 2018.

Figure 19 – SAXS data of WPUU/Ag NP membranes

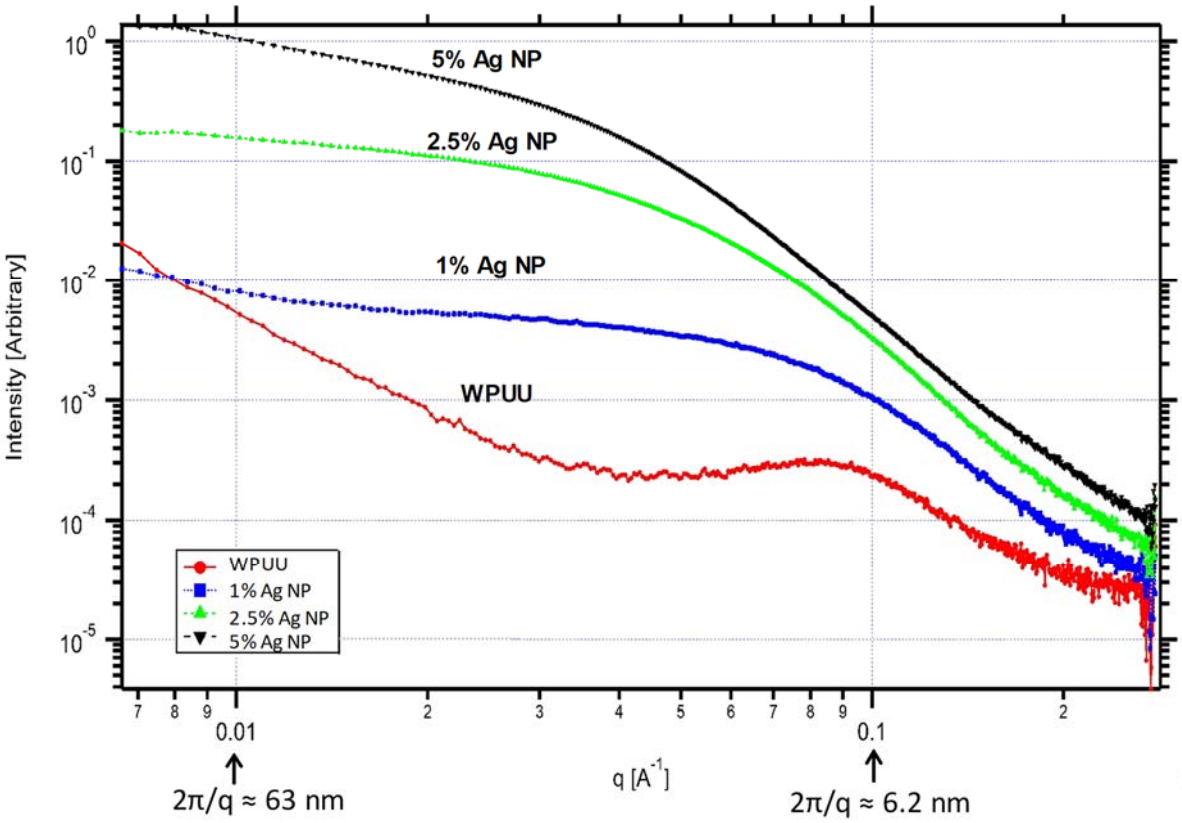

Source: The author, 2018.

Figure 20 – Fits of SAXS data

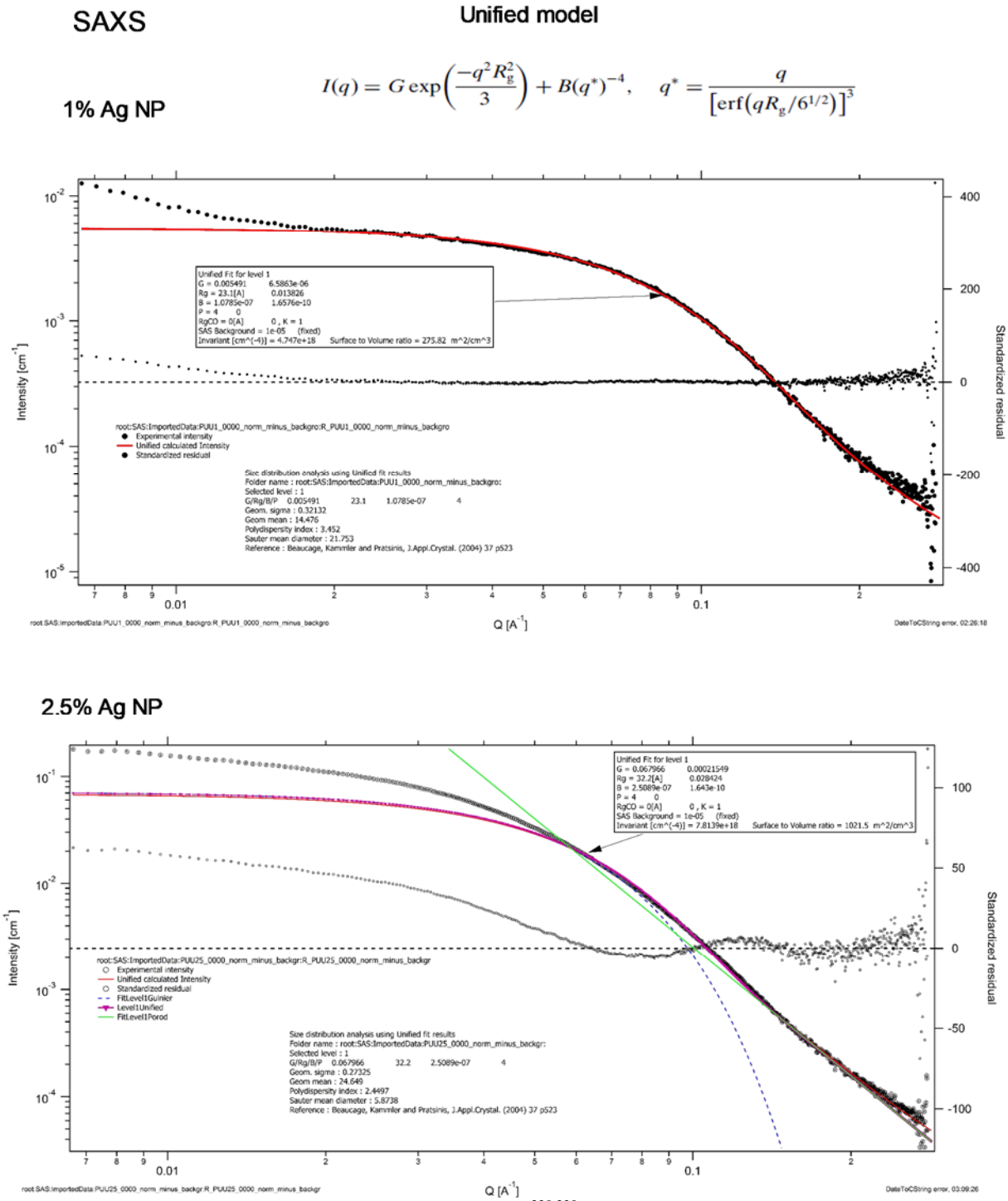

Note: Fits of SAXS data using the Beaucage unified model.[228,229]
Source: The author, 2018.

Figure 21 – Continued

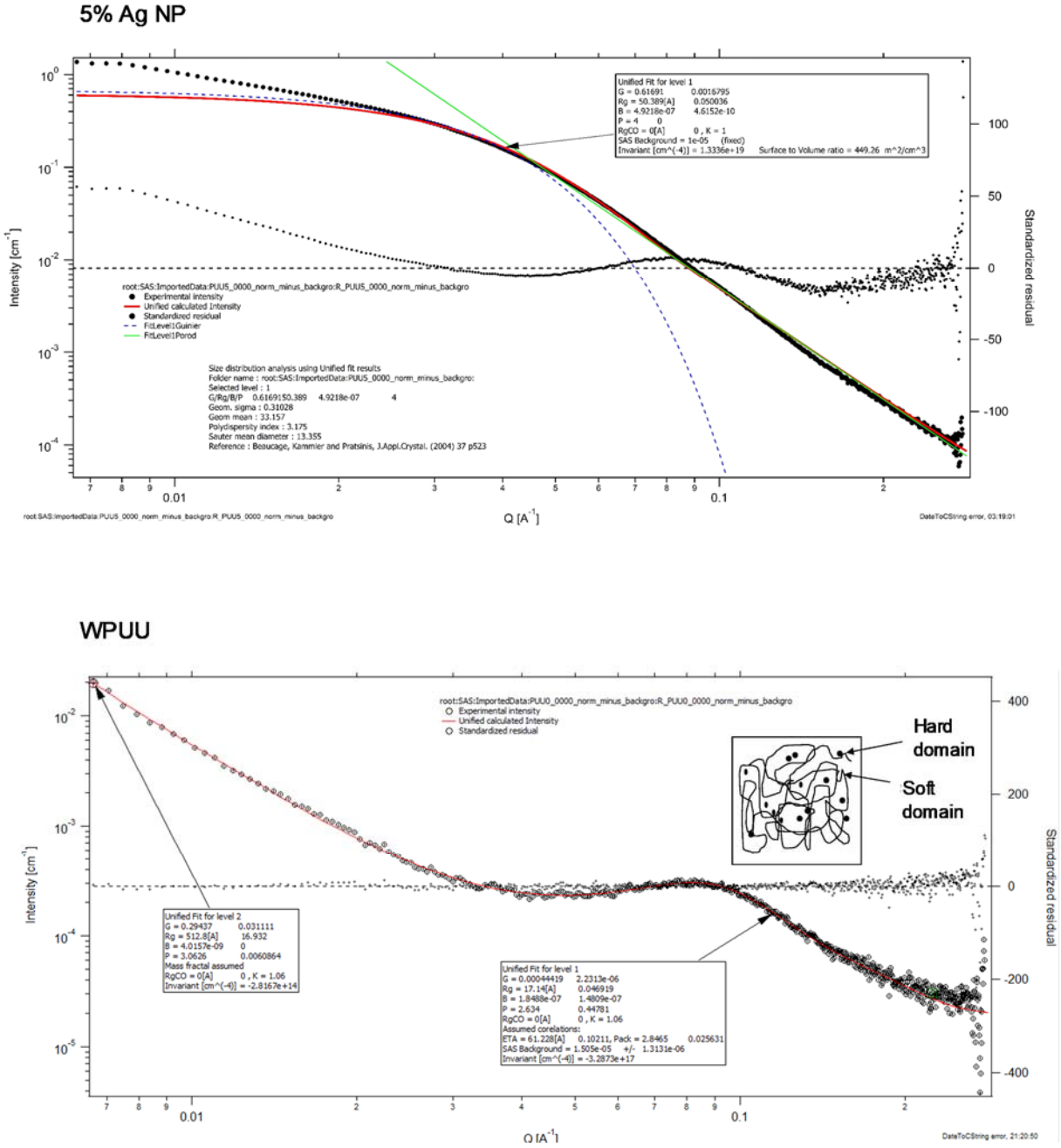

Note: Fits of SAXS data using the Beaucage unified model.[228,229]
Source: The author, 2018.

Table 12 – SAXS results for the WPUU/Ag NP membranes

Membrane	R_g (Å)	Diameter (nm)	Polydispersity index	k	d (nm)
1% Ag NP	23.1	3	3.4	—	—
2.5% Ag NP	32.2	5	2.4	—	—
5% Ag NP	50.4	7	3.2	—	—
WPUU	17.4	—	—	2.8	6.1

Note: P is fixed at -4 for the Ag NP membranes.
Source: The author, 2018.

2.4.2 X-ray diffraction (XRD)

The diffractograms of WPUU, 1% Ag NP, 10% Ag NP, 30% Ag NP_{ppt}, 30% Ag NP^*, and 50% Ag $NP^*$are shown in Figure 21. Ag NP have diffraction peaks at 2θ = 38º and 44º related to the (1 1 1) and (2 2 0) metallic silver crystal planes (JCPDS file no. 04–0783), which corresponds to a face-centered cubic structure.[230] The same diffraction pattern appeared in 10% Ag NP, 30% Ag NP_{ppt}, 30% Ag NP^*, and 50% Ag NP^* membranes, indicating the metallic nature of the Ag NP embedded in the polymer matrix. In the 10% Ag NP and 30% Ag NP_{ppt} materials, $NaNO_3$ diffraction peaks, resulting from the Ag NP synthesis, were also found.[231] The mean size of Ag NP was estimated by using the Scherrer's equation (18) applied to the data of peak associated to the (1 1 1) plane.[232,233] The geometric factor used for the calculus was 0.9. The mean size determined was 8.7, 15.6, 15.6, and 18.8 nm for the 10% Ag NP, 30% Ag NP_{ppt}, 30% Ag NP^*, and 50% Ag NP^*, respectively.

Figure 21 – XRD patterns of Ag NP and WPUU/Ag NP membranes

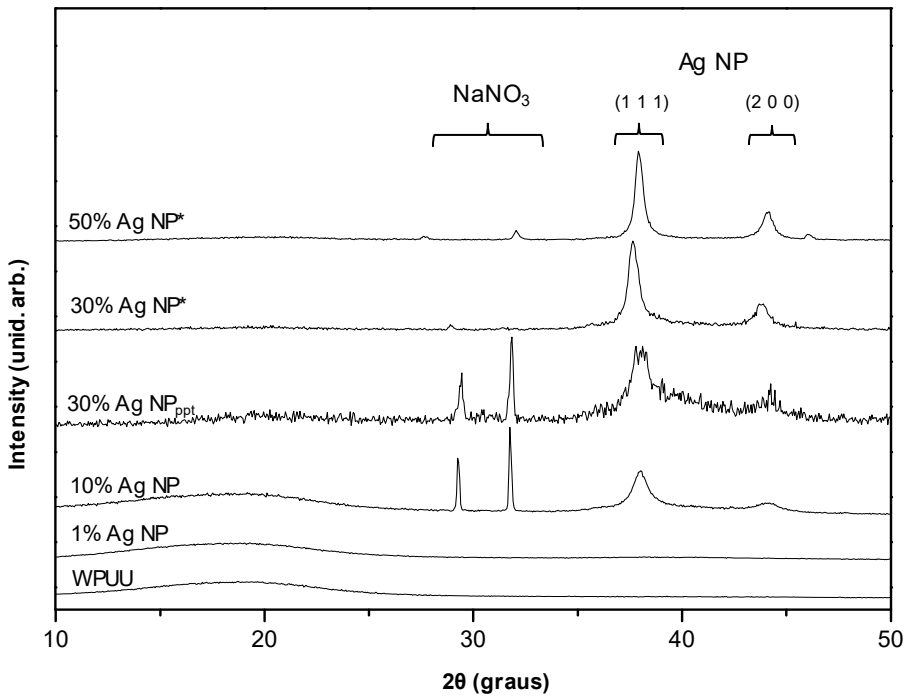

Source: The author, 2018.

By increasing the silver content in the membrane, the Ag NP size got larger, but yet nanometric scale. In the diffractogram of the 30% Ag NP^* and 50% Ag NP^* membranes, $NaNO_3$ peaks were practically absent, showing that salt removal by washing procedure was successful.

Moreover, the washing step and the solubilization in ethanol did not alter the size of the synthesized Ag NP, since the Ag NP in the 30% Ag NP_{ppt} and 30% Ag NP* had the same size. No silver peaks in the 1% Ag NP membrane are observed because of the lower amount of silver, which is not detected by the XRD analysis. The broad halo centered at $2\theta = 20^{o}$, which is mainly related to the amorphous structures of PPG in WPUU soft domains,[234] did not have significant changes.

2.4.3 Infrared Spectroscopy (FTIR)

FTIR analysis is an essential tool to evaluate the changes in proton donator and proton acceptor groups of WPUU.[113,223] From the neat WPUU up to the membrane with 5 wt% of silver content, there were no significant changes in the FTIR profile. Figure 22 shows the FTIR spectra of the WPUU and 10% Ag NP membranes, depicting the most significant changes in the main vibrational modes of –NH, C=O (urethane and urea), and ether (C-O-C) bonds. No FTIR spectrum shows any shoulder or split in C=O bands suggesting not only the absence of free carbonyl urethane (absorption at 1740-1716 cm^{-1}) and urea groups (1680-1695 cm^{-1} region), but also the absence of disordered urea hydrogen-bonded carbonyl group that absorbs at 1652–1679 cm^{-1} region. Noteworthy is that the presence of these groups should not be discarded due to the large profile of the bands in the region between 1600 and 1750 cm^{-1}, which could include a fraction of these species. In the carbonyl region (C=O) (Figure 22b), the frequency of urethane carbonyl decreases (Δ = -7 cm^{-1}), reflecting a hydrogen bonding rearrangement inside the polymer matrix, mainly in the interphase region, since the urea C=O band keeps the same frequency. The shifts to lower frequency indicate an intensification of hydrogen bonds related to urethane carbonyl groups. In the amide II region, the frequency shift indicates an alteration of intermolecular hydrogen bonds and polymeric chain conformation.[223]

In the 50% Ag NP^{*} membrane, there were no expressive shifts in the C=O (urethane and urea) bands. However, ether and –NH regions underwent some changes. In the ether region of FTIR spectra (Figure 23c), the former ether band was shifted to lower frequencies (Δ = -8 cm^{-1}) indicating that ether groups interacted intensely with another site inside the material, probably with the Ag NP surface or proton donator groups (N–H).[125,155] The N–H groups also seem to feel the Ag NP presence. To investigate this aspect, the area ratios (between baseline and the band) of absorption FTIR bands of N–H region was calculated (Figure 23b and Table 13). The ratio is necessary to make a fair comparison among bands intensities of different samples. The extinction coefficients of all vibration bands compared were considered the same

for the membranes. To calculate the areas, the fitting of Gaussian peaks assumed a constant base line between 3800 cm^{-1} and 3400 cm^{-1} (N–H region).[235] The number of bonded proton donators groups (bonded urethane and urea N-H)[113,236] increased with the loading of Ag NP 50 wt%. Moreover, the bonded N–H band shifts to lower frequency indicating an intensification of hydrogen bonds related to N–H groups. As the carbonyl region was not changed markedly upon the silver addition, there is just one more option to a proton donate interact, probably the ether group, which is a proton acceptor. This kind of interaction, between ether groups and N-H, favors the miscibility among hard and soft domains of the WPUU, in a certain extend.[223] The amide II region also changed corroborating the alteration in intermolecular hydrogen bonds (Figure 23a).[223] There are some differences in band frequencies between Figure 22 and Figure 23 because the FTIR analysis were carried out in different spectrophotometers.

Figure 22 – Comparison between FTIR spectra of the WPUU and Ag NP 10%

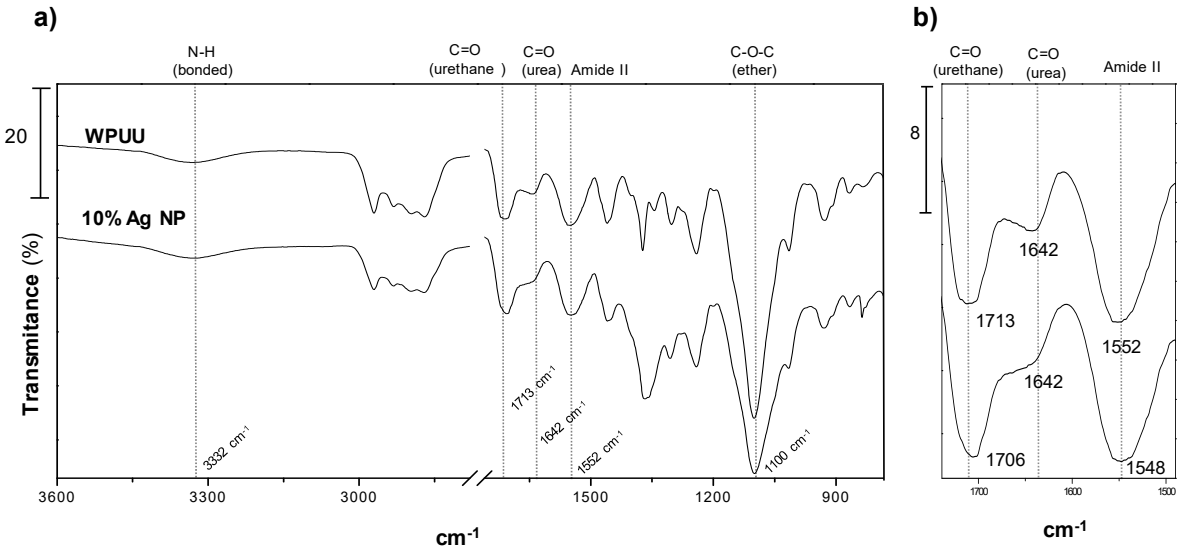

Source: The author, 2018.

Comparing 10% Ag NP and 50% Ag NP* membranes, it can be seen a carbonyl band shift in Ag NP 10% that does not take place in the 50% Ag NP*. This difference may be caused by the $NaNO_3$ present in the composite that can interact with the carbonyl groups of the material. This situation did not take place in 50% Ag NP* membrane because it passed by a washing procedure to remove the salt.

Figure 23 – Comparison between FTIR spectra of the WPUU and 50% Ag NP*

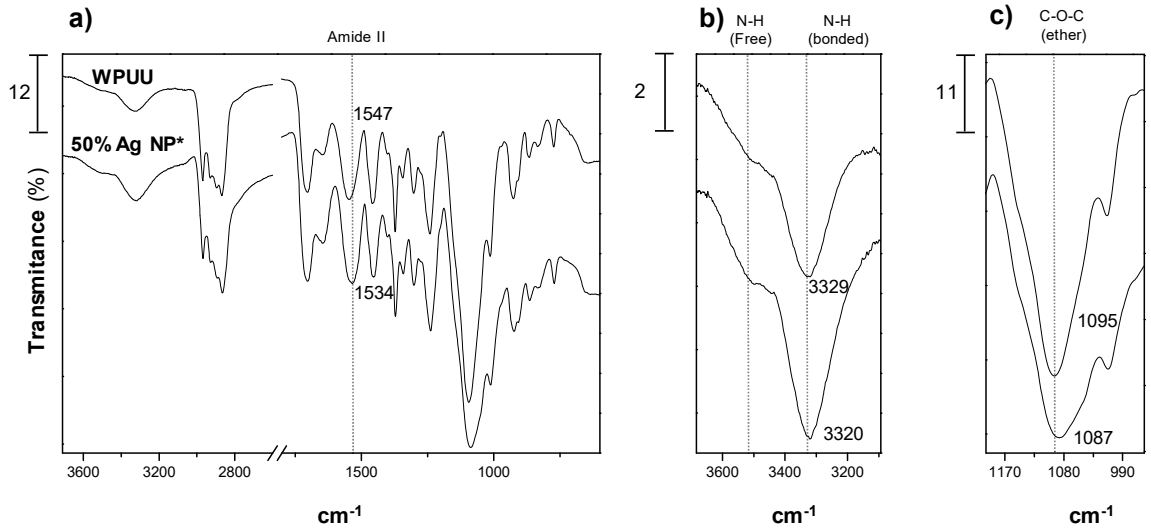

Source: The author, 2018.

Table 13 – Area ratios of the FTIR bands in N–H region of WPUU and 50% Ag NP* membranes

Membrane	N-H bonded/free[a]
WPUU	4.0
50% Ag NP*	9.5

Note: [a] The free is centered at 3580 cm^{-1} and bonded at 3330 cm^{-1}.
Source: The author, 2018.

2.4.4 Thermal Stability

The TGA allows to evaluate the degradation profile of the polymeric material. Some minor changes, not shown in TGA curves, can be evaluated by derivative thermogravimetry (DTG) curves. The thermal degradation of PUU films is basically a two-stage depolycondensation process. The first stage of degradation is related to the rigid domains of the polymer and the subsequent stage corresponds to flexible domains. Due to its association with rigid domains of PUU, the initial temperature of degradation (T_{onset}) can provide information on changes in the urethane and urea groups.[208,237]

In the DTG curves, several peaks appear, demonstrating the complexity of the degradation. They are associated with temperature at maximum rate of weight loss (T_{vmax}) at each stage of degradation. The higher T_{vmax}, which is relative to the last peak of the DTG curves,

is related to the degradation of polymer flexible domains; thus, variations in this T_{vmax} are closely associated to changes in ether groups present in PUU.[208,237]

TGA data of the membranes are reported in Table 14 and Table 15 for batch A and B of WPUU, respectively. The introduction of Ag NP into the polymer matrix decreased the initial degradation temperatures (T_{onset}) as general trend. This modification is related to the high thermal conductivity of silver compared to usual polymeric materials.[238,239] Since silver conducts more efficiently the heat inside the composite material, it anticipates the thermal decomposition process, reducing the T_{onset} as compared to neat WPUU.

Table 14 – Thermal degradation data of the WPUU/Ag NP membranes from batch A of WPUU

Membrane (Batch A)	**T_{onset} (°C)**	**T_{vmax} (°C)[a]**
WPUU	212(5)	386(1)
1% Ag NP	200(3)	384(3)
2.5% Ag NP	169(2)	386(1)
5% Ag NP	165(2)	385(2)

Note: The number in parenthesis is the standard deviation; a – T_{vmax} of the second degradation stage.
Source: The author, 2018.

Table 15 – Thermal degradation data of the WPUU/Ag NP membranes from batch B of WPUU

Membrane (Batch B)	**T_{onset} (°C)**	**T_{vmax} (°C)[a]**
WPUU	206(5)	373(1)
1% Ag NP	194(3)	370(3)
10% Ag NP	167(4)	361(3)
30% Ag NP_{ppt}	191(1)c	375(17)c
30% Ag NP*	179(1)c	386(15)c
50% Ag NP*	179(1)c	381(5)

Note: The number in parenthesis is the standard deviation; a – T_{vmax} of the second degradation stage; b – duplicate.
Source: The author, 2018.

Meanwhile, at the second thermal degradation stage, the temperature at maximum rate of weight loss (T_{vmax}), which is related to the soft domains decomposition,[208,240] seems to not have a single behavior upon the addition of Ag NP into the WPUU matrix. Up to 5% Ag NP membrane, there were no significant changes, but in the 10% Ag NP material the T_{vmax}

decreases and it has the tendency to increase in the free $NaNO_3$ membranes. This observation suggests that Ag NP and $NaNO_3$ were placed in the soft chains of the polymer interfering in the degradation of this domain. By removing the $NaNO_3$ from the membranes using the washing procedure, there is a trend to increase the T_{vmax} upon the addition of Ag NP. This behavior is related to interaction among Ag NP and the WPUU ether groups that favors the increasing of T_{vmax}.[239,241] The FTIR results confirm this kind of interaction showing a shift band in ether region for the 50% Ag NP* membrane.

2.5 Conclusions

The method adopted for the synthesis *in situ* of Ag NP, using WPUU aqueous dispersion as stabilizing agent, was able to overcome the challenges to controll the suitable dispersion and low polydispersity of Ag NP in aqueous medium. The WPUU/Ag NP dispersions were employed to prepare WPUU/Ag NP membranes with silver content up to 50wt%. During the preparation of higher concentrated Ag NP membranes, it was necessary to remove $NaNO_3$, which is a synthesis residue.

TEM, SAXS, and XRD results demonstrated that synthesized Ag NP were in nanometric scale, with less than 20 nm. For the 50% Ag NP* membrane, FTIR data showed an interaction among the Ag NP and WPUU ether groups, in addition, tendency of microphase miscibility among WPUU hard and soft domains was found. The Ag NP-ether interaction is also responsible for delaying the second thermal degradation stage of WPUU in free $NaNO_3$ composites; however, the Ag presence had an anticipative effect related to T_{onset} of the material.

By these results, the synthesis *in situ* of Ag NP in WPUU dispersion, without any additional stabilizing agent, was demonstrated as a proper procedure to the preparation of WPUU/Ag NP membranes with silver content up to 50wt%.

3 OLEFIN/PARAFFIN GAS PERMEATION

3.1 Introduction

Regarding membrane gas separation processes, olefin/paraffin gas separation is sometimes referred as the "holy grail" of membrane technology since ethylene and propylene are the most important building blocks for petrochemical industry.[28] The available commercial polymeric membranes using the solution–diffusion mechanism[109] do not achieve the desired performance for useful industrial operation. Much research is been undertaken aiming the production of appropriate materials for this kind of separation. The majority of studies investigates the facilitated transport membranes using carrier agents, which bind with olefins by the π-complexion reaction.[19,41] Generally, transport membranes using silver (Ag) salts as carrier agents have been demonstrating better selectivity and permeability, when compared to passive transport membranes.[40] Despite the superior separation properties of those systems, in general, some Ag salts carrier agents do not have enough stability to keep a long-term performance separation.[28] As an attempt to solve this problem, many authors have been pointing out to carrier agents based on Ag nanoparticles (NP), as promising chemical stable carriers for facilitated transport membranes.[19,42–46] Ag NP can introduce resistance to the membrane against exposure to light and poisonous agents, as hydrogen and acetylene, resulting in desirable chemical stability, during the separation process.[24] The investigation of new membranes based on Ag NP with long-term resistant performance is the challenge for many authors.[24,42,44,73]

Considering all suitable characteristics of Ag NP and WPUU, a study investigating the transport properties of petrochemical gases through WPUU/Ag NP material is reasonable to be proposed. To act as carrier, Ag NP require a suitable activator agent[42–44,71,72,74,75] to polarize their surface to form a partial charge, which is responsible by the interaction with olefins.[43,76] For the experiments in this Thesis, it was chosen p-benzoquinone (p-BQ) and 1-butil-3-methilimidazolium tetrafluoroborate ($BMImBF_4$) due to the lower price of these activator agents comparing with other compounds. The concentration of Ag NP inside the polymer matrix should be higher than 30 wt% and NP should have diameters smaller than 30 nm to achieve the facilitated transport.[46]

Other alternative that literature has shown as promising is the introduction of ionic liquids (IL) to stabilize Ag^+ salts in facilitated transport membranes. Relate to this option, Ortiz et al.[22,77] developed a material with promising characteristics for the separation of light olefins/paraffins. Composite films of poly (vinylidene fluoride-co-hexafluoropropylene)

(PVDF-HFP)/$BMImBF_4$–$AgBF_4$ reached C_3H_6/C_3H_8 mixture selectivity of 700 and propylene permeability of 6630 Barrer (*ca.* 55 GPU) in long-term permeation tests for 10 days. This remarkable performance motivated the use of this system ($AgBF_4$/$BMImBF_4$) in membrane of WPUU as attempt to overcome Ag^+ cation deactivation.

Therefore, the general objective of this chapter is to investigate the gas transport behavior in WPUU membranes with Ag NP/activator and $AgBF_4$/$BMImBF_4$ systems. The specific goals of this part of Thesis are:

(i) to perform permeation tests using WPUU/Ag NP membranes, which was analyzed in Chapter 2; moreover, to introduce $BMImBF_4$ and p-BQ as activator/polarizing agents;

(ii) to prepare WPUU/$AgBF_4$ membranes and test them in gas permeation experiments;

(iii) to check the influence of $BMImBF_4$ in the gas transport behavior of the WPUU/$AgBF_4$ membranes.

3.2 Experimental

3.2.1 Materials

The gases (C_2H_4, C_2H_6, and CO_2 with a minimum purity of 99.9%) were supplied by Linde do Brasil. Propylene and propane gas were purchased from Praxair with a minimum purity of 99.5%. Poly(urethane urea) used in this work was prepared as described in section 3.2.2. The ionic liquid (IL) $BMImBF_4$ (CAS number 174501-65-6) was provided by Iolitec, with a minimum purity of 99%. Silver tetrafluoroborate (CAS number 14104-20-2) of 99% purity was purchased from Apollo Scientific Ltd. Anhydrous ethanol (CAS number 64-17-5) and p-benzoquinone (p-Bq) (CAS number 106-51-4) were supplied by Sigma Aldrich. Microporous support of PVDF was purchased from Merck.

3.2.2 Membranes preparation

3.2.2.1 Membranes based on WPUU/Ag NP

Besides the membranes prepared as described in section 3.2.2., other membranes with IL or p-Bq were prepared by adding these compounds directly into alcoholic solution of WPUU/Ag NP under 5 min of mild stirring. After, the mixture was cast onto a Teflon mold and

placed inside a vacuum oven to form the membranes. For all mixture gas experiments, the tests were performed placing the membranes onto a PVDF-HFP microporous support to avoid any damage to the film.

An additional WPUU formulation, WPUU(2), was used to prepare the membranes. WPUU(2) was synthesized by using a NCO/OH ratio of 2, while WPUU formulation has NCO/OH ratio of 1.5. The expectation is that WPUU(2) should be less elastomeric than WPUU due to the higher content of hard segments when compared to WPUU. The same procedure, used to prepare WPUU/50% Ag NP salt free membrane (Chapter 2), was performed to prepared WPUU(2)/50% Ag NP salt free membrane. All WPUU/Ag NP membranes prepared for gas permeation experiments are listed in Table 16. The codes for each membrane are expressed as weight ratio based on 0.750g of dried polymer.

Table 16 – WPUU/Ag NP membranes prepared for gas permeation experiments

Membrane (weight ratio based on 0.750g of WPUU)
1 WPUU
1 WPUU : 1 Ag NP (equivalent to 50% Ag NP)
1 WPUU : 0.28 Ag NP : 0.2 IL**
1 WPUU : 0.42 Ag NP : 0.25 IL**
1 WPUU(2)
1 WPUU(2) : 1 Ag NP
1 WPUU(2) : 1 Ag NP : 0.5 IL
1 WPUU(2) : 1 Ag NP : 1 IL
1 WPUU(2) : 1 Ag NP : 1 IL : 0.85 p-Bq[43]

Note: *50% Ag NP: membrane prepared from alcoholic solution and salt free, see the preparation in chapter 2; **membrane prepared by adding WPUU alcoholic solution to dilute the original 1 WPUU : 1 Ag NP solution.
Source: The author, 2018.

3.2.2.2 Membranes based on WPUU/$AgBF_4$

During the synthesis of WPUU dispersions, dimethylolpropionic acid (DMPA) was neutralized by triethylamine (TEA) resulting in an aqueous media with pH = 9.5. High pH and amines are source of reduction for Ag^+ cation; thus, a pretreatment should be carried out previously to the use of WPUU dispersion.

WPUU dispersion was neutralized by $HCl_{(aq)}$ 37% w/w until complete precipitation of polymer. The neutralized polymer was washed several times with H_2O (pH<3). The resultant material was solubilized in ethanol at 75° C. After solvent removal, the dried final material, free of TEA, was used to prepare the WPUU/$AgBF_4$ membranes.

The membranes were prepared by the solubilization of 0.750 g of WPUU pretreated in ethanol. To alcoholic polymer solution was added $AgBF_4$ and $BMImBF_4$. After, the mixture was cast onto a PVDF-HFP microporous support and placed inside a vacuum oven to form the composite membranes. Due to the poor mechanical stability of the material, it was necessary to carry out the casting directly upon to PVDF-HFP microporous support. All $AgBF_4$/WPUU membranes prepared for gas permeation experiments are listed in Table 17. The codes for each membrane are expressed as weight ratio based on 0.750g of polymer. The base for weight ratio used in this work was 1polymer: 1 $AgBF_4$, the same as used in the work of Pinnau and Toy.[155] The base for weight ratio of polymer and IL was in according with Fallanza et al.[22]

Table 17 – $AgBF_4$/WPUU membranes prepared for gas permeation experiments

Membrane (weight ratio based on 0.750g of WPUU)
1 WPUU
1 WPUU : 0.25 IL
1 WPUU : 1 $AgBF_4$
1 WPUU : 1 $AgBF_4$: 0.25 IL
1 WPUU : 1 $AgBF_4$: 0.50 IL
1 WPUU : 2 $AgBF_4$: 0.50 IL

Source: The author, 2018.

3.2.3 Gas permeation tests

3.2.3.1 Simple gas experiments

The gas transport properties were determined in an apparatus for gas permeation measurements by using a variable pressure and constant volume method,[242] in which the permeate flux is measured by monitoring the pressure increase of collected permeate gas in a closed volume using a pressure transducer. The permeability of the gases was measured at 2 bar through the membrane, at 308 ± 0.2 K. Permeabilities, **P** (in Barrer), was calculated from the initial slope of the pressure curve on the permeation side *vs.* time, using the Equation (6), where the $\boldsymbol{dp^p/dt}$ (cmHg·s^{-1}) is the rate of pressure measured by the pressure sensor in the low-pressure downstream chamber, $\boldsymbol{V^p}$ (cm^3) is the downstream volume, $\boldsymbol{T}$ (K) is the temperature of the experiment, **δ** (cm) is the thickness of the film, $\boldsymbol{A_m}$ (cm^2) is the film effective area of permeation and $\boldsymbol{\Delta p}$ (cmHg) is the pressure difference through the film. For the experiments, $\boldsymbol{V^p}$ = 7 cm^3, $\boldsymbol{A_m}$ = 4.9 cm^2, and **δ** ≈ 0.300 cm or 300 µm. To check the reliability,

the measurements were made twice for each film, and the standard deviation between the replicates was less than 0.05 Barrer.

$$P = \frac{273.15}{76}\frac{dp^p}{dt}\frac{V^p}{TA_m}\frac{\delta}{\Delta p} \quad (6)$$

3.2.3.2 Mixture gas experiments

The membranes prepared were placed into a permeation cell (46.5 cm^2). The tests were performed inside an oven with temperature control (298 ± 0.2 K). Gas flow rates were controlled by a mass flow controller. The feed stream (20 ml/min - mixed gas 50/50% v/v C_3H_8/C_3H_6) flows through the upper chamber, while the nitrogen used as sweep gas (20 ml/min) flows through the permeate side. The pressure was controlled using micrometric valves. The feed and the permeate stream were analyzed by gas chromatography. The analysis was performed in a gas chromatograph HP 6890 equipped with a thermal conductivity detector (TCD) and a column HP Al/S (30m length, nominal diameter of 0.53 mm).

The experimental permeabilities of each gas were calculated using the Equation (3). At least two samples were collected to calculate the olefin or paraffin flux. The relative deviation of the gas composition analysis was *ca.* 5%. For some membranes, it was not possible to measure the thickness of the film; thus, the experiments results were reported in GPU (1 GPU=1×10^{-6} cm^3 (STP)/cm^2 s cmHg). All results reported in GPU were based on 0.750g of polymer. For all results reported in Barrer, the thickness of the membranes was *ca.* 100 µm.

3.3 Results

3.3.1 Membranes based on WPUU/Ag NP

The permeability values of CO_2, C_2H_4, and C_2H_6 in WPUU/Ag NP membranes are presented in Table 18. CO_2 was used in these tests due to its high affinity to the WPUU matrix, providing valuable information related to property changes in polymer matrix. CO_2 and C_2H_4 can interact with ether groups present in soft domains of WPUU matrix. Thus, both gases should have considerable solubility in WPUU. C_2H_6 does not share the same affinity by ether groups, making it less soluble in the material. WPUU used is elastomeric, consequently, sorption is the dominant step, which favors CO_2 and C_2H_4 transport in neat WPUU membrane.[110,213] The FTIR

analysis of this material (Chapter 2) did not show any significant change in ether region of spectra. Therefore, upon the addition of Ag NP, the WPUU membrane did not interact preferentially through ether groups. Since ether groups were not altered upon Ag NP addition, it is reasonable to discard expressive changes in the sorption behavior of the material. Thus, the main affect to be considered is the change in the diffusional pathway caused by tortuosity increase upon the Ag NP introduction. If this hypothesis is correct, the drop in the permeability should follow the molecular size of gases molecules, from large to small compound. This effect should be more evident in high Ag NP content; hence, it will be considered 30% Ag NP* membrane to analyze this behavior. The order of permeability drop is: C_2H_6 (68%) > C_2H_4 (64%) > CO_2 (48%) with similar C_2H_6 and C_2H_4 drop. The size order of molecules is: C_2H_6>C_2H_4>CO_2 with very close C_2H_6 and C_2H_4 sizes.[243] By this comparison, it is clear that the same trend was found, confirming the change in the diffusional pathway caused by Ag NP. Additionally, the gas transport results for membranes up to 30 wt% of Ag NP content did not show any facilitated transport of olefins as depicted by $\alpha^{**}(C_2H_4/C_2H_6)$ nearly to 1.

For membranes with 50 wt% of Ag NP content, permeation test was performed using propylene/propane gas mixture (50:50 vol%) (Table 19). Even with 50wt% of Ag NP (weigh ratio 1 WPUU: 1 Ag NP) in the membrane, it was not possible to observe the facilitated transport of olefin in both membranes, 50% Ag NP WPUU and WPUU(2) free salt. In 1 WPUU: 1 Ag NP membrane, the FTIR analysis showed an Ag NP/ether group interaction (Chapter 2); however, this interaction was not enough to activated Ag NP to the facilitated transport.

Therefore, an external activated agent is required.[19] For this purpose, an ionic liquid (IL), $BMImBF_4$,[22,45] and p-benzoquinone (p-Bq)[43] was selected to be introduced in WPUU/Ag NP membranes. IL improved discreetly the selectivity (the highest selectivity founded was 2.37 for 1 WPUU(2) : 1 Ag NP : 1 IL) of the membranes due to its affinity by olefin (Table 19). However, Ag NP activation by IL was not detectable in the test. The olefin flux did not increase as expected. The membrane with p-Bq achieved the best selectivity (2.92) among WPUU/Ag NP membranes. Nonetheless, the presence of this activator was not enough to provide the facilitated transport of olefin through the membrane. One hypothesis to the failure of p-Bq use as activator is the poor stability of this electron acceptor that can be reduced easily to hydroquinone. The reduced form of p-Bq is not active to polarize the surface of Ag NP demonstrating a real drawback to the application of this activator in WPUU/Ag NP membranes. Compounds like p-Bq, (7,7,8,8-tetracianequinodimethane) TCNQ and tetrathiafulvalene (TTF) work as electron acceptor; thus, they have a tendency of withdrawing electrons from other molecules. This feature makes polarizing agents susceptible to chemical attack similarly as it is

found in Ag^+ cation that results in reduced species unable to polarize the surface of Ag NP.

Table 18 – Permeability of CO_2, C_2H_6 and C_2H_4 in WPUU/Ag NP membranes

Membrane	**Permeability (Barrer)**			**α**(C_2H_4/C_2H_6)**	**Permeability drop related to neat WPUU**		
	CO_2	**C_2H_6**	**C_2H_4**		**CO_2**	**C_2H_6**	**C_2H_4**
WPUU	296	109	132	1.21	—	—	—
1% Ag NP	256	105	129	1.23	14%	4%	2%
10% Ag NP	219	82	98	1.20	26%	25%	26%
30% Ag NP*	154	35	47	1.30	48%	68%	64%

Note: Condition: 2 bar transmembrane pressure. *30% Ag NP: membrane prepared from alcoholic solution, see the preparation in chapter 2; **Ideal selectivity.
Source: The author, 2018.

Table 19 – Permeability of C_3H_8 and C_3H_6 in WPUU/Ag NP membranes

Membrane (weight ratio based on 0.750g of WPUU)	**Permeability**		**α^a(C_3H_6/C_3H_8)**
	C_3H_8	**C_3H_6**	
1 WPUU	140	245	1.75
1 WPUU : 1 Ag NP (50% Ag NP*)	—	—	1.73
1 WPUU : 0.28 Ag NP : 0.2 IL**	65.1	120	1.84
1 WPUU : 0.42 Ag NP : 0.25 IL**	62.6	140	2.00
1 WPUU(2)	92.1	171	1.84
1 WPUU(2) : 1 Ag NP	78.5	143	1.79
1 WPUU(2) : 1 Ag NP : 0.5 IL	67.7	144	2.12
1 WPUU(2) : 1 Ag NP : 1 IL	56.9	145	2.37
1 WPUU(2) : 1 Ag NP : 1 IL : 0.85 p-Bq	0.239[b]	0.700[b]	2.92

Note: Condition: 0.2 bar transmembrane pressure. WPUU: NCO/OH ratio of 1.5. WPUU(2): NCO/OH ratio of 2. *50% Ag NP: membrane prepared from alcoholic solution and salt free, see the preparation in chapter 2; **membrane prepared by adding WPUU alcoholic solution to dilute the original 1 WPUU : 1 Ag NP solution. a - mixed gas (50:50 vol % of propylene/propane mixture); b – permeance, long-term test of 104 h.
Source: The author, 2018.

3.3.2 Membranes based on WPUU/$AgBF_4$

FTIR analysis is an essential tool to evaluate the changes in proton donator and proton acceptor groups of WPUU.[113,223] The goals of this section is to evaluate the possible interactions of $AgBF_4$ and $BMImBF_4$ inside the polymer matrix and how these interactions affects the structure of the WPUU.

3.3.2.1 Infrared Spectroscopy (FTIR)

The FTIR spectra of $AgBF_4$ and H_2O are depicted in Figure 24.[244–246] Due to the hygroscopicity,[175] H_2O bands (v O-H and δ O-H) appear in the $AgBF_4$ spectrum. Moisture

bands are also present in membrane FTIR spectra when a high content of $AgBF_4$ is used in analyzed films.

Figure 24 – FTIR spectra of $AgBF_4$ and H_2O

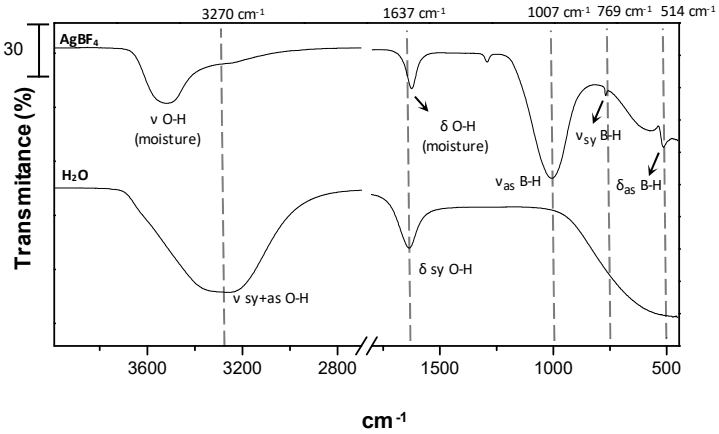

Source: The author, 2018.

Figure 25a shows the FTIR profile of the films prepared with different contents of $AgBF_4$. As $AgBF_4$ was added in WPUU matrix, the ether band shifted from 1095 cm^{-1}(neat polymer) to1047 cm^{-1} in the film with weight ratio of 1 WPUU:1 $AgBF_4$. This frequency decrease indicates an intensification of interaction among ether groups and the Ag^+ cations (Figure 25d).[154,155,157] The ether/Ag^+ interaction leads to a weakening of the former ether/N-H interaction that is depicted by the frequency increase of N-H bonded band from 3332 cm^{-1} to 3396 cm^{-1} (Figure 25b). Mainly in 1 WPUU:1 $AgBF_4$ film, Ag^+ cation also interacted with urethane C=O, which is at the interface between the hard and soft phase of WPUU. Urethane C=O band frequency decreased from 1712 cm^{-1} to 1677 cm^{-1} (Figure 25c), indicating an interaction intensification related to these groups. On the other hand, the urea C=O band frequency seems to increase from 1641 cm^{-1} to higher values (Figure 25c) (it was not possible to check it in 1 WPUU:1 $AgBF_4$ film due to moisture interference) that can be interpreted as a weakening of interactions among urea and urethane C=O since urea groups are inner inside WPUU hard domains. Presumably, Ag^+ cation did not reach the hard domain cores. The interaction weakening of urea groups was related to unavailability of urethane N-H groups that suffered Ag^+/urethane interference at the interfacial region.

Figure 25 – FTIR spectra of WPUU/$AgBF_4$ films

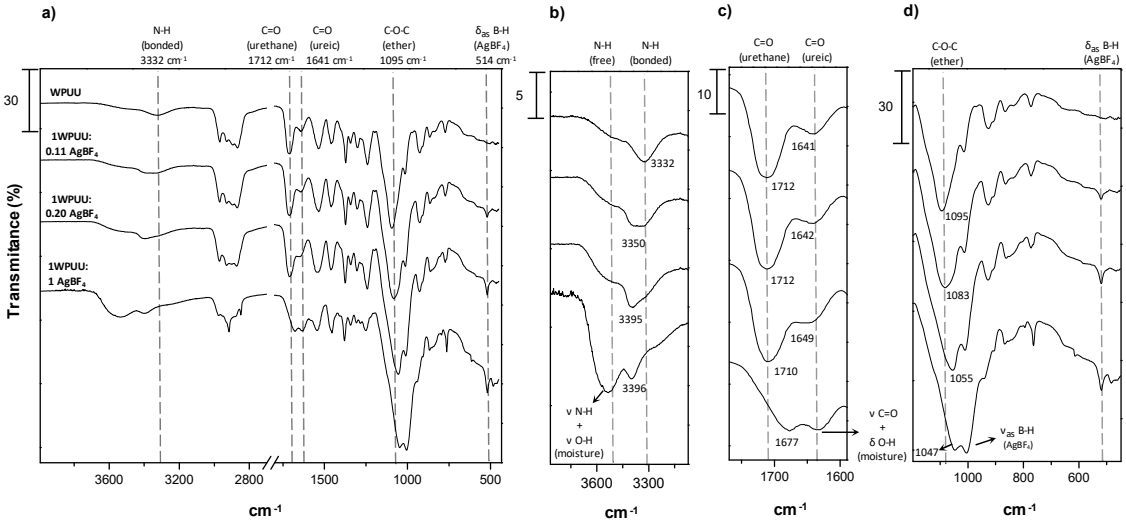

Source: The author, 2018.

Figure 26 – FTIR spectra of WPUU/IL and WPUU/$AgBF_4$/IL films

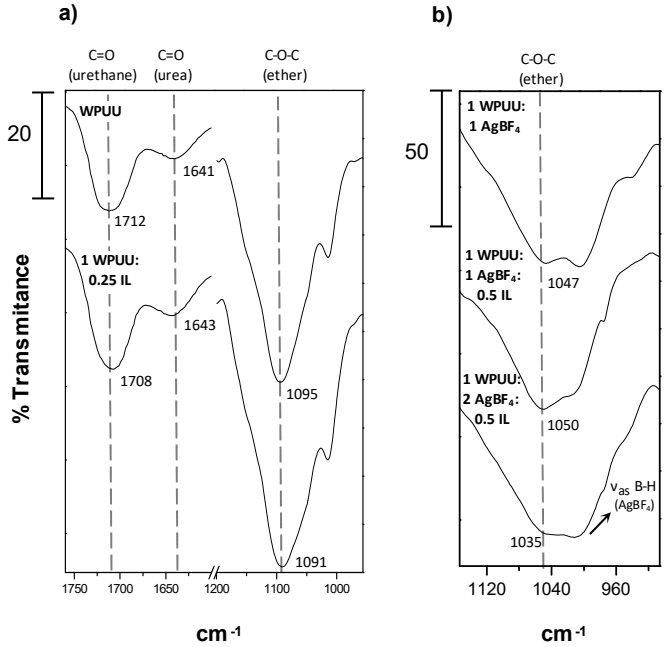

Source: The author, 2018.

The introduction of IL in the WPUU matrix seems to follow the same interaction behavior like in $AgBF_4$ case; however, less intense. In the film with weight ratio of 1 WPUU: 0.25 IL, the ether band and urethane C=O band frequencies decreased from 1095 cm^{-1} to 1091 cm^{-1} and from 1712 cm^{-1} to 1708 cm^{-1}, respectively. Additionally, the urea C=O band frequency increased from 1640 cm^{-1} to 1643 cm^{-1} (Figure 26a). These FTIR results suggest an IL cations (imidazolium) interaction with ether and urethane group to some extent.

The influence of IL upon the WPUU/$AgBF_4$ composite was also verified using FTIR. The main change was in the ether region. Compared to the 1 WPUU:1 $AgBF_4$ film, the material with weight ratio of 1 WPUU: 1 $AgBF_4$: 0.5 IL showed an ether band shift to high frequencies, from 1047 cm^{-1} to 1050cm^{-1} (Figure 26b). This frequency increase suggests a weakening of the interaction between the Ag^+ cations and the ether groups caused by the addition of IL.[26] However, the same IL behavior was not maintained when the $AgBF_4$ content was doubled. In 1 WPUU: 2 $AgBF_4$: 0.5 IL film, the Ag^+/ether interaction was intensified due to the high $AgBF_4$ content. It can be checked by the large shift to lower frequencies in ether band, from 1050 cm^{-1} to 1035 cm^{-1} (Figure 26b).

Therefore, by observing the ether region of WPUU FTIR spectrum is possible to investigate the main interaction, Ag^+/ether group, in the WPUU/$AgBF_4$ composites. Ag^+/ether group interaction is the principal responsible for the dissolution of the $AgBF_4$ salt in the polymer matrix. This interaction may be smoothed by the addition of IL in the formulation of WPUU/$AgBF_4$ composite material.

3.3.2.2 Gas permeation

To find out the $AgBF_4$ concentration that could provide the facilitated transport in WPUU matrix, it was prepared some WPUU/$AgBF_4$ membranes with different silver salt contents. The initial membrane composition able to perform the facilitated transport of olefin was the weight ratio of 1WPUU:1 $AgBF_4$ based on 0.750g of polymer.[155] During the permeation (Figure 27), olefin flux increased until 3.15h of experiment due to the growing number of olefin molecules that began to complex with Ag^+ cation and hop from carrier to carrier in order to cross the membrane.[154] Within the membrane, the Ag^+ can interact with coordination site of the WPUU matrix (i.e. ether oxygen atoms) to form desirable free ions pairs, which is more useful to the olefin complexation than the original crystal structure of salt. [69,165–167] However, instead of reaching a stable value, establishing the steady facilitated transport flux, the olefin flux started to decrease. Apparently, the decrease is because the removal of residual solvent or moisture trapped inside the polymer matrix. One important moisture holding inside the membrane is the $AgBF_4$, which is a very hygroscopic salt.[175] The few residual liquids were dragged while the dried gas mixture crossed the membrane.

Figure 27 – Flux of propylene, propane, and selectivity vs. permeation time for WPUU/$AgBF_4$ membranes

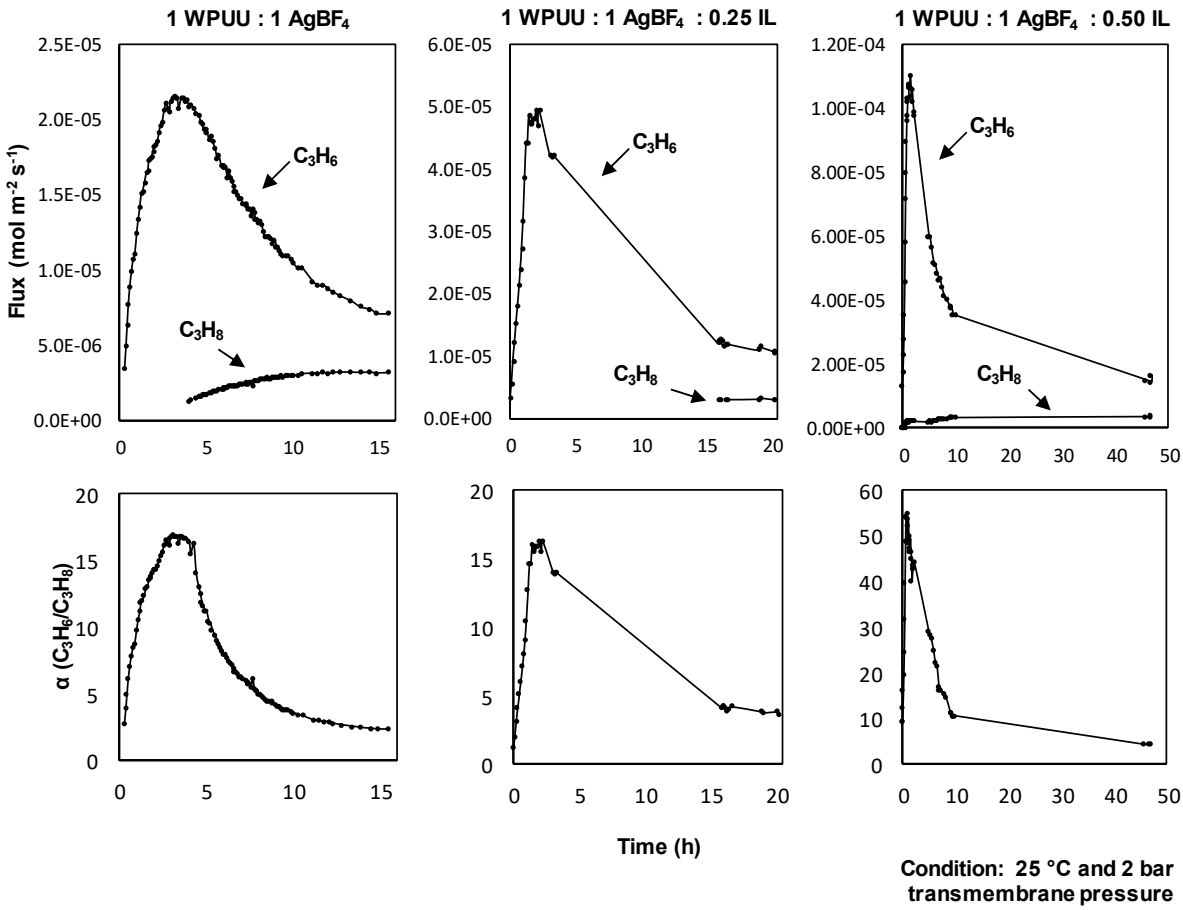

Source: The author, 2018.

Water can form Ag^+ aquo complex that supports the salt dissolution.[18] In its solvated form, Ag^+ cations are more available to the interaction with the olefin. The drying process leads to a loss of one of the dissolution sources remaining only the dissolution provided by the polar polymer chains. As the moisture was dragged from the membrane, the polymer dissolution did not show the ability to sustain the silver availability for the olefin reversible complexation. In this case, the WPUU interaction with the Ag^+ cation makes it so attached to ether groups that the metal becomes less available for the olefin interaction, in a certain extend. Presumably, this is one of possible reasons for the decreasing of olefin flux during the permeation experiment.

Another cause could be the reduction of Ag^+ by the polymer interaction, which can deactivate the Ag^+ transforming it into Ag^0. Roughly, the Ag^0 formation can just be detected by simple inspection of the membrane at the end of permeation, since agglomerations of Ag^0 is dark and the WPUU material is colorless. This verification was made, and no black spots were

observed at the end of the 63 h of permeation. This does not mean that any Ag^0 formation takes place, but it can be assumed that there was no evidence of a critical reduction process in the membrane. Another evidence that corroborated to this assumption was the difference about flux behavior of both gases. Silver nanoparticles growth during the permeation process leads to the formation of interfacial void that become large. Through this voids, both gases can pass instinctively resulting in the increase of flux but in the decreasing of selectivity.[65]

Initially, the silver reduction was discharged as hypothesis during the permeation experiment. Thus, to solve the unviability of the Ag^+ for the olefin complexation during the runs, ionic liquids were thought as an alternative to smooth the interaction between Ag^+ and WPUU ether groups. The ionic liquid (IL) chosen was the $BMImBF_4$ due to its known behavior in composite membrane of PVDF-HPF/$AgBF_4$ in the work of Ortiz et al.[22] Moreover, this IL adds a proper factor to the membrane. The system $BMImBF_4$/$AgBF_4$ can avoid the potential reduction of Ag^+ by the polymer chain interactions.[167,184]

Figure 28 and Table 20 show the effect of IL content in the olefin maximum flux (J_{max}) achieved. Compared to the membrane without IL, the olefin J_{max} increased 2.3 and 5.1 times in the membrane with weight ratio of 1 WPUU:1 $AgBF_4$:0.25 IL and 1 WPUU:1 $AgBF_4$:0.5 IL, respectively. In addition, membranes with a high IL content reach the J_{max} sooner. This J_{max} anticipation and the higher J_{max} values reached show the properly IL support to the olefin flux in the WPUU membranes. However, after membranes with IL reach the J_{max}, the olefin flux followed the same behavior of the membrane without IL. The olefin flux started to decrease, probably because the removal of residual solvent or moisture trapped inside the polymer or in the IL medium. At the end of permeation experiments, either the IL could not sustain the high values of olefin flux.

As an attempt to increase the olefin flux, a membrane with weight ratio of 1 WPUU:2 $AgBF_4$:0.5 IL was prepared. The membrane showed the same behavior of previous membranes. The initial olefin flux increased, afterward, it started to decrease during the permeation time (Figure 29). Compared to 1 WPUU:1 $AgBF_4$:0.5 IL membrane, this high content $AgBF_4$ film increased the olefin J_{max} 5.6 times. Moreover, the J_{max} was anticipated from 1.52 h to 0.42 h (Figure 30).

Figure 28 – Flux of propylene and propane vs. permeation time for WPUU/$AgBF_4$ membranes in the initial time of the experiments

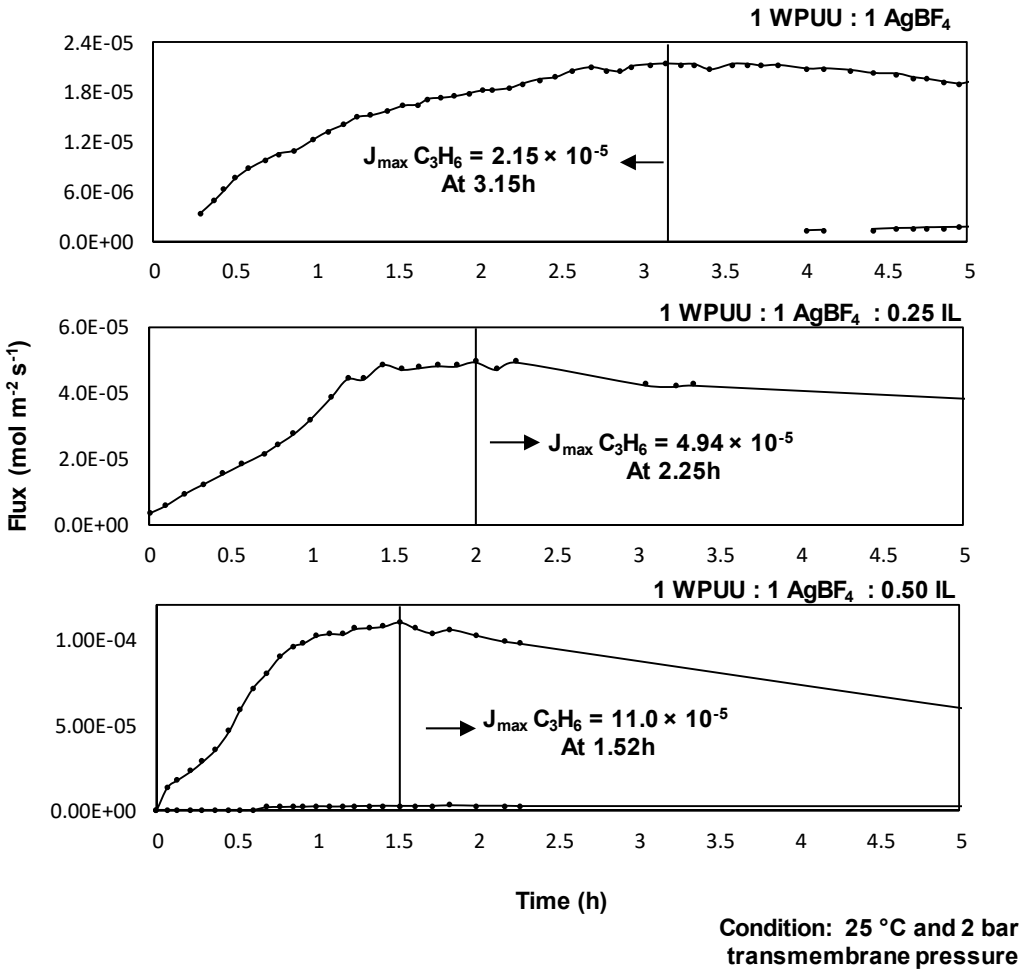

Source: The author, 2018.

Table 20 – Results for the WPUU/$AgBF_4$ membranes

Membrane (weight ratio based on 0.750g of WPUU)	J_{max} C_3H_6 (10^{-5} mol m^{-2} s^{-1})	α_{max} (C_3H_6/C_3H_8)	Permeance (GPU)		Time of maximum values (h)
			C_3H_8	C_3H_6	
1 WPUU	5.15*	1.80	0.59	1.06	—
1 WPUU : 0.25 IL	4.35*	1.95	0.45	0.86	—
1 WPUU : 1 $AgBF_4$	2.15	>16.8	0.02	0.44	3.15
1 WPUU : 1 $AgBF_4$: 0.25 IL	4.94	>16.2	0.06	1.01	2.25
1 WPUU : 1 $AgBF_4$: 0.50 IL	11.0	48.9	0.04	2.28	1.52
1 WPUU : 2 $AgBF_4$: 0.50 IL	61.6	97.5	0.15	13.94	0.42

Note: Condition: 25 °C and 2 bar transmembrane pressure. *Stationary flux values.
Source: The author, 2018.

Figure 29 – Flux of propylene, propane, and selectivity vs. permeation time for the membrane with high $AgBF_4$ content

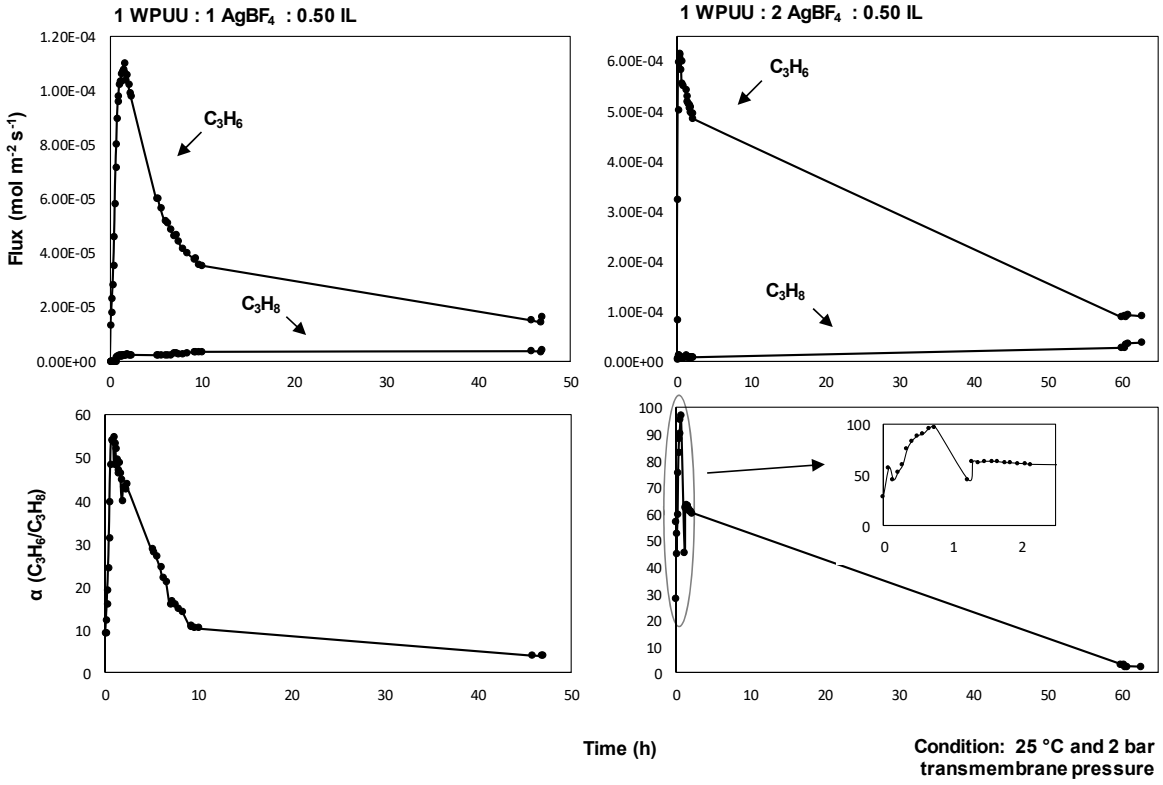

Source: The author, 2018.

Figure 30 – Flux of propylene, propane, and selectivity vs. permeation time for membrane with high $AgBF_4$ content in the initial time of the experiments

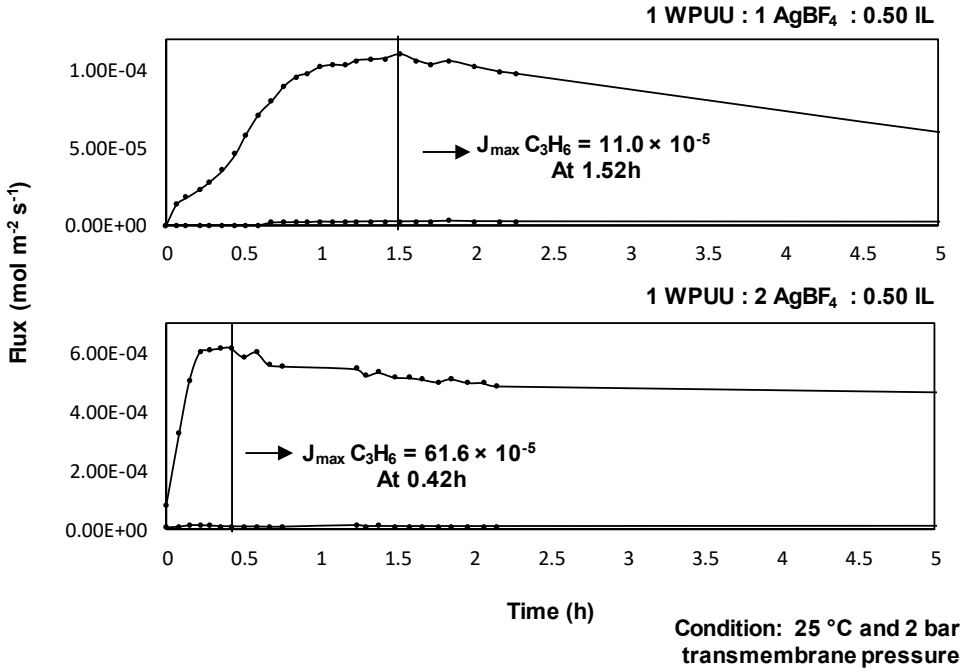

Source: The author, 2018.

To check the carrier properties of the membrane after the decline of olefin flux in the first hours of permeation, the permeation cell was opened (protected from light) and closed after 15 min. The permeation test was restarted to observe the olefin flux behavior (Figure 31). The membrane used for this test was with the weight ratio of 1WPUU : 1 $AgBF_4$: 0.25 IL. Initially, the membrane achieved the olefin J_{max} of 4.94 10^{-5} mol m^{-2} s^{-1}, afterward, the flux decline started until attain the olefin flux of 1.06 10^{-5} mol m^{-2} s^{-1} at 20.3 h of experiment. At this point, the cell was opened and closed after 15 min. Olefin flux was recovered 4.15 10^{-5} mol m^{-2} s^{-1} (recovery of 84%), but, after 27.2 h the olefin flux attain the value of 1.01 10^{-5} mol m^{-2} s^{-1}. This result shows that the initial olefin flux decline in WPUU/$AgBF_4$/IL membranes is mainly caused by moisture loss during experiments with dried gases. The recovery of olefin flux took place when the membrane was in contact with atmospheric air during 15 min., which repairs the moisture level inside the membrane. However, when the dried gases started to cross the membrane, again, the moisture level decreases and the Ag^+ cation becomes tightly attached to ether groups leading to metal unfeasibility for olefin interaction. If any critical Ag^+ reduction problem related to Ag^+/ether interaction might take place, probably, it should occur in larger long-term permeation tests.

Final performance values at the end of long-term permeation experiments are present in Table 21. Compared to WPUU membrane, 1 WPUU: 0.25 IL membrane presented lower values of olefin and paraffin permeance (permeance drop: paraffin 24% and olefin 19%). The FTIR analysis suggests a smooth imidazolium/ether group interaction and probably it could be the cause of olefin and paraffin permeance drops. In less extent, this interaction decreased the chain mobility of polymer matrix influencing on gas transport properties of the membrane. In 1 WPUU: 1 $AgBF_4$ membrane, the intensive Ag^+/ether interaction was responsible for reduce the polymer chain mobility; thus, the permeances of both gases decreased (permeance drop: paraffin 51% and olefin 69%) with selectivity nearly to 1. However, when IL was added the final selectivity of the membranes increased. In 1 WPUU: 1 $AgBF_4$: 0.25 IL membrane was 3.20 and in 1 WPUU: 1 $AgBF_4$: 0.5 IL membrane was 4.07. Compared to 1 WPUU: 1 $AgBF_4$ membrane, the main difference was the low paraffin flux found in the membrane with IL. Probably, the IL could protect the Ag^+ cation against the initial reduction process that produces Ag^0. Over the time, the Ag^0 growth and agglomeration cause the formation of some defects or holes at the interface between the metal particle and the polymer chains. Without discrimination, the gases can easily pass through this pathway with lower mass transport resistance that leads to selectivity loss in long-term permeation experiments.[26] In the membrane without IL, the selectivity nearly to 1 and the higher paraffin flux may be indicate the initial process of Ag^0 formation and growth. When IL is present this process seems to be under control to some extent. The intensive Ag^+/ether interaction was smoothed by the addition of IL, as shown in FTIR analysis. This is the reason for the protection against the silver reduction inside the polymer matrix.

Figure 31 – Flux of propylene and propane vs. permeation for 1 WPUU: 1 AgBF4: 0.25 IL membrane. In this experiment, the permeation cell was opened and closed to restart the run

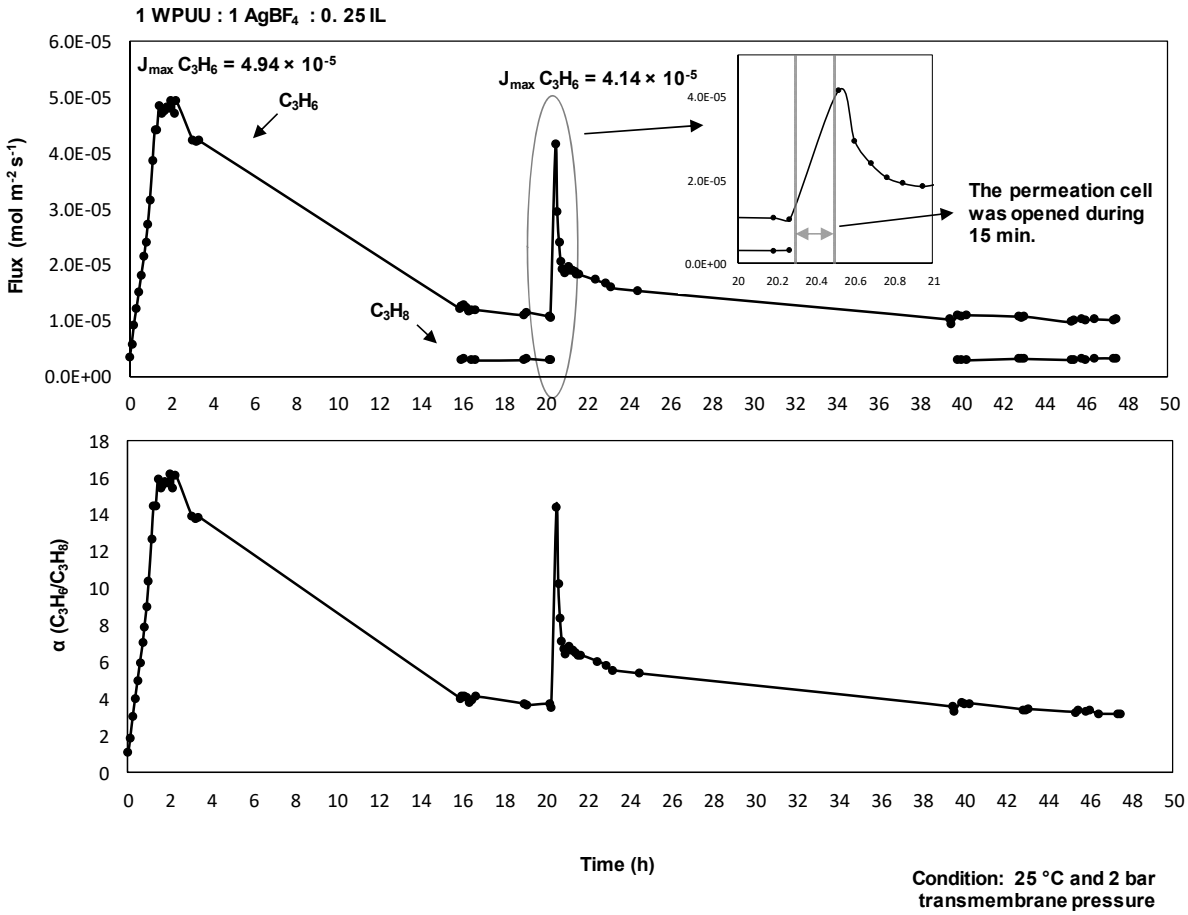

Source: The author, 2018.

Table 21 – Results for the WPUU/AgBF4 membranes at the end of gas permeation experiments

Membrane (weight ratio based on 0.750g of WPUU)	J C_3H_6 (10^{-5} mol m^{-2} s^{-1})	α (C_3H_6/C_3H_8)	Permeance (GPU)		Time of experiments values (h)
			C_3H_8	C_3H_6	
1 WPUU	5.15	1.80	0.59	1.06	28.8
1 WPUU : 0.25 IL	4.35	1.95	0.45	0.86	45.6
1 WPUU : 1 $AgBF_4$	1.63	1.12	0.29	0.33	63.1
1 WPUU : 1 $AgBF_4$: 0.25 IL	1.02	3.20	0.06	0.20	47.5
1 WPUU : 1 $AgBF_4$: 0.50 IL	1.65	4.07	0.08	0.33	46.9
1 WPUU : 2 $AgBF_4$: 0.50 IL	8.98	2.42	0.75	1.85	62.7

Note: Condition: 25 °C and 2 bar transmembrane pressure.
Source: The author, 2018.

In 1 WPUU: 2 $AgBF_4$: 0.5 IL membrane (Table 21), the high content of $AgBF_4$ indeed could provide a higher olefin flux compared to all membranes. However, paraffin flux also followed this behavior, and was the higher among the membranes. The result was a selectivity of 2.42. In this case, the high amount of silver salt maybe was forming some small silver

nanoparticles aggregates inside the polymer matrix during the permeation process, leading to the selectivity loss. Other possibility is the weight ratio of 2 $AgBF_4$: 0.5 IL used that was not enough to ensure the IL protection against the initial reduction process of Ag^+ cation. The FTIR analysis showed that the most intense Ag^+/ether interaction was found in this membrane. Thus, the IL added could not weaken the interaction between the Ag^+ cations and the ether groups avoiding the reduction process.[26]

3.4 Conclusions

It was possible to prepare WPUU/Ag NP membranes up to 50 wt% of silver content. The facilitated transport of olefin was not reached, even with the Ag NP/ether group interaction inside the polymer matrix, which could polarize Ag NP surface. In attempt to provide activation to Ag NP, it was added $BMImBF_4$ or p-Bq to the membranes. The presence of these activator agents improved discreetly the selectivity of the membranes (from 1.84 in 1 WPUU(2) membrane to 2.92 in 1 WPUU(2) : 1 Ag NP : 1 IL : 0.85 p-Bq membrane); however, the facilitated transport was not observed.

WPUU/$AgBF_4$ membranes with more than 50 wt% of $AgBF_4$ (weight ration of 1WPUU: 1 $AgBF_4$) provided a facilitated transport of olefin. However, the olefin flux decreased during the permeation experiment due to the intensive Ag^+/ether interaction in WPUU matrix. As an effort to solve this problem, IL ($BMImBF_4$) was introduced to the electrolyte membranes prepared. IL was able to smooth Ag^+/ether interaction leading to an increase of the final selectivity when compared with membrane without IL. The higher selectivity (4.07) was found in 1 WPUU: 1 $AgBF_4$: 0.5 IL membrane. Before the olefin flux drop, the maximum olefin permeance (13.94 GPU) and selectivity (97.5) was observed in 1 WPUU: 2 $AgBF_4$: 0.5 IL membrane.

The main cause of initial olefin flux decline was the moisture loss during experiments with dried gases. For the 1 WPUU: 1 $AgBF_4$: 0.25 IL membrane, it was possible to recovery (84%) of olefin flux when the permeation cell was opened, and the membrane was in contact with atmospheric air during 15 min., repairing the moisture level of the material. This result suggests that the initial source of olefin flux decline was not the Ag^+ reduction problem, but the moisture loss, which leads to Ag^+ cations unfeasibility for olefin interaction.

GENERAL CONCLUSIONS

Ag NP/activator and $AgBF_4$/$BMImBF_4$ systems were chosen to be tested in waterborne poly(urethane urea) (WPUU) matrix in order to evaluate the maintenance of light olefin/paraffin selectivity in long-term gas permeation tests. To prepare WPUU/Ag NP membranes, the method adopted for the synthesis *in situ* of Ag NP, using WPUU aqueous dispersion as stabilizing agent, was able to overcome the challenges to control the suitable dispersion and low polydispersity of Ag NP in aqueous medium. The WPUU/Ag NP dispersions were employed to prepare WPUU/Ag NP membranes with silver content up to 50 wt%. and free of synthesis residue. TEM, SAXS, and XRD results demonstrated that synthesized Ag NP were in nanometric scale, with less than 20 nm.

WPUU/Ag NP membranes up to 50 wt% of silver content could not reach the facilitated transport of olefin, even with an interaction Ag NP/ether group inside polymer matrix, which could polarize the Ag NP surface. In attempt to provide activation to Ag NP, it was added $BMImBF_4$ or p-Bq to the membranes. However, the facilitated transport was not observed probably because of low electron acceptor feature of $BMImBF_4$ and poor stability of p-Bq. The best result was achieved using the 1 WPUU(2) : 1 Ag NP : 1 IL : 0.85 p-Bq membrane that showed a mixture selectivity of 2.92 and propylene permeance of 0.7 GPU. On the other hand, the facilitated transport of olefins was reached in $AgBF_4$/$BMImBF_4$/WPUU membranes. However, the olefin flux decreased during the permeation experiment. The main cause of initial olefin flux decline was the moisture loss during experiments with dried gases. Therefore, the initial source of olefin flux decline was not the Ag^+ reduction problem, but the moisture loss, which leads to Ag^+ cations unfeasibility for olefin interaction. The best result after olefin flux decline was found in 1 WPUU: 1 $AgBF_4$: 0.5 IL membrane, mixture selectivity of 4.0 and propylene permeance of 0.33 GPU after 45 h of experiment. Before the olefin flux drop, the maximum olefin permeance of 13.94 GPU and selectivity of 97.5 was observed in 1 WPUU: 2 $AgBF_4$: 0.5 IL membrane.

This Thesis reviews the main problems related to the membrane instabilities in olefin/paraffin separations pointing out some perspective of solutions to solve the drawbacks. Among solutions, the use of Ag NP/activator and $AgBF_4$/$BMImBF_4$ systems were selected to be applied in WPUU membranes. These systems presented problems for use in WPUU matrix. The activating agents for Ag NP, $BMImBF_4$ and p-Bq, were not able to provide the facilitated transport of olefins. The $AgBF_4$/$BMImBF_4$ /WPUU membranes reached the facilitated transport of olefin; however, the initial olefin flux decreased during the tests due to humidification

requirement to flux maintenance. Although all efforts in this work, it is not an easy task to achieve or keep the facilitated transport even with promising alternatives highlighted during the Thesis review (Chapter 1). Therefore, the search for other alternatives, new materials to be applied in facilitated transport membrane for olefin separation remains as a challenge.

CHALLENGES FOR FUTURE RESEARCHES

Regarding the experience accumulated during the development of this Thesis, it is possible to point out some challenges for future researches.

Most of the results reported in the literature did not performer permeation test with the presence of poisonous agents. Thus, for future experiments, poisonous agents should be considered in the test to have accesses to more realistic data of operational conditions. With the development of some solutions highlighted in Chapter 1, probably, the future efforts will be dedicated to understand deeply the problems regarding poisonous agents, trying to figure out more robust solutions.

The olefin flux decrease during the initial hours of permeation, reported by many authors as consequence of silver deactivation by reduction, maybe, it can be caused by moisture loss during the passage of dried gases through the membrane. If any deactivation by reduction occurs, the effect of olefin flux decline should be isolated from the moisture loss to clarify the data. Thus, for a fair judgment, future works should present data with dried and humidified feed gases.

There is a clear tendency of using fluorinated polymers for facilitated transport membranes for olefin/paraffin separation (Chapter 1). Therefore, there is a huge gap to study various fluorinated polymer classes or other kind of inert polymer applied to facilitated transport of olefins.[247]

Related to Ag NP, some futures works could ask the following question. Could the shape of silver Ag NP influence in the gas transport? In a material where Ag NP can act properly as olefin carrier, may be very interesting to change the shape of Ag NP with different synthesis conditions and after checking the influence on olefin transport. Other step more audacious may be the orientation control of these Ag NP inside the polymer matrix. For instance, an orientation of flat Ag NP in the flux direction could maximize the olefin flux.

Finally, to avoid the use of polarizing agents for Ag NP activation, some polymers could act like a polarizing agent. Polymer applied in organic solar cell are photovoltaic materials. Normally, these polymers are formed by conjugated double bond structures like in current

polarizing molecules (p-Bq, TCNQ, TTF). One possible work to be proposed is the use of photovoltaic polymer in preparation of membranes with Ag NP for olefin/paraffin separation. This membrane also could be a blend of photovoltaic polymer with an usual polymer matrix that has already been applied for this separation.

REFERENCES

(1) *Petrochemicals Make Things Happen*. Petrochemicals Europe, 2017. Available online at: www.petrochemistry.eu. (Accessed: 1st March 2018)

(2) NAKAYAMA, N. Global Supply and Demand of Petrochemical Products Relied on LPG as Feedstock. In: INTERNATIONAL LP GAS SEMINAR, 2017, Tokyo.

(3) AMGHIZAR, I. et al. New Trends in Olefin Production. Engineering, v. 3, n. 2, p. 171–178, 2017.

(4) FOSTER, J. Can shale gas save the naphtha crackers? *Platts special report: Petrochemicals*, 3 p. 2013.

(5) BROOKS, R. E. Modeling the North American market for natural gas liquids. In: US ASSOCIATION OF ENERGY AND ECONOMICS (USAEE) CONFERENCE, 32., 2013, Anchorage.

(6) REN, T.; PATEL, M.; BLOK, K. Olefins from conventional and heavy feedstocks: Energy use in steam cracking and alternative processes. *Energy*, v. 31, n. 4, p. 425–451, 2006.

(7) CHUAPET, W. et al. A Study of Energy Intensity and Carbon Intensity from Olefin Plants in Thailand. In: INTERNATIONAL CONFERENCE ON INDUSTRIAL ENGINEERING AND APPLICATIONS, 3., 2016, Hong Kong.

(8) ZIMMERMANN, H.; WALZL, R. *Ethylene. Ullmann's Encyclopedia of Industrial Chemistry*. Weinheim: Wiley-VCH, 2012. v. 13. p. 465–529.

(9) FALQI, F. H. *The miracle of petrochemicals. Olefins industry: an in-depth look at steam-crackers.* Florida: Universal-Publishers Boca Raton, 2009.

(10) XU, L. et al. Olefins-selective asymmetric carbon molecular sieve hollow fiber membranes for hybrid membrane-distillation processes for olefin/paraffin separations. *Journal of Membrane Science*, v. 423–424, p. 314–323, 2012.

(11) BAKER, R. W.; LOW, B. T. Gas separation membrane materials: A perspective. *Macromolecules*, v. 47, n. 20, p. 6999–7013, 2014.

(12) PARK, J. et al. Performance Study of multistage membrane and hybrid distillation processes for propylene/propane separation. *The Canadian Journal of Chemical Engineering*, v. 95, n. 12, p. 2390–2397, 2017.

(13) SAFARIK, D. J.; ELDRIDGE, R. B. Olefin/Paraffin Separations by Reactive Absorption: A Review. *Industrial & Engineering Chemistry Research*, v. 37, n. 7, p. 2571–2581, 1998.

(14) BERNARDO, P.; DRIOLI, E.; GOLEMME, G. Membrane gas separation: A review/state of the art. *Industrial & Engineering Chemistry Research*, v. 48, n. 10, p. 4638–4663, 2009.

(15) POZUN, Z. D.; HENKELMAN, G. A model to optimize the selectivity of gas separation in membranes. *Journal of Membrane Science*, v. 364, n. 1–2, p. 9–16, 2010.

(16) ZARCA, R. et al. Optimized distillation coupled with state-of-the-art membranes for propylene purification. *Journal of Membrane Science*, v. 556, p. 321–328, 2018.

(17) AMEDI, H. R.; AGHAJANI, M. Economic Estimation of Various Membranes and Distillation for Propylene and Propane Separation. *Industrial & Engineering Chemistry Research*, v. 57, n. 12, p. 4366–4376, 2018.

(18) ANTONIO, M. R.; TSOU, D. T. Silver Ion Coordination in Membranes for Facilitated Olefin Transport. *Industrial & Engineering Chemistry Research*, v. 32, n. 2, p. 273–278, 1993.

(19) LI, Y. et al. Facilitated transport of small molecules and ions for energy-efficient membranes. *Chemical Society reviews*, v. 44, n. 1, p. 103–18, 2015.

(20) HO, W. S.; DALRYMPLE, D. C. Facilitated transport of olefins in Ag^+-containing polymer membranes. *Journal of Membrane Science*, v. 91, n. 1–2, p. 13–25, 1994.

(21) POLLO, L. D. et al. Polymeric membranes containing silver salts for propylene/propane separation. *Brazilian Journal of Chemical Engineering*, v. 29, n. 2, p. 307–314, 2012.

(22) FALLANZA, M. et al. Polymer-ionic liquid composite membranes for propane/propylene separation by facilitated transport. Journal of Membrane Science, v. 444, p. 164–172, 2013.

(23) MAJUMDAR, S. et al. *Thin film composite membranes for separation of alkenes from alkanes*. W.O. Patent WO2016/182887 A1, November 17, 2016.

(24) KIM, Y. R. et al. Chemical stability of olefin carrier based on silver cations and metallic silver nanoparticles against the formation of silver acetylide for facilitated transport membranes. *Journal of Membrane Science*, v. 463, p. 11–16, 2014.

(25) LEE, U. et al. Techno-economic feasibility study of membrane based propane/propylene separation process. *Chemical Engineering and Processing: Process Intensification*, v. 119, p. 62–72, 2017.

(26) PARK, Y. S. et al. Durable poly(vinyl alcohol)/$AgBF_4$/$Al(NO_3)_3$ complex membrane with high permeance for propylene/propane separation. *Separation and Purification Technology*, v. 174, n. 3, p. 39–43, 2017.

(27) FAIZ, R.; LI, K. Olefin/paraffin separation using membrane based facilitated transport/chemical absorption techniques. *Chemical Engineering Science*, v. 73, p. 261–284, 2012.

(28) MERKEL, T. C. et al. Silver salt facilitated transport membranes for olefin/paraffin separations: Carrier instability and a novel regeneration method. *Journal of Membrane Science*, v. 447, p. 177–189, 2013.

(29) STAUDT-BICKEL, C.; KOROS, W. J. Olefin/paraffin gas separations with 6FDA-based polyimide membranes. *Journal of Membrane Science*, v. 170, n. 2, p. 205–214, 2000.

(30) GIANNAKOPOULOS, I. G.; NIKOLAKIS, V. Separation of Propylene/Propane Mixtures Using Faujasite-Type Zeolite Membranes. *Industrial & Engineering Chemistry Research*, v. 44, n. 1, p. 226–230, 2005.

(31) NIKOLAKIS, V. et al. Growth of a faujasite-type zeolite membrane and its application in the separation of saturated/unsaturated hydrocarbon mixtures. *Journal of Membrane Science*, v. 184, n. 2, p. 209–219, 2001.

(32) LIU, D. et al. Gas transport properties and propylene/propane separation characteristics of ZIF-8 membranes. *Journal of Membrane Science*, v. 451, p. 85–93, 1 fev. 2014.

(33) ZHANG, C.; LIVELY, R. P.; et al. Unexpected molecular sieving properties of zeolitic imidazolate framework-8. *The Journal of Physical Chemistry Letters*, v. 3, n. 16, p. 2130–2134, 2012.

(34) KWON, H. T.; JEONG, H.-K. *In Situ* Synthesis of Thin Zeolitic–Imidazolate Framework ZIF-8 Membranes Exhibiting Exceptionally High Propylene/Propane Separation. *Journal of the American Chemical Society*, v. 135, n. 29, p. 10763–10768, 2013.

(35) KWON, H. T.; JEONG, H.-K. Highly propylene-selective supported zeolite-imidazolate framework (ZIF-8) membranes synthesized by rapid microwave-assisted seeding and secondary growth. *Chemical Communications*, v. 49, n. 37, p. 3854–3856, 2013.

(36) PAN, Y. et al. Effective separation of propylene/propane binary mixtures by ZIF-8 membranes. *Journal of Membrane Science*, v. 390–391, p. 93–98, 2012.

(37) LIU, J. et al. *Separation of gases via carbonized vinylidene chloride copolymer gas separation membranes and process for the preparation of the membranes*. W.O. Patent WO2017/160815 A1, September 21, 2017.

(38) LIU, J.; CALVERLEY, E. M.; et al. New carbon molecular sieves for propylene/propane separation with high working capacity and separation factor. *Carbon*, v. 123, p. 273–282, 2017.

(39) KOROS, W. J.; MA, Y. H.; SHIMIDZU, T. Terminology for Membranes and Membrane processes. *Pure & Applied Chemistry.* v. 68, n. 7, p. 1479–1489, 1996.

(40) KIM, J. H. et al. The structural transitions of pi-complexes of poly(styrene-b-butadiene-b-styrene) block copolymers with silver salts and their relation to facilitated olefin transport. *Journal of Membrane Science*, v. 281, p. 369–376, 2006.

(41) FAIZ, R.; LI, K. Polymeric membranes for light olefin/paraffin separation. *Desalination*, v. 287, p. 82–97, 2012.

(42) KANG, S. W.; KANG, Y. S. Silver nanoparticles stabilized by crosslinked poly(vinyl pyrrolidone) and its application for facilitated olefin transport. *Journal of Colloid and Interface Science*, v. 353, n. 1, p. 83–86, 2011.

(43) KANG, Y. S. et al. Interaction with olefins of the partially polarized surface of silver nanoparticles activated by p-benzoquinone and its implications for facilitated olefin transport. *Advanced Materials*, v. 19, n. 3, p. 475–479, 2007.

(44) KANG, S. W.; CHAR, K.; KANG, Y. S. Novel Application of Partially Positively Charged Silver Nanoparticles for Facilitated Transport in Olefin/Paraffin Separation Membranes. *Chemistry of Materials*, v. 20, n. 4, p. 1308–1311, 2008.

(45) KANG, S. W.; LEE, D. H.; et al. Effect of the polarity of silver nanoparticles induced by ionic liquids on facilitated transport for the separation of propylene/propane mixtures. *Journal of Membrane Science*, v. 322, n. 3, p. 281–285, 2008.

(46) LEE, J. H. et al. A strong linear correlation between the surface charge density on Ag nanoparticles and the amount of propylene adsorbed. *Journal of Materials Chemistry A*, v. 2, n. 19, p. 6987–6993, 2014.

(47) SIH, B. C. et al. Metal nanoparticle—conjugated polymer nanocomposites. *Chemical Communications*, v. 11, n. 27, p. 3375–3384, 2005.

(48) WU, C. et al. Preparation of Antibacterial Waterborne Polyurethane/silver Nanocomposite. *Journal of the Chinese Chemical Society*, v. 56, p. 1231–1235, 2009.

(49) DALLAS, P.; SHARMA, V. K.; ZBORIL, R. Silver polymeric nanocomposites as advanced antimicrobial agents: Classification, synthetic paths, applications, and perspectives. *Advances in Colloid and Interface Science*, v. 166, n. 1, p. 119–135, 2011.

(50) WILSON, J. L. et al. Synthesis and magnetic properties of polymer nanocomposites with embedded iron nanoparticles. *Journal of Applied Physics*, v. 95, n. 3, p. 1439, 2004.

(51) CROOKS, R. M. et al. Dendrimer-encapsulated metal nanoparticles: synthesis, characterization, and applications to catalysis. *Accounts of Chemical Research*, v. 34, n. 3, p. 181–190, 2001.

(52) PACHFULE, P. et al. One-dimensional confinement of a nanosized metal organic framework in carbon nanofibers for improved gas adsorption. *Chemical Communications*, v. 48, n. 14, p. 2009–2011, 2012.

(53) PEPONI, L. et al. Processing of nanostructured polymers and advanced polymeric based nanocomposites. *Materials Science and Engineering: R: Reports*, v. 85, n. 1, p. 1–46, 2014.

(54) PACIONI, N. L. et al. Synthetic routes for the preparation of silver nanoparticles. A mechanistic perspective. In: ALARCON, E. I.; GRIFFITH, M.; UDEKWU, K. I. *Silver Nanoparticle Applications. In the Fabrication and Design of Medical and Biosensing Devices*. Cham: Springer, 2015. p. 13–46.

(55) TAN, K. S.; CHEONG, K. Y. Advances of Ag, Cu, and Ag-Cu alloy nanoparticles synthesized via chemical reduction route. *Journal of Nanoparticle Research*, v. 15, n. 4, Article n. 1537, 2013.

(56) TOLAYMAT, T. M. et al. An evidence-based environmental perspective of manufactured silver nanoparticle in syntheses and applications: A systematic review and critical appraisal of peer-reviewed scientific papers. *Science of The Total Environment*, v. 408, n. 5, p. 999–1006, 2010.

(57) CREIGHTON, J. A.; BLATCHFORD, C. G.; ALBRECHT, M. G. Plasma resonance enhancement of Raman scattering by pyridine adsorbed on silver or gold sol particles of size comparable to the excitation wavelength. *Journal of the Chemical Society, Faraday Transactions 2*, v. 75, n. 0, p. 790-798, 1979.

(58) COUTINHO, F. M. B.; DELPECH, M. C.; GARCIA, M. E. F. Evaluation of gas permeability of membranes obtained from poly(urethane-urea)s aqueous dispersions based on hydroxyl-terminated polybutadiene. *Polymer Testing*, v. 21, n. 6, p. 719–723, 2002.

(59) COUTINHO, F. M. B.; DELPECH, M. C.; GARCIA, M. E. F. Avaliação das propriedades mecânicas e da permeabilidade a gases de membranas obtidas a partir de dispersões aquosas de poliuretanos à base de polibutadieno líquido hidroxilado. *Polímeros*, v. 14, n. 4, p. 230–234, 2004.

(60) BARBOZA, E. M.; DELPECH, M. C.; GARCIA, M. E. F. Avaliação das Propriedades de Barreira de Membranas Obtidas a partir de Dispersões Aquosas à Base de Poliuretanos e Argila. *Polímeros*. v. 24, n. 1, p. 94–100, 2014.

(61) BARBOZA, E. M. *Avaliação das propriedades de barreira a gases de membranas obtidas a partir de dispersões aquosas à base de poliuretanos e argila.* 2011. 131 p. Dissertação de Mestrado em Química - Instituto de Química, Universidade do Estado do Rio de Janeiro, 2011.

(62) REIS, R. A. et al. Waterborne poly(urethane-urea)s gas permeation membranes for CO_2/CH_4 separation. *Journal of Applied Polymer Science*, v. 135, n. 11, p. 46003, 2018.

(63) PEREIRA, H. C. P. *Caracterização de filmes formados por dispersões aquosas de poli (uretano-uréia)s para aplicação em membranas para permeação de gases*. 2012. 88 p. Dissertação de Mestrado em Engenharia Química - Instituto de Química, Universidade do Estado do Rio de Janeiro, 2012.

(64) CAMPOS, A. C. C. *Síntese e caracterização de filmes de nanopartículas de prata dispersas em poli(uretano-ureia) para separação de gases petroquímicos*. 2013. 85 p. Dissertação de Mestrado em Engenharia Química - Instituto de Química, Universidade do Estado do Rio de Janeiro, 2013.

(65) HONG, G. H. et al. Highly permeable poly(ethylene oxide) with silver nanoparticles for facilitated olefin transport. *RSC Advances*, v. 4, n. 10, p. 4905–4908, 2014.

(66) REZENDE, C. G. F.; BORGES, C. P.; HABERT, A. C. Sorption of propylene and propane in polyurethane membranes containing silver nanoparticles. *Journal of Applied Polymer Science*, v. 133, n. 4, p. 6–11, 2016.

(67) PARK, H. H. et al. Effect of nonionic n-octyl β-D-glucopyranoside surfactant on the stability improvement of silver polymer electrolyte membranes for olefin/paraffin separation. *Journal of Membrane Science*, v. 217, n. 1–2, p. 285–293, 2003.

(68) KANG, S. W. et al. Chemical activation of $AgNO_3$ to form olefin complexes induced by strong coordinative interactions with phthalate oxygens of poly(ethylene phthalate). *Industrial & Engineering Chemistry Research*, v. 45, n. 11, p. 4011–4014, 2006.

(69) KANG, S. W. et al. Suppression of silver ion reduction by $Al(NO_3)_3$ complex and its application to highly stabilized olefin transport membranes. *Journal of Membrane Science*, v. 445, n. 3, p. 156–159, 2013.

(70) SONG, D.; KANG, Y. S.; KANG, S. W. Highly permeable and stabilized olefin transport membranes based on a poly(ethylene oxide) matrix and $Al(NO_3)_3$. *Journal of Membrane Science*, v. 474, n. 0, p. 273–276, 2015.

(71) KIM, J. H.; WON, J.; KANG, Y. S. Olefin-induced dissolution of silver salts physically dispersed in inert polymers and their application to olefin/paraffin separation. *Journal of Membrane Science*, v. 241, n. 2, p. 403–407, 2004.

(72) WANG, Y. et al. Impact of ionic liquids on silver thermoplastic polyurethane composite membranes for propane/propylene separation. *Arabian Journal of Chemistry*, p. in press.

(73) CHAE, I. S. et al. Surface energy-level tuning of silver nanoparticles for facilitated olefin transport. *Angewandte Chemie - International Edition*, v. 50, n. 13, p. 2982–2985, 2011.

(74) SHIN, H. S. et al. Mechanism of growth of colloidal silver nanoparticles stabilized by polyvinyl pyrrolidone in γ-irradiated silver nitrate solution. *Journal of Colloid and Interface Science*, v. 274, n. 1, p. 89–94, 2004.

(75) CHOI, H. et al. Tetrathiafulvalene as an electron acceptor for positive charge induction on the surface of silver nanoparticles for facilitated olefin transport. *Chemical Communications*, v. 50, n. 24, p. 3194–3196, 2014.

(76) POZUN, Z. D. et al. Why silver nanoparticles are effective for olefin/paraffin separations. T*he Journal of Physical Chemistry C*, v. 115, p. 1811–1818, 2011.

(77) FALLANZA, M. et al. Propylene and propane solubility in imidazolium, pyridinium, and tetralkylammonium based ionic liquids containing a silver salt. *Journal of Chemical and Engineering Data*, v. 58, n. 8, p. 2147–2153, 2013.

(78) HYDE, B. *Light Olefins Market Review*. In: FORO PEMEX PETROQUIMICA, 2012.

(79) RAPPAPORT, H. Ethylene and Polyethylene Global Overview. In: PLASTICS INDUSTRY TRADE ASSOCIATION (SPI) FILM AND BAG CONFERENCE, 2011, Chicago.

(80) SATTLER, J. J. H. B. et al. Catalytic Dehydrogenation of Light Alkanes on Metals and Metal Oxides. *Chemical Reviews*, v. 114, n. 20, p. 10613–10653, 2014.

(81) GALADIMA, A.; MURAZA, O. Revisiting the oxidative coupling of methane to ethylene in the golden period of shale gas: A review. *Journal of Industrial & Engineering Chemistry*, v. 37, p. 1–13, 2016.

(82) TIAN, P. et al. Methanol to olefins (MTO): From fundamentals to commercialization. *ACS Catalysis*, v. 5, n. 3, p. 1922–1938, 2015.

(83) AKAH, A.; AL-GHRAMI, M. Maximizing propylene production via FCC technology. *Applied Petrochemical Research*, v. 5, n. 4, p. 377–392, 2015.

(84) EUROPEAN COMMISSION. Reference document on best available techniques in the large volume organic chemical industry. *Integrated Pollution Prevention and Control (IPPC)*, 432 p., 2003.

(85) HUANG, H. Y.; PADIN, J.; YANG, R. T. Comparison of π-complexations of ethylene and carbon monoxide with Cu^+ and Ag^+. *Industrial & engineering chemistry research*, v. 38, n. 7, p. 2720–2725, 1999.

(86) TIAN, Y. et al. In-situ reduction of $Cu(CH_3COO)_2$ to prepare π-complexation adsorbent for propylene/propane separation by slurry bed. *Separation Science and Technology*, v. 52, n. 12, p. 1959–1966, 2017.

(87) ANSON, A. et al. Adsorption of ethane and ethylene on modified ETS-10. *Chemical Engineering Science*, v. 63, n. 16, p. 4171–4175, 2008.

(88) REGE, S. U.; PADIN, J.; YANG, R. T. Olefin/paraffin separations by adsorption: π-Complexation vs. kinetic separation. *AIChE Journal*, v. 44, n. 4, p. 799–809, 1998.

(89) AGUADO, S. et al. Absolute Molecular Sieve Separation of Ethylene/Ethane Mixtures with Silver Zeolite A. *Journal of the American Chemical Society*, v. 134, n. 36, p. 14635–14637, 2012.

(90) BAO, Z. et al. Potential of microporous metal–organic frameworks for separation of hydrocarbon mixtures. *Energy and Environmental Science*, v. 9, n. 12, p. 3612–3641, 2016.

(91) LI, P. et al. A microporous six-fold interpenetrated hydrogen-bonded organic framework for highly selective separation of C_2H_4/C_2H_6. *Chemical Communications*, v. 50, n. 86, p. 13081–13084, 4 set. 2014.

(92) HUANG, L.; CAO, D. Selective adsorption of olefin–paraffin on diamond-like frameworks: diamondyne and PAF-302. *Journal of Materials Chemistry A*, v. 1, n. 33, p. 9433, 2013.

(93) LUNA-TRIGUERO, A. et al. Effective Model for Olefin/Paraffin Separation using (Co, Fe, Mn, Ni)-MOF-74. *ChemistrySelect*, v. 2, n. 2, p. 665–672, 2017.

(94) PENG, J. et al. Efficient kinetic separation of propene and propane using two microporous metal organic frameworks. Chemical Communications, v. 53, n. 67, p. 9332–9335, 2017.

(95) WANG, Y. et al. Silver-decorated hafnium metal-organic framework for ethylene/ethane separation. *Industrial & Engineering Chemistry Research*, v. 56, n. 15, p. 4508–4516, 2017.

(96) GAJBHIYE, S. B. Membranes of poly(phenylene oxide) and its copolymers: Synthesis, characterization, and application in recovery of propylene from a refinery off-gas mixture. *Journal of Applied Polymer Science*, v. 127, n. 4, p. 2497–2507, 2013.

(97) TANG, Z. et al. *Mixed matrix membranes for olefin/paraffin separation and method of making thereof*. U.S. Patent US2017/291147 A1, October 12, 2017.

(98) ZHANG, C.; DAI, Y.; et al. High performance ZIF-8/6FDA-DAM mixed matrix membrane for propylene/propane separations. *Journal of Membrane Science*, v. 389, p. 34–42, 2012.

(99) SHEN, X. et al. Separation of propylene and propane by functional mixture of imidazolintum chloride ionic liquid – Organic solvent – Cuprous salt. *Separation and Purification Technology*, v. 175, p. 177–184, 2017.

(100) INSTITUTE FOR OCCUPATIONAL SAFETY AND HEALTH OF THE GERMAN SOCIAL ACCIDENT INSURANCE. *Gestis substance database*, 2018.

(101) SHOLL, D. S.; LIVELY, R. P. Seven chemical separations to change the world. *Nature*, v. 532, p. 435–437, 2016.

(102) BAKER, R. W. *Membrane Technology and Applications*. 3. ed. Chichester: John Wiley & Sons, Ltd, 2012.

(103) MERKEL, T. et al. *Separation of Olefin / Paraffin Mixtures with Carrier Facilitated Membranes*. Final report prepared by Membrane Technology and Research, Inc. Report DE-FC36-04GO14151, U.S. Department of Energy, 2007.

(104) LISKEY, C. W.; LIU, C.; TRAN, H. Q. *Polyimide membranes with very high separation performance for olefin/paraffin separation*. U.S. Patent US2015/0328594 A1, November 19, 2015.

(105) CHEVRON PHILLIPS CHEMICAL COMPANY LP. Available online at: www.cpchem.com/en-us/Pages/default.aspx. (Accessed: 1st March 2018).

(106) BAKER, R. W. Future directions of membrane gas separation technology. *Industrial & Engineering Chemistry Research*, v. 41, n. 6, p. 1393–1411, 2002.

(107) DAS, M. *Membranes for olefin/paraffin separations*. 2009. 206 f. Doctoral Thesis - School of Chemical & Biomolecular Engineering of Georgia Institute of Technology, 2009.

(108) HABERT, A. C.; BORGES, C. P.; NOBREGA, R. *Processo de Separação por Membranas*. Rio de Janeiro: E-papers, 2006.

(109) BAKER, R. W. Gas Separation. In: _____. *Membrane Technology and Applications*. 2. ed. Chichester: John Wiley & Sons, Ltd, 2004. p. 301–353.

(110) LIN, H.; FREEMAN, B. D. Gas solubility, diffusivity and permeability in poly(ethylene oxide). *Journal of Membrane Science*, v. 239, n. 1, p. 105–117, 2004.

(111) GHOSAL, K.; CHERN, R. T.; FREEMAN, B. D. Effect of basic substituents on gas sorption and permeation in polysulfone. *Macromolecules*, v. 29, n. 12, p. 4360–4369, 1996.

(112) MULDER, M. *Basic principles of membrane technology*. 2. ed. Dordrecht: Kluwer Academic Publishers, 1996.

(113) NING, L. et al. Hydrogen-Bonding Properties of Segmented Polyether Poly(urethane urea) Copolymer. *Macromolecules*, v. 30, n. 15, p. 4405–4409, 1997.

(114) WOLINSKA-GRABCZYK, A. Effect of the hard segment domains on the permeation and separation ability of the polyurethane-based membranes in benzene/cyclohexane separation by pervaporation. *Journal of Membrane Science*, v. 282, n. 1–2, p. 225–236, 2006.

(115) DELPECH, M. C.; COUTINHO, F. M. B. Waterborne anionic polyurethanes and poly(urethane-urea)s: Influence of the chain extender on mechanical and adhesive properties. *Polymer Testing*, v. 19, n. 8, p. 939–952, 2000.

(116) LI, H.; FREEMAN, B. D.; EKINER, O. M. Gas permeation properties of poly(urethane-urea)s containing different polyethers. *Journal of Membrane Science*, v. 369, n. 1–2, p. 49–58, 2011.

(117) SURYA, R. M.et al. Separation of binary mixtures of propylene and propane by facilitated transport through silver incorporated poly(ether-block-amide) membranes. *Oil & Gas Science and Technology – Revue d'IFP Energies nouvelles*, v. 70, n. 2, p. 381–390, 2015.

(118) ISANEJAD, M.; AZIZI, N.; MOHAMMADI, T. Pebax membrane for CO2/CH4 separation: Effects of various solvents on morphology and performance. *Journal of Applied Polymer Science*, v. 134, n. 9, p. 1–9, 2017.

(119) WANG, Y.; REN, J.; DENG, M. Ultrathin solid polymer electrolyte PEI/Pebax2533/$AgBF_4$ composite membrane for propylene/propane separation. *Separation and Purification Technology*, v. 77, n. 1, p. 46–52, 2011.

(120) ARMSTRONG, S. et al. Gas permeability of melt-processed poly(ether block amide) copolymers and the effects of orientation. *Polymer*, v. 53, n. 6, p. 1383–1392, 2012.

(121) BAI, S.; SRIDHAR, S.; KHAN, A. A. Metal-ion mediated separation of propylene from propane using PPO membranes. *Journal of Membrane Science*, v. 147, n. 1, p. 131–139, 1998.

(122) KROL, J. J.; BOERRIGTER, M.; KOOPS, G. H. Polyimide hollow fiber gas separation membranes: preparation and the suppression of plasticization in propane/propylene environments. *Journal of Membrane Science*, v. 184, n. 2, p. 275–286, 2001.

(123) OKAMOTO, K. et al. Permeation and separation properties of polyimide membranes to 1,3-butadiene and n-butane. *Journal of Membrane Science*, v. 134, n. 2, p. 171–179, 1997.

(124) BURNS, R. L.; KOROS, W. J. Defining the challenges for C_3H_6/C_3H_8 separation using polymeric membranes. *Journal of Membrane Science*, v. 211, n. 2, p. 299–309, 2003.

(125) KANG, S. W.; HONG, J.; PARK, J. H.; et al. Nanocomposite membranes containing positively polarized gold nanoparticles for facilitated olefin transport. *Journal of Membrane Science*, v. 321, n. 1, p. 90–93, 2008.

(126) KIM, J. H.; MIN, B. R.; WON, J.; JOO, S. H.; et al. Role of polymer matrix in polymer/silver complexes for structure, interactions, and facilitated olefin transport. *Macromolecules*, v. 36, n. 16, p. 6183–6188, 2003.

(127) CUSSLER, E. L.; ARIS, R.; BHOWN, A. On the limits of facilitated diffusion. *Journal of Membrane Science*, v. 43, n. 2–3, p. 149–164, 1989.

(128) DEWAR, M. J. S. A review of the p-complex theory. *Bulletin de la Socie´te´ Chimique*, v. 18, p. C71-9, 1951.

(129) CHATT, J., DUNCANSON, L. A. Olefin co-ordination compounds. Part III. Infrared spectra and structure: Attempted preparation of acetylene complexes. *Journal of the Chemical Society*, v. 0, p. 2939–2947, 1953.

(130) MIESSLER, G. L.; FISCHER, P. J.; TARR, D. A. Inorganic Chemistry. 5th. ed. Upper Saddle Rive, NJ: Pearson, 2014.

(131) COTTON, F. A. et al. *Advanced Inorganic Chemistry.* 6. ed. New York: Wiley-Interscience, 1999.

(132) SCHOLANDER, P. F. Oxygen transport through hemoglobin solutions. *Science*, v. 131, p. 585–590, 1960.

(133) KANG, Y. S. et al. *Solid state polymer electrolyte facilitated transport membranes containing surfactants*. U.S. Patent US6,645,276 B2, November 11, 2003.

(134) KIM, J. H.; KANG, Y. S.; WON, J. Silver polymer electrolyte membranes for facilitated olefin transport: carrier properties, transport mechanism and separation performance. *Macromolecular Research*, v. 12, n. 2, p. 145–155, 2004.

(135) BRYAN, P. F. Removal of propylene from fuel-grade propane. *Separation and Purification Reviews*, v. 33, n. 2, p. 157–182, 2004.

(136) SUN, Y. et al. A novel copper(I)-based supported ionic liquid membrane with high permeability for ethylene/ethane separation. *Industrial & Engineering Chemistry Research*, v. 56, n. 3, p. 741–749, 2017.

(137) STEIGELMANN, E. F.; HUGHES, R. D. *Process for Separation of Unsaturated Hydrocarbons*. U.S. Patent 3,758,603, September 11, 1973.

(138) HUGHES, R. D.; MAHONEY, J. A.; STEIGELMANN, E. F. Olefin separation by facilitated transport membranes. In: LI, N. N.; CALO, J. M. *Recent Developments in Separation Science*. Boca Raton: CRC Press, 1986. p. 173–196.

(139) DUAN, S.; ITO, A.; OHKAWA, A. Separation of propylene/propane mixture by a supported liquid membrane containing triethylene glycol and a silver salt. *Journal of Membrane Science*, v. 215, n. 1–2, p. 53–60, 2003.

(140) FALLANZA, M. et al. Experimental study of the separation of propane/propylene mixtures by supported ionic liquid membranes containing Ag^{+}–RTILs as carrier. *Separation and Purification Technology*, v. 97, p. 83–89, 2012.

(141) PITSCH, F. et al. An adaptive self-healing ionic liquid nanocomposite membrane for olefin-paraffin separations. *Advanced Materials*, v. 24, n. 31, p. 4306–4310, 2012.

(142) KÁRÁSZOVÁ, M. et al. Progress in separation of gases by permeation and liquids by pervaporation using ionic liquids: A review. *Separation and Purification Technology*, v. 132, p. 93–101, 20 ago. 2014.

(143) TERAMOTO, M. et al. Separation of ethylene from ethane by supported liquid membranes containing silver nitrate as a carrier. *Journal of Chemical Engineering of Japan*, v. 19, n. 5, p. 419–424, 1986.

(144) RAVANCHI, M. T.; KAGHAZCHI, T.; KARGARI, A. Facilitated transport separation of propylene-propane: Experimental and modeling study. *Chemical Engineering and Processing: Process Intensification*, v. 49, n. 3, p. 235–244, 2010.

(145) RAVANCHI, M. T.; KAGHAZCHI, T.; KARGARI, A. Supported liquid membrane separation of propylene-propane mixtures using a metal ion carrier. *Desalination*, v. 250, n. 1, p. 130–135, 2010.

(146) OLIVER H. L. et al. Facilitated transport in ion-exchange membranes. *Journal of Membrane Science*, v. 6, p. 339–343, 1980.

(147) ERIKSEN, O. I.; AKSNES, E.; DAHL, I. M. Facilitated transport of ethene through Nafion membranes. Part II. Glycerine treated, water swollen membranes. *Journal of Membrane Science*, v. 85, n. 1, p. 99–106, 1993.

(148) ERIKSEN, O. I.; AKSNES, E.; DAHL, I. M. Facilitated transport of ethene through Nafion membranes. Part I. Water swollen membranes. *Journal of Membrane Science*, v. 85, n. 1, p. 89–97, 1993.

(149) RABAGO, R.; NOBLE, R. D.; KOVAL, C. A. Effects of Incorporation of Fluorocarbon and Hydrocarbon Surfactants into Perfluorosulfonic Acid (Nafion) Membranes. *Chemistry of Materials*, v. 6, n. 7, p. 947–951, 1994.

(150) SUNGPET, A. et al. Reactive polymer membranes for ethylene/ethane separation. *Journal of Membrane Science*, v. 136, n. 1–2, p. 111–120, 1997.

(151) YAMAGUCHI, T. et al. Olefin separation using silver impregnated ion-exchange membranes and silver salt/polymer blend membranes. *Journal of Membrane Science*, v. 117, n. 1–2, p. 151–161, 1996.

(152) THOEN, P. M.; NOBLE, R. D.; KOVAL, C. A. Unexpectedly large selectivities for olefin separations utilizing silver ion in ion-exchange membranes. *The Journal of Physical Chemistry*, v. 98, n. 4, p. 1262–1269, 1994.

(153) KOVAL, C. et al. Facilitated transport of unsaturated hydrocarbons in perfluorosulfonic acid (Nafion) membranes. In: BARTSCH, R.; WAY, J. D. *Chemical Separations with Liquid Membranes*. Washington, DC: ACS Symposium Series; American Chemical Society, 1996. v. 642. p. 286–302.

(154) LIU, L.; FENG, X.; CHAKMA, A. Unusual behavior of poly(ethylene oxide)/$AgBF_4$ polymer electrolyte membranes for olefin-paraffin separation. *Separation and Purification Technology*, v. 38, n. 3, p. 255–263, 2004.

(155) PINNAU, I.; TOY, L. G. Solid polymer electrolyte composite membranes for olefin/paraffin separation. *Journal of Membrane Science*, v. 184, n. 1, p. 39–48, 2001.

(156) KIM, J. H.; MIN, B. R.; KIM, C. K.; WON, J. New Insights into the coordination mode of silver ions dissolved in poly (2-ethyl-2-oxazoline) and its relation to facilitated olefin. *Macromolecules*, v. 35, p. 5250–5255, 2002.

(157) SUNDERRAJAN, S. et al. Propane and propylene sorption in solid polymer electrolytes based on poly(ethylene oxide) and silver salts. *Journal of Membrane Science*, v. 182, n. 1–2, p. 1–12, 2001.

(158) MORISATO, A. et al. Transport properties of PA12-PTMO/AgBF4 solid polymer electrolyte membranes for olefin/paraffin separation. *Desalination*, v. 145, n. 1, p. 347–351, 2002.

(159) MERKEL, T. C. et al. Olefin/paraffin solubility in a solid polymer electrolyte membrane. *Chemical Communications*, v. 37, n. 13, p. 1596, 2003.

(160) KIM, J. H.; KANG, S. W.; KANG, Y. S. Threshold silver concentration for facilitated olefin transport in polymer/silver salt membranes. *Journal of Polymer Research*, v. 19, n. 1, p. 9753, 2012.

(161) KIM, J. H.; MIN, B. R.; KIM, H. S.; et al. Facilitated transport of ethylene across polymer membranes containing silver salt: effect of HBF_4 on the photoreduction of silver ions. *Journal of Membrane Science*, v. 212, n. 1, p. 283–288, 2003.

(162) KANG, Y. S. et al. Solid-State Facilitated Transport Membranes for Separation of Olefins / Paraffins and Oxygen / Nitrogen. In: YAMPOLSKII, Y.; PINNAU, I.; FREEMAN, B. *Materials Science of Membranes for Gas and Vapor Separation*. Chichester: John Wiley & Sons, Ltd., 2006. p. 391–410.

(163) KIM, J. H.; WON, J.; KANG, Y. S. Silver polymer electrolytes by π-complexation of silver ions with polymer containing C=C bond and their application to facilitated olefin transport membranes. *Journal of Membrane Science*, v. 237, n. 1–2, p. 199–202, 2004.

(164) KIM, J. H.; MIN, B. R.; WON, J.; KANG, Y. S. Revelation of facilitated olefin transport through silver-polymer complex membranes using anion complexation. *Macromolecules*, v. 36, n. 12, p. 4577–4581, 2003.

(165) KIM, J. H.; MIN, B. R.; WON, J.; et al. Complexation mechanism of olefin with silver ions dissolved in a polymer matrix and its effect on facilitated olefin transport. *Chemistry European Journal*, v. 8, n. 3, p. 650–654, 2002.

(166) KIM, J. H.; MIN, B. R.; KIM, C. K.; WON, J.; et al. Spectroscopic interpretation of silver ion complexation with propylene in silver polymer electrolytes. *Journal of Physical Chemistry B*, v. 106, n. 10, p. 2786–2790, 2002.

(167) KANG, S. W.; CHAR, K.; et al. Control of ionic interactions in silver salt-polymer complexes with ionic liquids: Implications for facilitated olefin transport. *Chemistry of Materials*, v. 18, n. 7, p. 1789–1794, 2006.

(168) DUARTE, L. T.; HABERT, A. C.; BORGES, C. P. Preparation and morphological characterization of polyurethane/polyethersulfone composite membranes. *Desalination*, v. 145, n. 1–3, p. 53–59, 2002.

(169) FERRAZ, H. C. et al. Recent achievements in facilitated transport membranes for separation processes. *Brazilian Journal of Chemical Engineering*, v. 24, n. 01, p. 101–118, 2007.

(170) KANG, S.; KIM, J.; WON, J. Enhancement of facilitated olefin transport by amino acid in silver-polymer complex membranes. *Chemical Communications*, v. 2, n. 3, p. 768–769, 2003.

(171) KIM, J. H. et al. Unusual separation property of propylene/propane mixtures through polymer/silver complex membranes containing mixed salts. *Journal of Membrane Science*, v. 248, n. 1–2, p. 171–176, 2005.

(172) PREECHATIWONG, W.; SCHULTZ, J. M. Electrical conductivity of poly(ethylene oxide)-alkali metal salt systems and effects of mixed salts and mixed molecular weights. *Polymer*, v. 37, n. 23, p. 5109–5116, 1996.

(173) JOSE, B. et al. Effect of phthalates on the stability and performance of AgBF4-PVP membranes for olefin/paraffin separation. *Chemical communications*, v. 37, p. 2046–2047, 2001.

(174) PASTORIZA-SANTOS, I.; LIZ-MARZÁN, L. M. Formation and stabilization of silver nanoparticles through reduction by N , N -dimethylformamide. *Langmuir*, v. 15, n. 4, p. 948–951, 1999.

(175) WISTRAND, L. Silver Tetrafluoroborate. In: *e-EROS Encyclopedia of Reagents for Organic Synthesis*. John Wiley & Sons, 2005. p. 1–8.

(176) PARK, Y. S.; KANG, Y. S.; KANG, S. W. Cost-effective facilitated olefin transport membranes consisting of polymer/$AgCF_3SO_3$/$Al(NO_3)_3$ with long-term stability. *Journal of Membrane Science*, v. 495, n. 3, p. 61–64, 2015.

(177) KANG, S. W.; HONG, J.; CHAR, K.; et al. Correlation between anions of ionic liquids and reduction of silver ions in facilitated olefin transport membranes. *Desalination*, v. 233, n. 1–3, p. 327–332, 2008.

(178) PARK, Y. S.; KANG, S. W. Role of ionic liquids in enhancing the performance of the polymer/AgCF3SO_3/$Al(NO_3)_3$ complex for separation of propylene/propane mixture. *Chemical Engineering Journal*, v. 306, p. 973–977, 2016.

(179) ARCELLA, V.; TROGLIA, C.; GHIELMI, A. Hyflon Ion membranes for fuel cells. *Industrial & Engineering Chemistry Research*, v. 44, n. 20, p. 7646–7651, 2005.

(180) HUANG, Y.; MERKEL, T. C.; BAKER, R. W. Pressure ratio and its impact on membrane gas separation processes. *Journal of Membrane Science*, v. 463, p. 33–40, 2014.

(181) CHAE, I. S.; KANG, S. W.; KANG, Y. S. Olefin separation via charge transfer and dipole formation at the silver nanoparticle-tetracyanoquinoid interface. *RSC Advances*, v. 4, n. 57, p. 30156–30161, 2014.

(182) GÖRNER, H. Photoprocesses of p -Benzoquinones in Aqueous Solution. *The Journal of Physical Chemistry A*, v. 107, n. 51, p. 11587–11595, 2003.

(183) SZATYLOWICZ, H. et al. Why 1,2-quinone derivatives are more stable than their 2,3-analogues? *Theoretical Chemistry Accounts*, v. 134, p. 35, 2015.

(184) KANG, S. W. et al. Ionic liquid as a solvent and the long-term separation performance in a polymer/silver salt complex membrane. *Macromolecular Research*, v. 15, n. 2, p. 167–172, 2007.

(185) SHALU et al. Thermal stability, complexing behavior, and ionic transport of polymeric gel membranes based on polymer PVDF-HFP and ionic liquid, [BMIM][BF_4]. *Journal of Physical Chemistry B*, v. 117, n. 3, p. 897–906, 2013.

(186) ZARCA, R. et al. Generalized predictive modeling for facilitated transport membranes accounting for fixed and mobile carriers. *Journal of Membrane Science*, v. 542, p. 168–176, 2017.

(187) ZARCA, G. et al. Synthesis and gas separation properties of poly(ionic liquid)-ionic liquid composite membranes containing a copper salt. *Journal of Membrane Science*, v. 515, p. 109–114, 2016.

(188) ZARCA, R. et al. Facilitated transport of propylene through composite polymer-ionic liquid membranes. Mass transfer analysis. *Chemical Product and Process Modeling*, v. 11, n. 1, p. 77–81, 2016.

(189) ZARCA, R. et al. A practical approach to fixed-site-carrier facilitated transport modeling for the separation of propylene/propane mixtures through silver-containing polymeric membranes. *Separation and Purification Technology*, v. 180, p. 82–89, 2017.

(190) ORTIZ, A. et al. Reactive Ionic Liquid Media for the Separation of Propylene / Propane Gaseous Mixtures. *Industrial & Engineering Chemistry Research*, v. 49, n. 16, p. 7227–7233, 2010.

(191) GUO, C. G. et al. Synthesis and characterization of Ag2C2·2AgClO4·2H2O: a novel layer-type structure with the acetylide dianion functioning in a μ6- η1, η1 : η2, η2 : η2, η2 bonding mode inside an octahedral silver cage. *Chemical Communications*, n. 3, p. 339–340, 1998.

(192) COMPACT MEMBRANE SYSTEMS COMPANY. Available online at: www.compactmembrane.com. (Accessed: 20th December 2017)

(193) THE GLOBAL DELAWARE BLOG, *Delaware company is overall winner of petrochemical innovation awards*. Wilmington, DE, 2016. Available online at: www.global.delaware.gov/2016/11/03/delaware-company-is-overall-winner-of-icis-innovation-awards. (Accessed: 1st March 2018)

(194) KATTULA, M. et al. Designing ultrathin film composite membranes: The impact of a gutter layer. *Scientific Reports*, v. 5, p. 1–9, 2015.

(195) GALIZIA, M. et al. 50th Anniversary Perspective: Polymers and Mixed Matrix Membranes for Gas and Vapor Separation: A Review and Prospective Opportunities. *Macromolecules*, v. 50, n. 20, p. 7809–7843, 2017.

(196) RAMON, G. Z.; WONG, M. C. Y.; HOEK, E. M. V. Transport through composite membrane, part 1: Is there an optimal support membrane? *Journal of Membrane Science*, v. 415–416, p. 298–305, 2012.

(197) LUNDY, K. A.; CABASSO, I. Analysis and construction of multilayer composite membranes for the separation of gas mixtures. *Industrial & Engineering Chemistry Research*, v. 28, n. 6, p. 742–756, 1989.

(198) ERIKSEN, O. I. et al. Use of silver-exchanged ionomer membranes for gas separation. U.S. Patent US5,191,151 A, March 2, 1993.

(199) FEIRING, A. E.; LAZZERI, J.; MAJUMDAR, S. Membrane separation of olefin and paraffin mixtures. U.S. Patent US2015/0025293 A1, January 22, 2015.

(200) HE, Y.; XIE, D.; ZHANG, X. The structure, microphase-separated morphology, and property of polyurethanes and polyureas. *Journal of Materials Science*, v. 49, n. 21, p. 7339–7352, 2014.

(201) ROLPH, M. S. et al. Blocked isocyanates: from analytical and experimental considerations to non-polyurethane applications. *Polymer Chemistry*, v. 7, n. 48, p. 7351–7364, 2016.

(202) MADBOULY, S. A.; OTAIGBE, J. U. Recent advances in synthesis, characterization and rheological properties of polyurethanes and POSS/polyurethane nanocomposites dispersions and films. *Progress in Polymer Science*, v. 34, n. 12, p. 1283–1332, 2009.

(203) QUEIROZ, D. P.; NORBERTA DE PINHO, M. Structural characteristics and gas permeation properties of polydimethylsiloxane/poly(propylene oxide) urethane/urea bi-soft segment membranes. *Polymer*, v. 46, n. 7, p. 2346–2353, 2005.

(204) KRÓL, P. Synthesis methods, chemical structures and phase structures of linear polyurethanes. Properties and applications of linear polyurethanes in polyurethane elastomers, copolymers and ionomers. *Progress in Materials Science*, v. 52, n. 6, p. 915–1015, 2007.

(205) MATTIA, J.; PAINTER, P. A Comparison of Hydrogen Bonding and Order in a Polyurethane and Poly(urethane−urea) and Their Blends with Poly(ethylene glycol). *Macromolecules*, v. 40, n. 5, p. 1546–1554, 2007.

(206) SHETH, J. P. et al. Influence of system variables on the morphological and dynamic mechanical behavior of polydimethylsiloxane based segmented polyurethane and polyurea copolymers: a comparative perspective. *Polymer*, v. 45, n. 20, p. 6919–6932, 2004.

(207) HICKS, E. M.; ULTEE, A. J.; DROUGAS, J. Spandex Elastic Fibers: Development of a new type of elastic fiber stimulates further work in the growing field of stretch fabrics. Science (New York, N.Y.), v. 147, n. 3656, p. 373–9, 1965.

(208) COUTINHO, F. M. B. et al. Degradation profiles of cast films of polyurethane and poly(urethane-urea) aqueous dispersions based on hydroxy-terminated polybutadiene and different diisocyanates. *Polymer Degradation and Stability*, v. 81, n. 1, p. 19–27, 2003.

(209) PATRICIO, P. S. D. O. et al. Tailoring the morphology and properties of waterborne polyurethanes by the procedure of cellulose nanocrystal incorporation. *European Polymer Journal*, v. 49, n. 12, p. 3761–3769, 2013.

(210) COUTINHO, F. M. B. et al. Síntese e caracterização de dispersões aquosas de poliuretanos à base de copolímeros em bloco de poli(glicol etilênico) e poli(glicol propilênico). *Química Nova*, v. 31, n. 6, p. 1437–1443, 2008.

(211) MISHRA, A. K.; JENA, K. K.; RAJU, K. V. S. N. Synthesis and characterization of hyperbranched polyester-urethane-urea/K10-clay hybrid coatings. *Progress in Organic Coatings*, v. 64, p. 47–56, 2009.

(212) BAKER, R. W. Carrier facilitated transport. In: _____. *Membrane Technology and Applications*. 2. ed. Chichester: John Wiley & Sons, Ltd, 2004. p. 425–463.

(213) LAU, C. H. et al. Reverse-selective polymeric membranes for gas separations. *Progress in Polymer Science*, v. 38, n. 5, p. 740–766, 2013.

(214) RAVEENDRAN, P.; WALLEN, S. L. Cooperative C-H...O hydrogen bonding in CO_2-Lewis base complexes: Implications for solvation in supercritical CO2. *Journal of the American Chemical Society*, v. 124, n. 42, p. 12590–12599, 2002.

(215) HORNYAK, G. L. et al. *Introduction to Nanosciences*. Boca Raton: CRC Press, 2008.

(216) ZHANG, R. et al. Nucleation and growth of nanoparticles in the atmosphere. *Chemical Reviews*, v. 112, n. 3, p. 1957–2011, 2012.

(217) ZHANG, R. Getting to the critical nucleus of aerosol formation. *Science*, v. 328, n. 5984, p. 1366–1367, 2010.

(218) GITTINS, D. I.; CARUSO, F. Spontaneous Phase Transfer of Nanoparticulate Metals from Organic to Aqueous Media. *Angewandte Chemie - International Edition*, v. 40, n. 16, p. 3001–3004, 2001.

(219) KUMAR, A. et al. Phase transfer of silver nanoparticles from aqueous to organic solutions using fatty amine molecules. *Journal of Colloid and Interface Science*, v. 264, n. 2, p. 396–401, 2003.

(220) LIU, Y. C.; LIN, L. H. New pathway for the synthesis of ultrafine silver nanoparticles from bulk silver substrates in aqueous solutions by sonoelectrochemical methods. *Electrochemistry Communications*, v. 6, n. 11, p. 1163–1168, 2004.

(221) PINTO, V. V. et al. Long time effect on the stability of silver nanoparticles in aqueous medium: Effect of the synthesis and storage conditions. *Colloids and Surfaces A: Physicochemical and Engineering Aspects*, v. 364, n. 1–3, p. 19–25, 2010.

(222) SOLOMON, S. D. et al. Synthesis and Study of Silver Nanoparticles. *Journal of Chemical Education*, v. 84, n. 2, p. 322–325, 2007.

(223) DELPECH, M. C.; MIRANDA, G. S. Waterborne polyurethanes: influence of chain extender in FTIR spectra profiles. *Central European Journal of Engineering*, v. 2, n. 2, p. 231–238, 2011.

(224) DONG, P. V. et al. Chemical synthesis and antibacterial activity of novel-shaped silver nanoparticles. *International Nano Letters*, v. 2, n. 1, p. 1–9, 2012.

(225) MAVANI, K.; SHAH, M. Synthesis of Silver Nanoparticles by using Sodium Borohydride as a Reducing Agent. *International Journal of Engineering Research & Technology (IJERT)*, v. 2, n. 3, p. 1–5, 2013.

(226) BONSAK, J. *Chemical synthesis of silver nanoparticles for light trapping applications in silicon solar cells*. 2010. 136 p. Doctoral Thesis - Faculty of Mathematics and Natural Sciences, University of Oslo, 2010.

(227) ASTM INTERNATIONAL. *ASTM E2550 - 07*: Standard Test Method for Thermal Stability by Thermogravimetry. West Conshohocken, 2007

(228) BEAUCAGE, G. Approximations leading to a unified exponential power-law approach to small-angle scattering. *Journal of Applied Crystallography*, v. 29, n. 6, p. 717–28, 1995.

(229) BEAUCAGE, G.; KAMMLER, H. K.; PRATSINIS, S. E. Particle size distributions from small-angle scattering using global scattering functions. *Journal of Applied Crystallography*, v. 37, n. 4, p. 523–535, 2004.

(230) LANJE, A. S.; SHARMA, S. J.; PODE, R. B. Synthesis of silver nanoparticles: a safer alternative to conventional antimicrobial and antibacterial agents. *Journal of Chemical and Pharmaceutical Research*, v. 2, n. 3, p. 478–483, 2010.

(231) LAFUENTE, B. et al. The power of databases: the RRUFF project. In: ARMBRUSTER, T.; DANISI, R. M. *Highlights in Mineralogical Crystallography*. Berlim: W. De Gruyter, 2015. p. 1–30.

(232) THEIVASANTHI, T.; ALAGAR, M. Electrolytic Synthesis and Characterization of Silver Nanopowder. *eprint arXiv:1111.0260*, 2011.

(233) KONWAR, U.; KARAK, N.; MANDAL, M. Vegetable oil based highly branched polyester/clay silver nanocomposites as antimicrobial surface coating materials. *Progress in Organic Coatings*, v. 68, n. 4, p. 265–273, 2010.

(234) SRIDHAR, S. et al. Modified poly(phenylene oxide) membranes for the separation of carbon dioxide from methane. *Journal of Membrane Science*, v. 280, n. 1–2, p. 202–209, 2006.

(235) SHAHROOZ, M. et al. Elucidating the significance of segmental mixing in determining the gas transport properties of polyurethanes. *Macromolecules*, v. 49, n. 11, p. 4220–4228, 2016.

(236) AYRES, E.; ORÉFICE, R. L. Nanocompósitos derivados de dispersões aquosas de poliuretano e argila: influência da argila na morfologia e propriedades mecânicas. *Polímeros*, v. 17, n.4, p. 339–345, 2007.

(237) COUTINHO, F. M. B.; DELPECH, M. C. Degradation profile of films cast from aqueous polyurethane dispersions. *Polymer Degradation and Stability*, v. 70, n. 1, p. 49–57, 2000.

(238) HAYNES, W. M.; LIDE, D. R.; BRUNO, T. J. *CRC Handbook of Chemistry and Physics*, 93rd Edition. Boca Raton: CRC Press Book, 2013.

(239) SANTOS, W. N. et al. Propriedades térmicas de polímeros por métodos transientes de troca de calor. *Polímeros: Ciência e Tecnologia*. v. 13, n. 4, p. 265–269, 2003.

(240) CAKIC, S. M. et al. Synthesis and degradation profile of cast films of PPG-DMPA-IPDI aqueous polyurethane dispersions based on selective catalysts. *Polymer Degradation and Stability*, v. 94, n. 11, p. 2015–2022, 2009.

(241) MILANESE, A. C.; CIOFFI, M. O. H.; VOORWALD, H. J. C. Flexural behavior of Sisal/Castor oil-Based Polyurethane and Sisal/Phenolic Composites. *Materials Research*, v. 15, n. 2, p. 191–197, 2012.

(242) ROMERO, A. I. et al. Synthesis of polyetherimide/silica hybrid membranes by the sol–gel process: influence of the reaction conditions on the membrane properties. *Journal of Materials Science*, v. 46, n. 13, p. 4701–4709, 2011.

(243) MATTEUCCI, S. et al. Transport of Gases and Vapors in Glassy and Rubbery Polymers. In: YAMPOLSKII, Y.; PINNAU, I.; FREEMAN, B. *Materials Science of Membranes for Gas and Vapor Separation*. Chichester: John Wiley & Sons, Ltd., 2006. p. 1–47.

(244) PADMA, D. K. A novel synthetic route for the preparation of silver salts of hexafluorophosphate, tetrafluoroborate and hexafluorosilicate. *Synthesis and Reactivity in Inorganic and Metal-Organic Chemistry*, v. 18, n. 4, p. 401–404, 1988.

(245) HEIMER, N. E. et al. Vibrational spectra of imidazolium tetrafluoroborate ionic liquids. *Journal of Molecular Liquids*, v. 124, n. 1–3, p. 84–95, 2006.

(246) MOJET, B. L.; EBBESEN, S. D.; LEFFERTS, L. Light at the interface: the potential of attenuated total reflection infrared spectroscopy for understanding heterogeneous catalysis in water. *Chemical Society Reviews*, v. 39, n. 12, p. 4643, 2010.

(247) OKAMOTO, Y. et al. New amorphous perfluoro polymers: Perfluorodioxolane polymers for use as plastic optical fibers and gas separation membranes. *Polymers for Advanced Technologies*, v. 27, n. 1, p. 33–41, 2016.

(248) JUSTICE, R. S. *Small-angle scattering from nanocomposites: elucidation of hierarchical morphology/property relationships*. 2007. 163 p. Doctoral Thesis - Division of Research and Advanced Studies, University of Cincinnati, 2007.

(249) POROD, G. Die Rontgenkleinwinkelstreuung con dichtgepackten kolloiden systemin. I. Teil. (X-ray low angle scattering of dense colloid systems. Part I). *Kolloid-Zeitschrift*, v. 124, p. 83–114, 1951.

(250) SCHAEFER, D. Polymers, Fractals, and Ceramic Materials. *Science*, v. 243, n. 4894, p. 1023–1027, 1989.

(251) SCHAEFER, D.W.; AGAMALIAN, M. A. Ultra-small-angle neutron scattering: a new tool for materials research. *Current Opinion in Solid State & Materials Science*, v. 8, n. 1, p. 39–47, 2004.

(252) G BEAUCAGE, D. S. structural studies of complex-systems using small-angle scattering: a unified guinier power-law approach. *Journal of Non-Crystalline Solids*. v. 172-174, p. 797–805, 1994.

(253) BEAUCAGE, G. et al. Multiple Size Scale Structures in Silica—Siloxane Composites Studied by Small-Angle Scattering. In: MARK, J .E.; LEE, C. Y. C.; BIANCONI, P. A. *Hybrid Organic-Inorganic Composites*. Washington, DC: ACS Symposium Series; American Chemical Society, 1995. p. 97–111.

(254) DAS, R. et al. Preparation of Silver Nanoparticles and Their Characterization. AZojomo *Journal of Nanotechnology Online*, 2009. Available online at: www.azonano.com/article.aspx?ArticleID=2318. (Accessed: 1st March 2018)

APPENDIX — Brief description of the main analytical techniques used to characterize the composites materials studied in this Thesis

The objective of this appendix is to present briefly the main analytical techniques used to characterize the WPUU composites studied in this Thesis and how to interpret the results to get the desired information. Transmission electron microscopy (TEM), small angle scattering X-ray (SAXS), X-ray diffraction (XRD), Fourier transform infrared spectroscopy (FTIR), and thermogravimetric analysis (TGA) are presented with special attention related to the Ag NP size and the interaction between the polymer chains and silver species (Ag^0 and Ag^+).

Transmission electron microscopy (TEM), Small angle X-ray scattering (SAXS), and X-ray diffraction (XRD)

In the study of nanomaterials, a set of techniques is used to check the morphology of NP analyzed. Beginning with transmission electron microscopy (TEM), which is a microscopy technique used to generate high resolution images of NP. To be performed, TEM requires a primary step of sample preparation. The sample prepared must be thin enough to allow the crossing of an electron beam generating images by transmission. For polymer material containing NP, it is necessary to prepare the samples in an ultramicrotome equipament. Thus, it is possible to prepare very thin slices in a range of few tens of nanometers. When the polymer material has a very low glass transition temperature (T_g), i.e., an elastomeric polymer, it is necessary to cut the material using an ultramicrotome with cryoscopy. Cryoscopy temperatures get the polymer very rigid allowing the normal utilization of the ultramicrotome knife. Without low temperatures, it is not possible to perform proper cuts in the material. Although TEM can provide high resolution images, this technique scans a very small part of the sample, in the order of cubic micrometers. As a very small percentage of the sample is analyzed, some errors in the conclusions obtained may occur, especially if the best regions are selected by the microscopist to the detriment of other areas unattended.[248]

To avoid these types of interpretation problems, TEM analyses should always be complemented by SAXS (small angle X-ray scattering) analyzes. The sample volume analyzed by SAXS is usually in the order of cubic millimeters or more, making the analysis much more representative of the sample reality. However, by using SAXS, a resolution loss takes place compared to TEM.[248]

In SAXS technique for nanocomposites characterization, when two phases (the matrix and the nanofiller) are irradiated by the X-ray beam, the electron density contrast between two phases provides information about the geometry and the three-dimensional arrangement of smaller phase (the nanofiller). Depending on the resolution quality of the SAXS equipment used, information on the arrangement of nanofiller, which ranges from 1 nm and a few micrometers, is obtained. The information is obtained by measuring the scattered intensity ***I*** as a function of the scattering vector ***q*** that is related to the scattering angle ***θ*** by the Bragg law, Equation (7) :

$$q = \frac{4\pi \sin(\theta/2)}{\lambda} \tag{7}$$

Where ***λ*** is the wavelength of the X-ray radiation used. The scattering profile of ***I(q)*** function (when plotted on log-log scale) typically shows regions of exponential scattering (Guinier region) and decaying scattering in the form of power-law. From the Guinier region, it is possible to determine the average structural size of the nanofiller according to Guinier's law according to Equation (8)**:**[248]

$$I(q) = G\ exp\left(-\frac{q^2 R_g^2}{3}\right) \tag{8}$$

Where ***G*** is the extrapolation of the value of ***I(0)*** and it is related to the volume $\boldsymbol{v^2}$ of the nanofiller inside polymer matrix, the number ***N*** of uniform particles per unit volume, and the composition $\mathbf{\Delta\rho^2}$ (electronic density difference between the phases) by equation (9). Additionally, $\boldsymbol{R_g}$ is the Guinier Radius (or for independent particles $\mathbf{R_g}$ = **R** = radius of rotation), which is related to the mean size (**D** = diameter) of nanofiller by Equation (10).

$$G = N\ \Delta\rho^2\ v^2 \tag{9}$$

$$R_g = \frac{D}{2}\sqrt{\frac{3}{5}} \tag{10}$$

The power-law region that follows the Guinier region (as ***q*** increases) is calculated as:

$$I(q) = \frac{B}{q^P} \tag{11}$$

Where ***B*** is the prefactor of the power-law that is not very significant in scattering of nanocomposites, and ***P*** is the power-law exponent that provides information about the nanofiller surface.

The surface area of colloid can be calculated from the scattering intensity under power-law regime.[249] Considering the Equation (11), if the nanofiller surface morphology is smooth, then $\mathbf{I} \approx \mathbf{q}^{-4}$ with $\boldsymbol{P} = 4$, which better known as Porod law. With $\boldsymbol{P} = 4$ as reference, deviations from this value provide information related to nanofiller morphology within polymer matrix. For example, $\boldsymbol{P}$ values in the range of $3 \leq \boldsymbol{P} < 4$ are related to a surface morphology that contains roughnesses and it is called rough or fractal surface. If the power-law presents an exponent $1 < \boldsymbol{P} < 3$, it is said that the nanofiller has a morphology of mass fractal. For NP with simple Euclidean geometries, ***P*** can provide a signature for the morphology of the nanofiller. It is possible to distinguish between rods, discs and spheres if the slope of ***log I(q) vs. log q*** is -1, -2 or -4, respectively (Figure 32).[249–251]

The equation for a single level of scattering profile can be reached by combining the Guinier's law to the related power-law regime equation as follows:

$$I(q) = G\ exp\left(-\frac{q^2 R_g^2}{3}\right) + B\left\{\frac{\left[erf\left(qR_g/\sqrt{6}\right)\right]^3}{q}\right\}^P \tag{12}$$

Equation (12) represents suitably the scattering profile of monodisperse systems. However, for not too much polydisperse systems with multiple hierarchical structures with different size scales (in the case of nanocomposites), the Equation (12) needs to be expanded to take into account the multiple hierarchical levels of organization, so the Equation (13) is expanded to:

$$I(q) \approx \sum_{i=1}^{n}\left\{G_i\ exp\left(-\frac{q^2 R_{G_i}^2}{3}\right) + B_i G\ exp\left(-\frac{q^2 R_{G_{(i+1)}}^2}{3}\right)\left\{\frac{\left[erf\left(qR_{G_i}/\sqrt{6}\right)\right]^3}{q}\right\}^{P_i}\right\} \tag{13}$$

Figure 32 – Slopes of power-law region from **log I(q) vs. log q** and respective nanofiller morphology

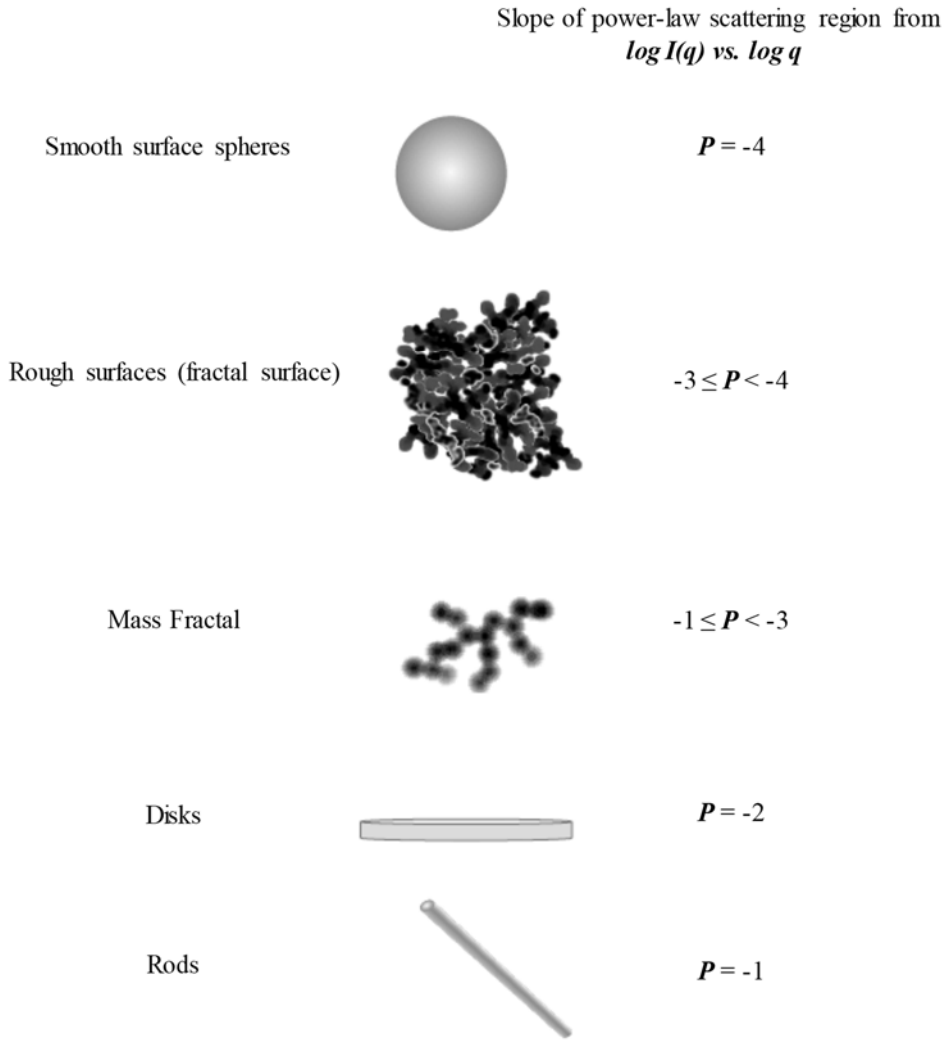

Source: The author, 2018.

Where ***i*** define the structural level related to the size scale; thus, ***i*** = 1 is the lower size hierarchical level (higher **q** values). This model represented by Equation (13) is known as unified model proposed by Beaucage *et al*.[228,252]

When a spatial correlation between the domains is present, i.e., for systems with higher nanoparticles concentration, an interference peak appears in the experimental curves. All previous equations for ***I(q)*** considered dilute systems of nanofiller. For systems with spatial correlation, a structural factor ***S(q)*** is added to the ***I(q)*** equation. Beaucage et al. proposed a semiempirical Equation (14) for the structure factor ***S(q)***. Where ***k*** is defined as a packing factor, which is proportional to the volume fraction occupied in the matrix by the correlated heterogeneities (reaching its theoretical maximum of 5.9 for close-packed crystal), and ***θ*** is a term associated with spatial correlations that occur at average distance ***d***. For spherical domains,

$\boldsymbol{\theta}$ is given by Equation (15). The mean distance between domains, $\boldsymbol{d}$, can be determined by Equation (16), where $\boldsymbol{q_{max}}$ corresponds to the maximum of the peak interference function, $\boldsymbol{I(q)}$, visible in the experimental curves.[253]

$$S(q) = (1 + k\theta)^{-1} \tag{14}$$

$$\theta = 3\frac{\sin(qd) - qd\cos(qd)}{(qd)^3} \tag{15}$$

$$d = \frac{2\pi}{q_{max}} \tag{16}$$

As a measure of polydispersity of nanoparticles embedded in a polymer matrix, a generalized index of polydispersity (**PDI**) for symmetric particles was propped by Beaucage et al.[229] as follows:

$$PDI = \frac{BR_g^4}{(1.62G)} \tag{17}$$

Where $\boldsymbol{B}$ is Porod constant, $\boldsymbol{G}$ is the Guinier prefactor, and $\boldsymbol{R_g}$ is the particles radius of gyration. Polydispersity, as well as asymmetry, of the particles serves to increase the dimensionless ratio of $BR_g^4/(1.62G)$. This ratio, normalized by the value for monodisperse spheres of 1.62 (the lowest possible value), serves as an index for polydispersity, **PDI**.

Another technique that also uses X-ray radiation during analysis is X-ray diffraction (XRD). Differently from SAXS, which analyzes scattered radiation detected at smaller angles, XRD detects X-rays that diffracts in the crystalline structure of the NP, and this diffracted radiation is detected at higher angles. The distance between the chemical bonds of the atoms participating in the crystalline lattice of the material has the same order of magnitude of the incident X-ray radiation. For this reason, the phenomenon of diffraction occurs caused by the crystalline network of the material that acts as a diffraction grating for incident X-rays. From the data of XRD is possible to determine the position and distance of atoms in the crystalline structure of the material. Information about distinct phases that may be present and mean diameter of crystals can also be found.[230,248,254]

Regarding the problems addressed in the Thesis, XRD analysis will be used to check crystalline structures of NP using comparison with diffraction patterns found in diffractogram

libraries. Another utility is the estimation of the mean diameter of NP crystals using the Debye-Scherrer equation (Equation (18)), where ***D*** is the mean particle diameter, λ is the wavelength of incident radiation, ***k*** is the geometric factor (constant that depends on the shape of the crystal), ***B*** is the full width at half maximum (FWHM) of the diffraction peak, and $\boldsymbol{\theta}$ is the Bragg`s angle.[230,254]

$$D = \frac{K\lambda}{B\cos\theta} \tag{18}$$

Infrared spectroscopy (FTIR)

FTIR analysis is an essential tool to evaluate the changes in proton donator and proton acceptor groups of PUU[113,223] The vibrational modes of –NH, C=O (urethane and urea), and ether (C-O-C) bonds receive great attention make it possible to analyze changes and rearrangements of hydrogen bonds that can occur among polymer chains.[113,209] The analysis of the bonded urethane carbonyl (*st* C=O) band at 1702 cm^{-1} and bonded urea (*st* C=O) at 1645 cm^{-1} allows a discussion about microseparation between the rigid and flexible domains of PUU.[64,223] The band region of ether group (*st* C-O-C) at 1100 cm^{-1} also deserves attention because of the possible ether-silver interactions (Ag^{+} or Ag^{0}).

Comparing the spectrum of a neat polymer, band shifts toward higher or lower wavenumber can take place upon the addition of fillers/compounds in the polymer matrix. Generally, shifts to lower wavenumbers suggest an interaction intensification between the functional group and the filler/compound or other group in the polymer backbone. On the other hand, shifts to higher wavenumbers imply in an opposite behavior, i.e., an interaction decrease related to the functional group.[69]

Thermogravimetric analysis (TGA)

The TGA allows to evaluate the degradation profile of the polymeric material. Some minor changes, not shown in TGA curves, can be evaluated by derivative thermogravimetry (DTG) curves. The thermal degradation of PUU films is basically a two-stage depolycondensation process. The first stage of degradation is related to the rigid domains of the polymer and the subsequent stage corresponds to flexible domains. Due to its association with rigid domains of

PUU, the initial temperature of degradation (T_{onset}) can provide information on changes in the urethane and urea groups.[208,237]

In the DTG curves, several peaks appeared, demonstrating the complexity of the degradation. They are associated with temperature at maximum rate of weight loss (T_{vmax}) at each stage of degradation. The higher T_{vmax}, which is relative to the last peak of the DTG curves, is related to the degradation of polymer flexible domains; thus, variations in this T_{vmax} are closely associated to changes in ether groups present in PUU.[208,237]